Natalia Frühmann

The ostracod fauna of two siliciclastic successions in the Retznei Quarries (Badenian, Styrian Basin, Austria)

Master's Thesis

To be awarded with the degree of

Master of Science

Institute of Earth Sciences

(Geology and Paleontology)

University of Graz

Supervisor:

o. Univ. Prof. Dr. phil. Werner E. Piller

Content

List of figures

List of tables

List of plates

Acknowledgments

At this point I would like to thank Prof. Dr. Werner E. Piller for his continuous support and scientific guidance. His vast experience and knowledge, critical remarks as well as his endless patience helped me tremendously throughout my study.

I would also like to thank Dr. Martin Gross for the invaluable help he provided with his experience and knowledge.

I am very grateful to Angela García and Gerald Auer for the critical and constructive discussions and their kind words. They really boosted my confidence and cheered me up in times of need.

I want to express my gratitude to the scientific and non-scientific staff of the Institute of Earth Science of the University of Graz, especially Gertraud Bauer and Georg Stegmüller for their kind words and technical and administrative help during the intense finish.

Finally, I am deeply thankful to my family and friends who always showed their belief and trust in me and gave me a place to back down to gain new energy and strength. Sincere and earnest thanks to my mom and my boyfriend Stephan Liegle, they are the pillars that hold me upright.

Abstract

For the purpose of this Master's thesis, the siliciclastic sections of the Retznei quarries (Old quarry and Rosenberg quarry) were investigated in terms of their ostracod content to reconstruct paleoenvironmental conditions. The investigated siliciclastic sections were deposited below (Rosenberg quarry section) and above (Old quarry section) the Lower Badenian (Middle Miocene) Leitha Limestone body which corresponds to the Middle Miocene Climate Optimum (MMCO; Zachos et al., 2001; Böhme, 2003). The results are based on the quantitative analysis of the ostracod fauna compared with geochemical (organic carbon, carbonate content, sulphur content, stable isotopes) and sedimentological (grain size analysis) data provided by Strahlhofer (2013).

The combination of these data with multivariate statistical methods (cluster analysis and NMDS), the ecological demands and the occurrence of the marker taxa *Krithe/Parakrithe, Henryhowella* and *Pterygocythereis* allowed a paleoecological reconstruction of the Old quarry. The lower part of the section is characterised by elevated primary production and relatively stagnant bottom waters. This led to the development of dysoxic to anoxic bottom waters in the middle of the section. Above a massive turbiditic layer, which disturbed the environment, lower temperatures and larger fluctuations in primary production were observed in the upper part of the section based on an increasing trend in $\delta^{18}O$ and variating TOC values.

The extremely sparse ostracod content of the Rosenberg quarry did not provide any detailed information, but the ecological demands of the occurring ostracods match to the established paleoecological reconstruction of Strahlhofer (2013).

Zusammenfassung

In dieser Masterarbeit wurden zwei Profile (Profil Alter Bruch, Profil Rosenberg Bruch) des Steinbruchareals von Retznei (Steirisches Becken, Österreich) mit dem Ziel einer paläoökologischen Rekonstruktion auf ihren Ostrakodengehalt untersucht. Die untersuchten siliziklastischen Abfolgen wurden unterhalb (Rosenberg Bruch) bzw. über (Alter Bruch) dem rotalgendominierten Leithakalk-Bioherm des unteren Badenium (mittleres Miozän), welcher Ablagerungen des mittelmiozänen Klimaoptimums (MMCO; Zachos et al., 2001; Böhme, 2003) entspricht, abgelagert. Die Ergebnisse stützen sich auf die quantitative Bestimmung von Ostrakoden sowie auf geochemische (organischer Kohlenstoff, Karbonatgehalt, Schwefel, stabile Isotope) und sedimentologische Messungen (Korngrößenanalyse) von Strahlhofer (2013).

Die Kombination dieser Daten mit den Ergebnissen von multivariaten statistischen Analysen (Clusteranalyse, NMDS) der Ostrakodenvorkommen sowie das Auftreten der „Markertaxa“ *Krithe/Parakrithe, Henryhowella* und *Pterygocythereis* erlaubte eine paläoökologische Rekonstruktion des Alten Bruchs. Der untere Profilteil zeichnet sich durch eine konstant hohe Primärproduktion in einem Bereich mit geringer Bodenwasserzirkulation aus, was zu dys- bis anoxischen Bedingungen in der Mitte des Profils führte. Eine mächtige, turbiditische Sandschicht in der Profilmitte unterbricht diese Entwicklung. Im oberen Profilteil, über dieser Sandlage, wurden anhand des ansteigenden $\delta^{18}O$ - Trends und schwankenden TOC-Werten niedrigere Temperaturen und schwankende Primärproduktion nachgewiesen.

Eine derartig detaillierte Interpretation des Rosenberg Bruchs war aufgrund der geringen Ostrakodenvorkommen nicht möglich, jedoch passen die ökologischen Ansprüche der vorkommenden Taxa zu dem etablierten paläoökologischen Modell von Strahlhofer (2013), das von einem deepening-upwards-Trend in einem marinen Randbereich ausgeht.

1. Introduction

Earth's climate during the late early Miocene was characterised by the onset of the Middle Miocene Climate Optimum (MMCO; Zachos et al., 2001; Böhme, 2003) which is the most recent period of significantly warmer climate. The MMCO is followed by the Middle Miocene Climate Transition (MMCT; Shevenell et al., 2004; Lewis et al., 2007; Harzhauser et al., 2011) that subsequently leads towards the Pleistocene glacial climate (Zachos et al., 2001).

In the Central Paratethys the MMCO is represented by the wide-spread development of reef belts and the migration of other tropical biota north of the Mediterranean Sea (Harzhauser and Piller, 2007; Kroh, 2007; Reuter et al., 2012). During the Langhian and the early Serravallian (Badenian on the regional stratigraphic time scale of the Central Paratethys; Piller et al., 2007), the most important wide-spread shallow-water carbonate in the entire Central Paratethys is the Leitha Limestone (Riegl and Piller, 2000a; Piller et al., 2007). It was usually formed in areas that were protected from coarse siliciclastic influx, like isolated basement highs (Dullo, 1983; Piller and Kleemann, 1991). In accordance with this, corallinacean carbonates and coral constructions also formed in the Styrian Basin around basement highs such as the Middle Styrian High and the South Burgenland High and around volcanic islands (Gross et al., 2007).

The Retznei cement quarries in southern Styria (fig. 1) expose an approximately 25 m thick Leitha Limestone build-up that lies in between two siliciclastic successions, of which the basal one represents sediments deposited before the onset of the MMCO and the overlying one represents the cooling during the MMCT (Strahlhofer, 2013). This provides a great opportunity to study the ecological impact of the Badenian climate changes on a local scale.

Its long mining history and easy accessibility made the Retznei quarries a location of scientific interest for a long time, hence, a lot of scientific work was done (e.g. Friebe, 1988, 1989, 1990, 1991, 1993; Fenninger & Hubmann, 1997; Riegl & Piller, 2000; Fritz & Hiden, 2001; Spezzaferri et al., 2002; Bojar et al., 2004; Erhart, 2004; Ćorić et al., 2007; Gross et al., 2007; Hohenegger et al., 2009; Reuter & Piller, 2011; Reuter et al., 2012; Strahlhofer, 2013). Although some of these studies deal with the siliciclastic sections beneath and above the carbonate build-up, most of them are focussing on the

structure and the development of the Leitha Limestone build-up. A detailed paleoenvironmental reconstruction, based on both benthic and planktic foraminiferal assemblages as well as geochemical proxies, was done by Strahlhofer (2013).

However, the ostracod fauna hasn't been investigated in detail until now; this is provided in the present study. Ostracods are excellent bioindicators, because they react very sensibly to environmental changes (e.g., water salinity, temperature, oxygen content).

The aim of this study is a reconstruction of the paleoenvironment based on ostracods and to compare this reconstruction with the established paleoenvironmental model from previous studies.

2. Geological setting

During the Cenozoic Era Africa moved towards Eurasia with a northwards shift and a generally counterclockwise rotation (Kovác et al., 1998; Márton et al., 2003, 2006; Márton 2006; Seghedi, et al. 2004; Piller et al,. 2007). This continental movement led to the change of the Eurasian paleogeography from vast marine areas interrupted by archipelagos into dry land (Piller et al., 2007). Around the Eocene/Oligocene boundary, Africa's northward movement and resulting European plate subduction caused the final disintegration of the ancient (Western) Tethys Ocean (Báldi 1980; Harzhauser et al., 2002; Harzhauser & Piller 2007; Piller et al., 2007) and led to the formation of the Indo-Pacific Ocean in the east and various relic east-west elongated marine basins in the west (Harzhauser & Piller, 2007; Piller et al., 2007). South of the Alpine orogene the Western Tethys (= Proto-Mediterranean) still continued, while to the north the vast Eurasian Paratethys Sea came into existence (Gross et al., 2007). During its maximum extent, the Paratethys Sea spread from the Rhône Basin in France towards Inner Asia. It was partitioned into two geotectonic units, a smaller part that consists of the Western Paratethys and the Central Paratethys, and the larger Eastern Paratethys, which underwent different paleoenvironmental histories due to differently timed geotectonic events and global sea level fluctuations controlling marine and non-marine phases (Popov et al., 2004; Harzhauser & Piller, 2007). The Western Paratethys includes the Rhône Basin and the Alpine Foreland Basins of Switzerland, western Bavaria and Upper Austria. The Central Paratethys includes the Eastern Alpine - Carpathian Foreland basins, from Lower Austria to Moldavia, and the Pannonian Basin System. The Eastern Paratethys comprises the Euxinian (Black Sea), Caspian and Aral Sea basins (Nevesskaja et al. 1993; Piller et al., 2007). Related to this is a complex pattern of changing seaways and landbridges between the Paratethys and the Mediterranean Sea as well as the western Indo-Pacific (e.g., Rögl, 1998, 1999), which created a complex pattern of biogeographic relationships between these paleobiogeographic units and resulted in complicated stratigraphic correlations within the Paratethys itself and between the Paratethys and the Mediterranean and global stratigraphy, respectively (Harzhauser et al., 2002; Piller et al., 2007).

2.1 Evolution of the Styrian Basin

The Styrian Neogene Basin is about 100 km long and 60 km wide and represents the westernmost embayment of the Central Paratethys. In the north, west and south-west it is confined by the crystalline Austroalpine units and the Graz Paleozoic. The Güns Mountains (Penninic units) mark the north-eastern boundary of the basin (Gross et al., 2007). The basin is part of the Pannonian Basin System, which is surrounded by the Alps, Dinarids and Carpathians (Gross et al., 2007). The NE – SW striking South Burgenland Swell separates the Styrian Basin from the Western Pannonian Basin (Gross et al., 2007). Several swells and Austroalpine basement spurs subdivide the Styrian Basin into different subbasins (Kröll et al., 1988). The main structure is the Middle Styrian Swell that separates the shallow (up to 1000 m) Western Styrian Basin from the more than 4000 m deep Eastern Styrian Basin (Sachsenhofer et al., 1997; Schreilechner & Sachsenhofer, 2007). The genesis and evolution of the Styrian Basin is closely linked with the final stages of the Alpine Orogeny (Ebner & Sachsenhofer, 1995). The initiation of the basin formation occurred during the final collision stage of the Adriatic with the European Plate (late Oligocene to Miocene; Gross et al., 2007). The basement is formed by the Austroalpine nappe system. The subsidence of the basin started during the early Miocene, respectively in the Ottnangian, as a result of lateral extrusions of crustal wedges along strike-slip faults towards the Pannonian Basin (Decker & Peresson, 1996; Frisch et al., 2000; Hohenegger et al., 2009). A combination of block tilting, subsidence and uplift led to the formation of different sub-basins. The sedimentation in the Styrian Basin started during the Ottnangian (the Ottnanigan is a regional stratigraphic stage of the Central Paratethys and is a part of the Burdigalian on the international stratigraphic time scale; Piller et al., 2007) with the deposition of limnic-fluvial sediments in the central Eastern Styrian Basin (“Limnic Series”; Kollmann, 1965) and shallow marine sediments in the western Gnas sub-basin (Ebner & Sachsenhofer, 1995). During the Karpatian (late Burdigalian) increasing tectonic activities caused increasing subsidence. This went alongside a marine ingression from the south and led to the deposition of several hundred meters thick offshore mud and siltstones with sandy, turbiditic intercalations (Styrian Schlier; Gross, 2007). The extensional tectonics during the Karpatian went along with acidic to intermediate volcanism, which produced an island complex built up by huge shield volcanoes, like in Bad Gleichenberg and

Weitendorf. Weathered volcanic ash layers in fossil-free or -poor areas indicate that this volcanism remained active at least to the end of the early Badenian. The tectonic activity increased during the latest Karpatian and at the Karpatian/Badenian boundary, forming the “Styrian Tectonic Phase”, first described by Stille (1924). The tectonic movements caused tilting of crustal blocks, the uplift of the western hinterlands and the uplift of the Sausal Mountains (= Middle Styrian Swell; Ebner & Sachsenhofer, 1995). These tectonic movements, in combination with a eustatic sea level lowstand, resulted in the “Styrian unconformity” (Friebe, 1991; Ebner & Sachsenhofer, 1995), an angular unconformity that is exposed at the Wagna brickyard (type locality), the Retznei quarries and in the Katzengraben/Spielfeld (Fenninger & Hubmann, 1997). However, the stratigraphic correlation of the Styrian tectonic phase is still subject of discussion: e.g. Friebe (1991) relates it to the latest Karpatian, while Auer (1996) suggests an early Badenian age for this phase. In the early Badenian, marine sedimentation in the Styrian Basin reached its maximum extent despite reduced tectonic activities and subsidence. This was connected with a eustatic sea level rise during the Middle Miocene Climate Optimum (MMCO; Friebe, 1990; Rögl, 1998; Zachos et al., 2001; Kovac et al., 2004). At this time a stable seaway (Trans-Tethyan Trench Corridor) via Slovenia as well as intermittent seaways into eastern directions connected the Pannonian Basin System with the Mediterranean Sea (Piller et al., 2007). These connections enabled three marine transgressions that correlate with the TB 2.3–2.5 sea level cycles of Haq et al. (1988) (Piller et al., 2007). These seaways enabled the immigration of tropical and subtropical taxa from the Mediterranean Sea (Harzhauser et al., 2003; Harzhauser & Piller, 2007). In addition, the carbonate production in the Central Paratethys reached its maximum during the early Badenian (Piller et al., 2007). Coralline algal limestones developed around basement swells and volcanos. In areas of low terrigenous sedimentation, such as the Middle Styrian High, coral growth was prolific (Friebe, 1990, 1993; Reuter & Piller, 2011). Siliciclastic influx was mainly controlled by sea level changes, delta dynamics and volcanic activity (Friebe, 1993; Reuter & Piller, 2011). The limestone, regionally known as Leitha Limestone, is grouped together with other shallow water sediments in the Weissenegg Formation, which overlies Karpatian sediments (Kreuzkrumpel Formation; Schell, 1994) above the Styrian Unconformity (Friebe, 1988, 1990) (fig.6).

2.2 Study Area

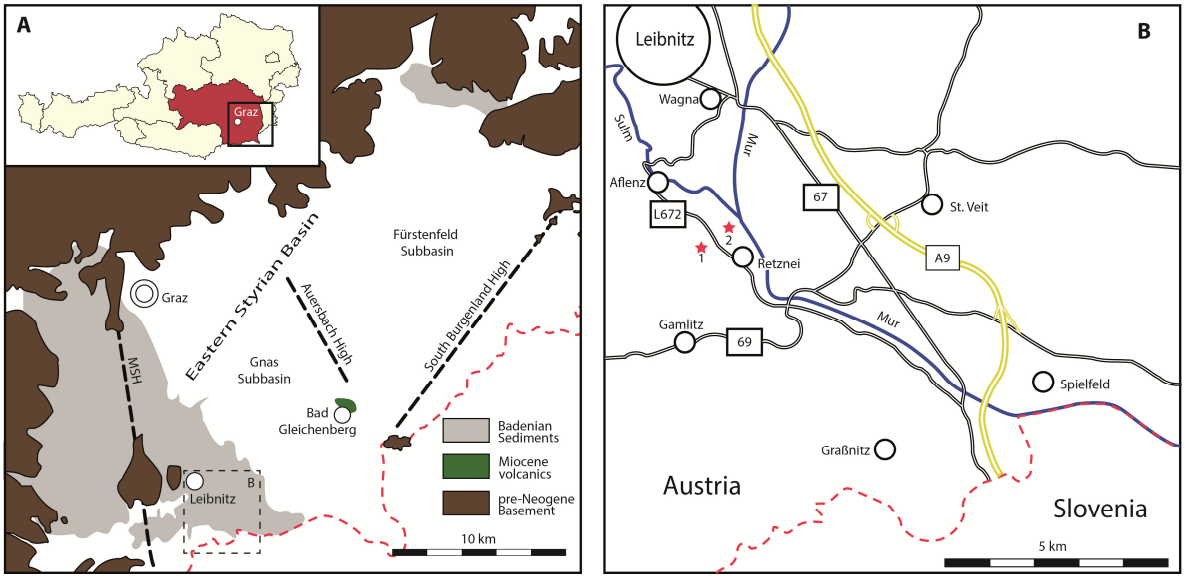

Fig. 1: Geological and geographical overview of the study area. A: Simplified geological map of the Styrian Basin showing the main structural elements and the distribution of the Badenian sediments and Miocene volcanic rocks at the surface (MSH = Middle Styrian High; modified after Reuter et al., 2012). B: Location of the Retznei quarries (1 = Old quarry, 2 = Rosenberg quarry, modified after Reuter et al., 2012).

The two studied sections are exposed in the Retznei Lafarge-Perlmooser cement quarries, which are located in Southern Styria, approximately 40 km south of Graz and approximately 6.8 km south-east of Leibnitz. The mining area is about 3 km^2 wide and includes the Old quarry (46°44'22.18''N, 15°33'27.35''E, 281 m above s.l.) and the New quarry, also known as the Rosenberg quarry; 46°44'34.67''N, 15°33'48.85''E, 293 m above s.l.). The two sections are about 250 m apart from each other and are separated by the road from Retznei to Aflenz (L672). The Rosenberg quarry is actively mined, whereas the Old quarry is abandoned, poorly preserved and currently used as a waste dump.

The Retznei quarries expose a heterogeneous, approximately 25 m thick Leitha Limestone body which mainly consists of coralline algal and coral-rich shallow-marine limestones, shows strong influence of terrigenous sedimentation (Reuter et al., 2012) and corresponds to the Middle Miocene Climate Optimum (MMCO; Zachos et al., 2001). Recent studies on the carbonate complex describe at least four depositional units and six different facies (e.g. Reuter & Piller, 2011; Reuter et al., 2012). This carbonate body is under- and overlain by fine-grained, fossil-rich siliciclastic successions. The basal

siliciclastics are exposed in the Rosenberg quarry. According to the study of Strahlhofer (2013), these sediments point towards a partly freshwater-influenced, marginal marine to fluvial marine environment. The overlying siliciclastics are exposed in both the Old quarry and the Rosenberg quarry, although the Old quarry section has a much greater thickness. Studies on these successions suggest a deepening-upwards trend (Hohenegger et al., 2009), which was accompanied by a decrease in surface water temperature, most likely caused by the expansion of the East Antarctic Ice Shield during the Middle Miocene Climate Transition (MMCT; Bojar et al., 2004; Shevenell et al., 2004; Strahlhofer, 2013).

Beside macrofossils, the siliciclastic sediments are rich in calcareous nannoplankton as well as microfossils, such as dinoflagellates and foraminifers. In comparison to the other microfossils, the ostracod content is relatively low.

2.2.1 Section description

The Retznei quarries have been of scientific interest for a long time. Therefore, a lot of work has been done prior to this study. The following description of the Old quarry section and the Rosenberg quarry section is based on Gross et al. (2007), Hohenegger et al. (2009), Reuter et al. (2012) and Strahlhofer (2013). A more detailed description of the Old quarry section and the Rosenberg quarry section is given in Strahlhofer (2013).

2.2.1.1 Old Quarry section

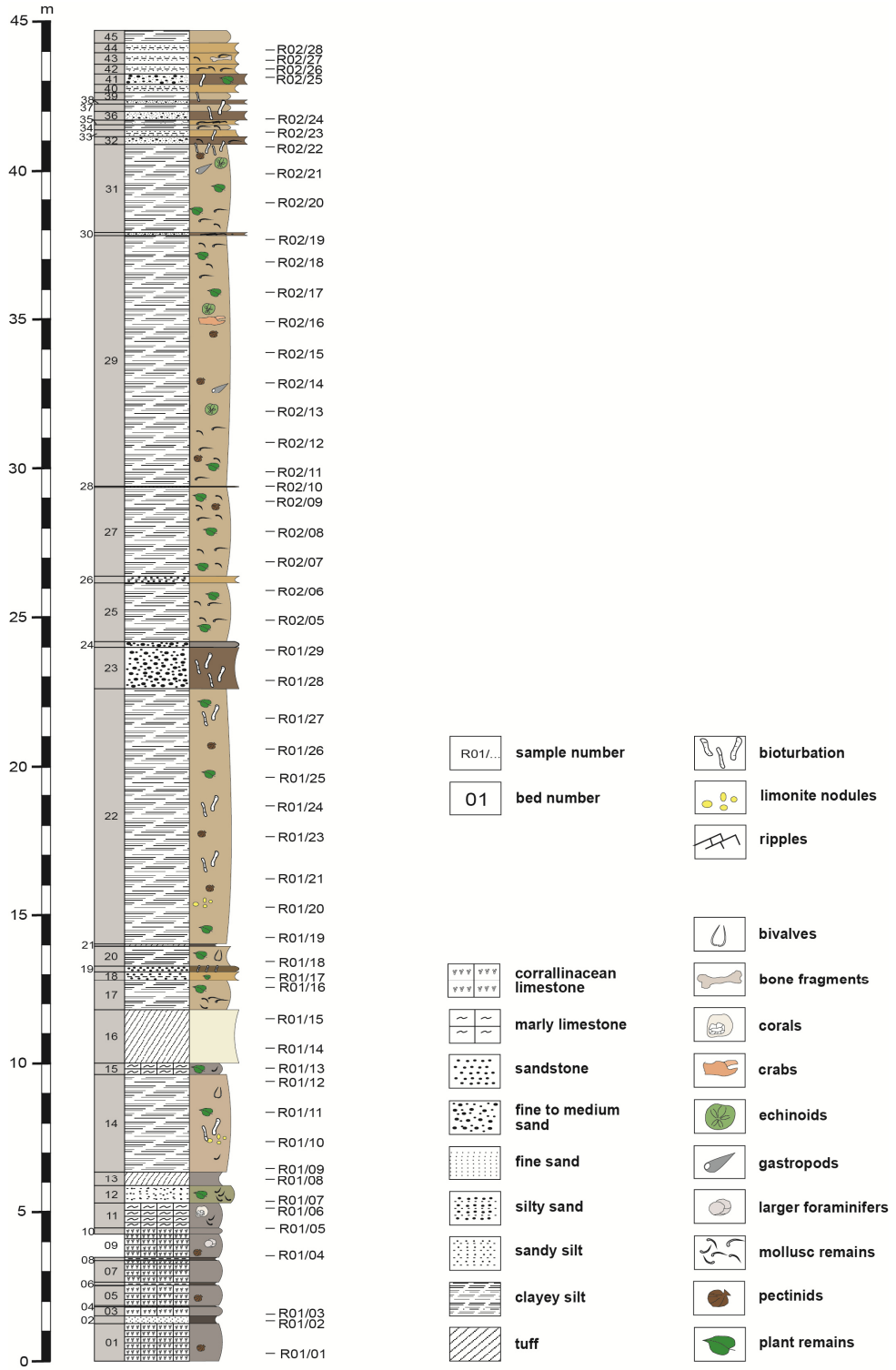

Fig. 2: Litholog of the Old quarry section showing the sample localities after Hohenegger et al. (2009), originally sampled in two overlapping sub-sections (R01 and R02); modified based on previous studies (Gross et al., 2007; Hohenegger et al., 2009; Strahlhofer, 2013).

The siliciclastic succession that overlies the carbonate complex was originally sampled in two overlapping sub-sections (R01 and R02) and correlated into an approximately 45 m thick composite section by using a distinct sand horizon for correlation (fig. 2). The siliciclastic succession of the Old quarry overlies the uppermost 5.2 m of the Leitha Limestone body that is interrupted by several thin marl layers. The carbonates frequently contain pectinids, but also bryozoans, accumulations of larger foraminifers and corals. After an erosional surface on top of the limestone body, the approximately 35 m thick siliciclastic succession, which consists of siltstones and turbiditic sandstones and is rich in plant remains, molluscs, foraminifers and dinocysts (Friebe, 1988; Gross et al., 2007; Hohenegger et al., 2009; Reuter et al., 2012; Strahlhofer, 2013), starts with a 60 cm thick sandy silt layer. It is followed by a 50 cm thick volcanic ash layer that consists of feldspar, quartz, idiomorphic zircons and biotites and was radiometrically dated to 14.21 ± 0.07 Ma (Bojar et al., 2004) or 14.39 ± 0.12 Ma (Handler et al., 2006). An approximately 1.8 m thick tuffitic layer that contains unaltered feldspar phenocrysts, idiomorphic biotites and bentonite occurs about 10 m above the limestone body. In the middle of the section, an approximately 1.5 m thick sandstone layer and an overlying 5 cm thick fine to medium sand layer, deposited about 18 m above the carbonates, mark the top of sub-section R01 (fig. 2). These sandstone layers were used for the correlation with sub-section R02.

The following approximately 18 m thick sub-section R02 shows a higher frequency of intercalated sandstone layers towards its top as well as a high amount of plant, fish, mollusc, echinoid and crab remains (fig. 2).

The siltstones in sub-section R01 are mostly bioturbated, whereas in sub-section R02 bioturbation only occurs in the intercalated sandstone layers (fig. 2).

2.2.1.2 Rosenberg quarry section

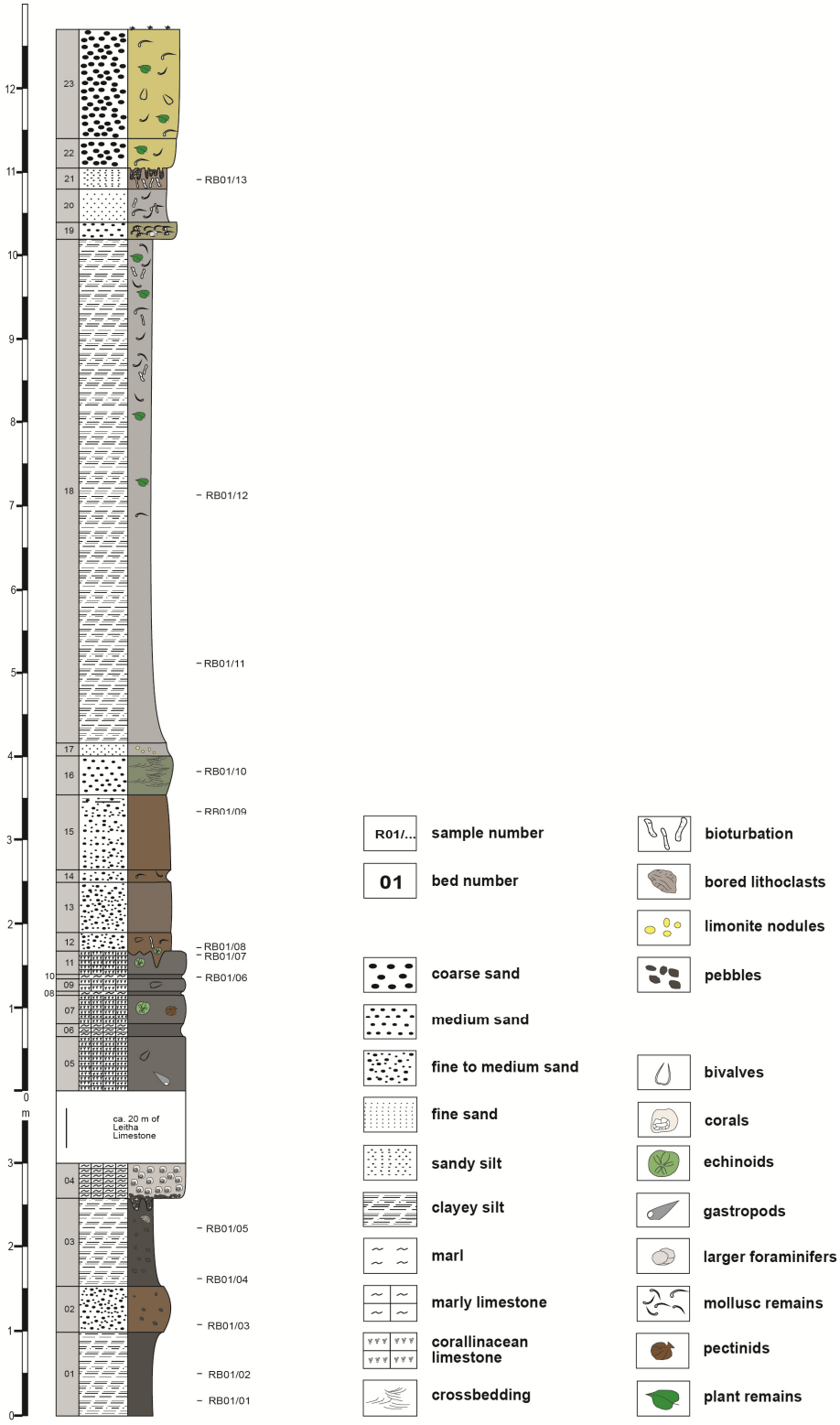

Fig. 3: Litholog of the Rosenberg quarry section showing the sample localities, after Strahlhofer (2013).

The Rosenberg quarry section consists of two mainly siliciclastic sub-sections that lie beneath and above an approximately 20 m thick Leitha Limestone build-up (fig. 3).
The basal part of the section is about 3 m thick and starts approximately 2.6 m below the limestone body with an approximately 1 m thick homogenous, fossil-free siltstone layer, which is overlain by about 1.6 m thick conglomerates that consist of fine-grained silt and sandstones with heavily bored polymict pebbles. The erosive top of the conglomerates exhibits incisions of up to 20 cm and is overlain by a grain-supported pebble layer. The top of the basal sub-section as well as the base of the overlying sub-section consist of marly limestones of the Retznei carbonate body (fig. 3), which has been the subject of many authors (e.g., Gross et al., 2007; Reuter & Piller, 2011; Reuter et al., 2012). The overlying section starts with the approximately 1.7 m thick uppermost part of the limestone body that shows an alternation of limestone and marl layers (fig. 3). The top of the carbonate body is highly erosive and exhibits an irregular surface that shows distinct parallel up to 15 cm deep and 50 cm wide runnels and up to 30 cm deep fissures (fig. 3). The carbonate complex is overlain by an approximately 11 m thick succession of sand and silt stones, which contain bivalves and echinoids as well as plant remains and strong bioturbation in the upper part (fig. 3).

2.2.2 Geochemistry

Geochemical data originate from measurements of bulk samples from the Old quarry and the Rosenberg quarry by Strahlhofer (2013). A detailed data table is provided in appendix 3 (App. 3 Tab. 1-2): Geochemical data.

2.2.2.1 Old quarry section

The trends of the geochemical measurements in the Old quarry section are depicted in figure 4. The following trends are visible:

- The carbonate content in the Old quarry is relatively constant, except of increased contents in the limestone body and reduced contents in the intercalated tuffitic layers.
- The sulfur content in the lower part of the Old quarry is generally lower than in the upper part. The middle part of the section shows a drastic increase in sulfur.
- Generally, the TOC content in the lower part is higher and more constant than in the upper part, where it is highly fluctuating.
- The TOC/S ratios in the lower part of the section are generally higher than in the upper part of the section. Towards the middle part of the section, a clear decreasing trend is visible. Extremely high TOC/S values were measured in tuffitic layers and sand layers.
- Except of a few samples with considerably lower values, the $\delta^{13}C$ values show a slight increasing-upwards trend throughout the section.
- The $\delta^{18}O$ values show strong variations. While in the lower part a slight decreasing-upwards trend is visible, the upper part of the section shows a slight increasing-upwards trend.

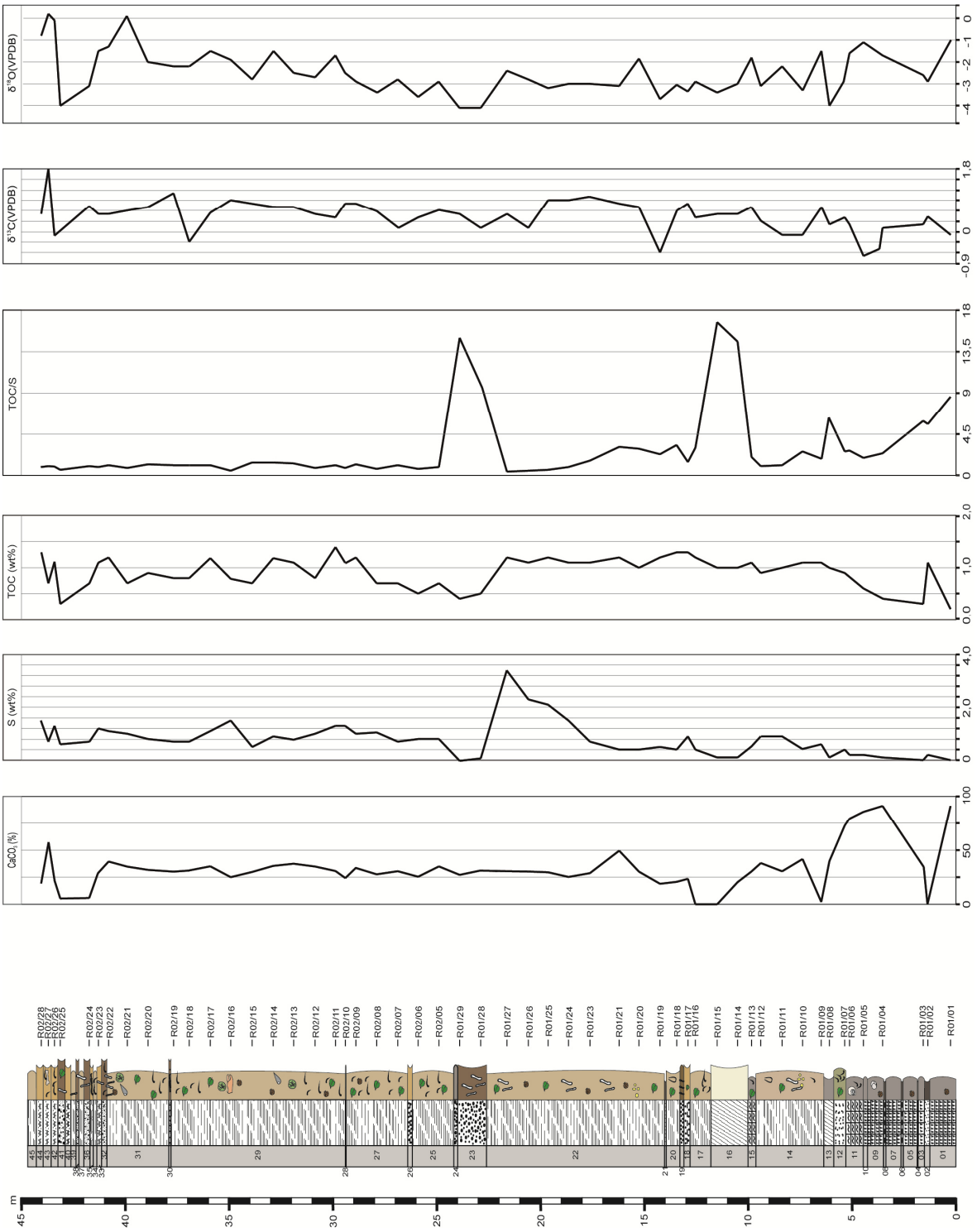

Fig. 4: Litholog of the Old quarry section showing Calcium carbonate ($CaCO_3$), Sulfur (S), total organic carbon (TOC), TOC/S-ratio, $\delta^{13}C$ and $\delta^{18}O$ values (data from Strahlhofer, 2013)

2.2.2.2 Rosenberg quarry section

The trends of the geochemical measurements in the Rosenberg quarry section are depicted in figure 5. The following trends are visible:

- The carbonate contents in the basal siliciclastics are slightly higher than the carbonate contents in the overlying siliciclastics. The highest content was measured in the Leitha Limestone body.
- The sulfur contents in the basal siliciclastics are slightly higher than in the overlying siliciclastics.
- The TOC contents in the basal siliciclastics show high variation and are generally higher than in the overlying siliciclastics.
- The TOC/S ratios are low throughout the section, except of sample RB01/13 where an extremely high value was calculated due to the missing sulfur content in this sample.
- The $\delta^{13}C$ values in the basal siliciclastics are slightly higher than in the overlying siliciclastics.
- The $\delta^{18}O$ values in the basal siliciclastics show strong variations. The samples above the limestone body show a decreasing upwards trend and generally more stable $\delta^{18}O$ values.

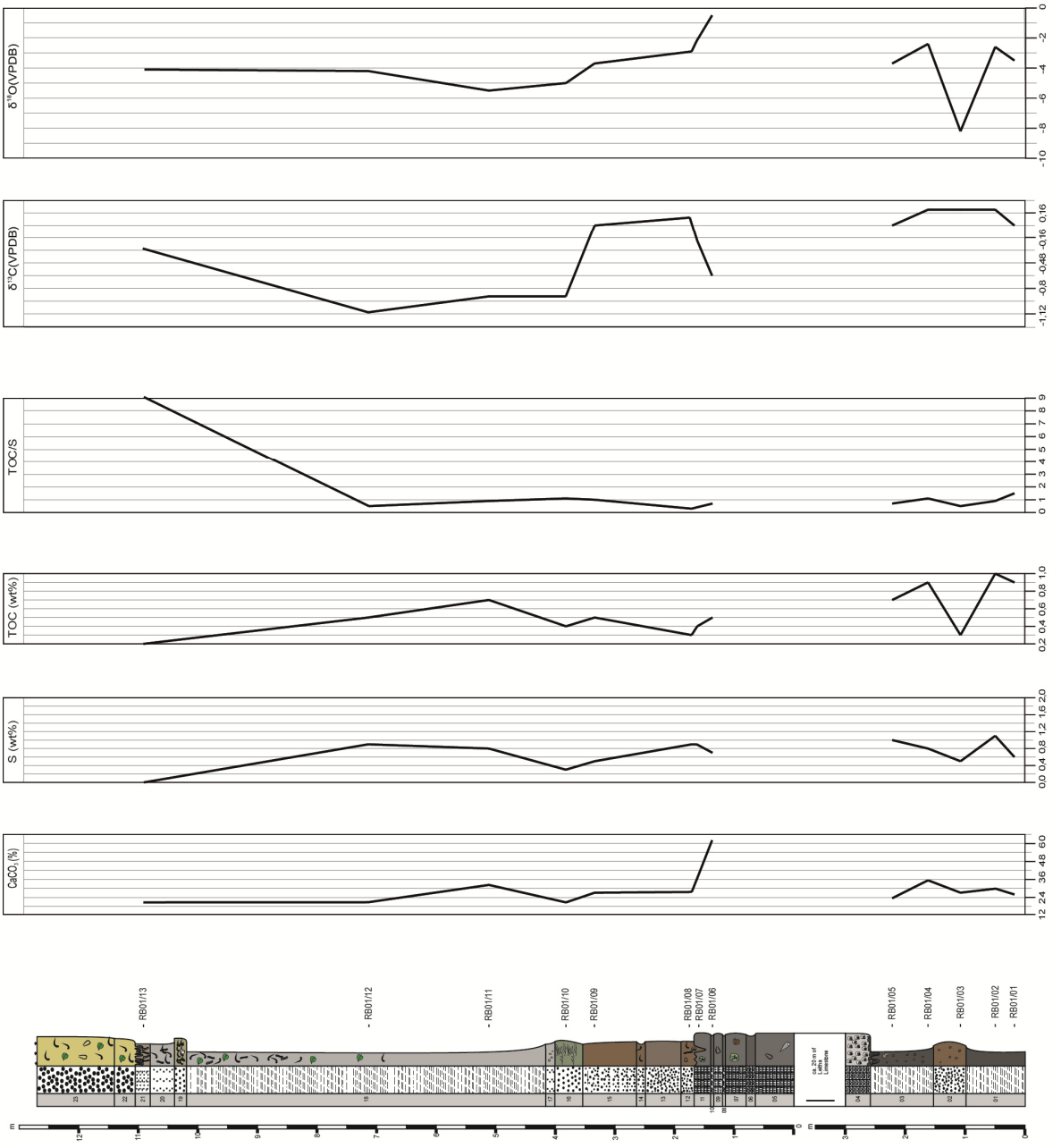

Fig. 5: Litholog of the Rosenberg quarry section showing calcium carbonate ($CaCO_3$), sulfur (S), total organic carbon (TOC), TOC/S-ratio, $\delta^{13}C$ and $\delta^{18}O$ values (data from Strahlhofer, 2013)

2.2.3 Sedimentary development

Local tectonic activities, volcanic ash falls and the development of the Middle Styrian High strongly influenced the sedimentary environment of the two sections of the Retznei quarries (Reuter & Piller, 2011; Reuter et al., 2012). The top of the basal siliciclastics exposed in the Rosenberg quarry section consists of the so-called “Geröllmergel” (e.g., Kollmann, 1965; Friebe, 1988), which is represented by an approximately 1.5 m thick, poorly sorted conglomeratic layer with components up to 40 cm in diameter (Fenninger & Hubmann, 1997; Reuter et al., 2012). This conglomerate consists of Karpatian silt- and sandstones, Paleozoic limestone and dolomite, gneiss, micaschist, phyllite, and quartz in a siltstone matrix with intercalated layers of fine-grained sandstone (Reuter et al., 2012). Larger components are heavily bored by bivalves and encrusted by oysters, serpulids and bryozoans (Fenninger & Hubmann, 1997; Gross et al., 2007; Hohenegger et al., 2009; Reuter et al., 2012). High-energy currents are indicated by the occurrence of well-rounded pebbles. These siliciclastics are interpreted as sediments of a fluvial-marine channel system, as a result of a relative sea level lowstand during the earliest Badenian (Friebe, 1993; Fenninger & Hubmann, 1997; Hohenegger et al., 2009; Reuter et al., 2012), which were deposited above the Styrian Unconformity. The top of the conglomerates is erosive and overlain by an a few cm thick polymict grain-supported pebble horizon, which is interpreted as a transgressive lag sediment (Reuter et al., 2012) that acted as a stable substrate for corals and other sessile organisms. This enabled the development of the approximately 25 m thick, vertically as well as laterally very heterogeneous Retznei Leitha Limestone carbonate complex with fairly diverse patch reefs (Friebe, 1993; Reuter & Piller, 2011; Reuter et al., 2012). The Retznei carbonate build-up represents a shallow-marine depositional environment and is correlated with the sea level rise of the second Badenian transgression into the Central Paratethys by Friebe (1993), corresponding to the global cycle TB 2.4 of Haq. et al. (1988). The carbonate production in the Retznei quarries corresponds to the Middle Miocene Climate Optimum (MMCO; Zachos et al., 2001; Böhme, 2003). Short-term volcanoclastic sedimentation, terrigenous input from delta systems and local alluvial fans highly influenced the carbonate production (Friebe, 1990; Reuter & Piller, 2011; Reuter et al., 2012). Increased nutrient input into the basin by river runoff that led to eutrophication events that terminated the carbonate production is indicated by thin marl

layers within the uppermost part of the limestone build-up. Based on the faunal assemblages within the carbonate body, Gross et al. (2007) suggest a tropical to sub-tropical climate with pronounced seasonality. Subtropical climate with high seasonal variations in water temperature is also indicated by an isotope study on brachiopod and pectinid shells by Bojar et al. (2004). The top of the carbonate body is highly eroded and exhibits deep karst fissures, which developed during prolonged emergence at the end of the carbonate production (Friebe, 1993; Reuter et al., 2012). Compared to the Old quarry, this erosive surface is much more prominent in the Rosenberg quarry due to its higher position on the bioherm, which resulted in a longer exposure period (Strahlhofer, 2013). Above the carbonate build-up, a highly bioturbated succession of fine siliciclastics with frequent mollusc and plant remains together with less common crustaceans, echinoids and fish remains follows. Three distinct diagenetically altered tuffitic horizons in the lower part of the siliciclastics of the Old quarry section indicate synsedimentary volcanic activity. Tuffitic layers are missing in the Rosenberg quarry section, probably due to reworking and alteration processes on the sea floor (cp. Reuter & Piller, 2011; Reuter et al., 2012). Throughout the Old quarry section, sand layers are intercalated with an increase in their frequency in the upper part. These sand layers mostly show a fining-upwards trend and bioturbation (e.g., *Thalassinoides*, *Ophiomorpha*; Hohenegger et al., 2009). Sedimentary structures such as flute casts and ripples suggest that these sand layers represent turbiditic deposits. Towards the top of the Rosenberg quarry section, increased terrigenous input is indicated by coarse-grained, poorly sorted sand layers that frequently contain molluscs (e.g., pectinids, oysters) and plant remains.

In contrast to the warm water carbonates, stable isotope data from Bojar et al. (2004) suggest cooler mean water temperatures with less seasonality for the siliciclastic deposits above the limestone body. The cooler temperatures, in combination with the clear lithological shift from carbonates to siliciclastics with an accompanying change in the faunal assemblages, are correlated with the major expansion of the East Antarctic Ice Sheet at about 14 Ma (Bojar et al., 2004). Corresponding to this, the radiometric dating of a tuffitic layer between the carbonates and the overlying siliciclastics of the Old quarry section gave an age of 14.21 ± 0.07 and 14.39 ± 0.12 Ma, respectively (Bojar et al., 2004; Handler et al., 2006; Gross et al., 2007).

Increased tectonic activities went alongside this climatic change and led to higher subsidence and the uplift of the hinterland (Friebe, 1993). Deepening is indicated by dinocyst and foraminiferal assemblages (Friebe, 1993; Gross et al., 2007; Hohenegger et al., 2009; Reuter et al., 2012), while plant remains point towards increased terrigenous sediment input from the close hinterland (Reuter et al., 2012).

3. Stratigraphy

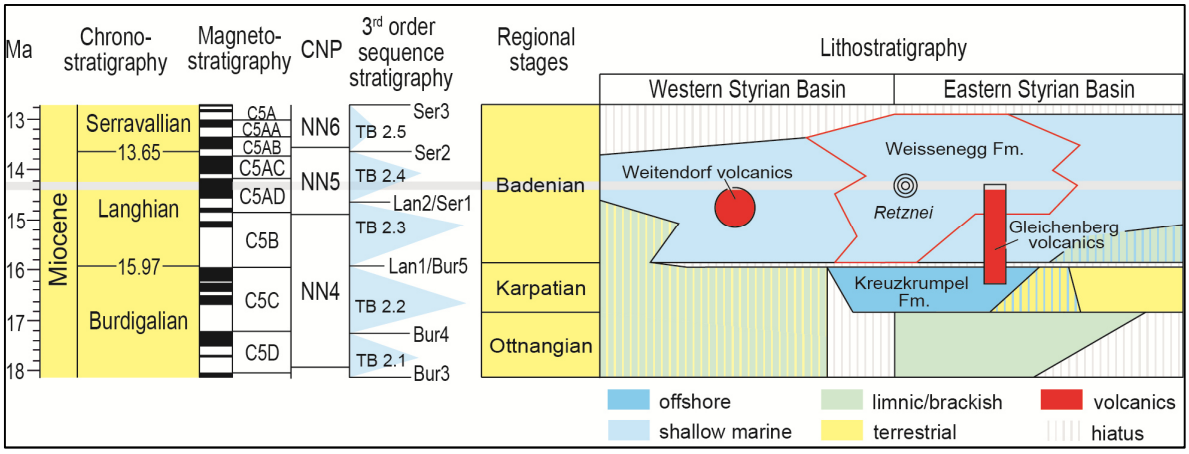

Fig. 6: Stratigraphic position of the Retznei quarries according to Reuter et al. (2012). The correlation of the chronostratigraphy of Gradstein et al. (2012), the magnetostratigraphy and the calcareous nannoplankton (CNP) with the regional stages follows Piller et al. (2007). The lithostratigraphy is according to the stratigraphic chart of Austria (Piller et al., 2004). The grey line marks the radiometrically dated tuffitic layer reported in Bojar et al. (2004) and Handler et al. (2006).

The approximately 1-2 m thick lowermost part of the siliciclastics below the Leitha limestone build-up can be correlated to the *Helicosphaera ampliaperta* Zone (NN4) of Martini (1974) based on the continuous presence of *Helicosphaera ampliaperta* and *Sphenolithus heteromorphus* (Spezzaferri et al., 2002; Fig. 6). The upper part of the basal siliciclastics can be assigned to the zone NN5 (Hohenegger et al., 2009; Fig. 6). The overlying Retznei carbonate build-up is correlated with the sea level rise of the second Badenian transgression into the Central Paratethys (=TB 2.4 of Haq et al., 1988; Strauss et al., 2006; Reuter & Piller, 2011; Reuter et al., 2012; Fig.6) by Friebe (1993). *Helicosphaera waltrans* and *Sphenolithus heteromorphus* point to nannoplankton zone NN5 for the carbonates as well as for the overlying siliciclastics (Gross et al., 2007; Hohenegger et al., 2009; Reuter & Piller, 2011). For the base and the top of the exposed carbonate succession normal polarity is proven (Hohenegger et al., 2009). Benthic foraminiferal assemblages of the siliciclastic sediments above the Leitha Limestone body correspond to the typical fauna of the Lagenidae Zone (Hohenegger et al., 2009).

The study of the dinoflagellate cysts carried out by Soliman in Gross et al. (2007) indicates a middle Miocene (Badenian) age, based on the occurrences of *Cerebrocysta poulsenii*, *C. placacanthum*, *Habibacysta tectata*, *Labyrinthodinium truncatum*, *Operculodinium*? *borgerholtense*, *Palaeocystodinium miocaenicum* and *Unipontidinium aquaeductum.* Radiometric dating of a tuff layer with black biotite and sandine on top of the limestones using the $^{40}Ar/^{39}Ar$ method indicates a depositional age between 14.21 ± 0.07 and 14.39 ± 0.12 Ma (Bojar et al., 2004; Handler et al., 2006) and correlates with polarity chron C5ADn (Hohenegger et al., 2009; Fig. 6).

4. Material and Methods

4.1 Lithology and sampling

The studied sections from the Retznei quarries were logged and sampled in spring 2001 during a collaborative field course by the Institute of Earth Sciences of the University of Graz and the Natural History Museum Vienna. The graphics of both the Old quarry section and the Rosenberg quarry section are based on previous studies of the Retznei quarries (e.g. Hohenegger et al., 2009; Strahlhofer, 2013). The investigated material of the present study is stored in the collection of the Institute of Earth Sciences at the University of Graz.

4.2 Geochemical proxies

In the present study the geochemical measurements of the bulk sediments (total carbon (TC), total organic carbon (TOC), sulfur content (S), stable isotopes) from Strahlhofer (2013) were utilised for the reconstruction of the depositional environment.

Sulfur mainly reflects the degree of sulfate-reducing bacterial activity and serves as an indicator of bottom-water oxygenation (Peters et al., 2005).

The content of **TOC** is an indicator for the quantity of organic matter (OM) in a given sample (Hunt, 1996). The preservation of OM is suggested to be more important for TOC than the production of OM by many authors, as there is no systematic correlation of primary production and TOC observed in present oceans (Demaison and Moore, 1980; Peters et al., 2005). The origin of the OM (terrestrial/marine), the sedimentation rates, the amount of bioturbation and the oxygenation of the bottom-water column and the sediment are controlling factors for the preservation of TOC (Demaison & Moore, 1980; Hunt, 1996; Peters et al., 2005). Thus, the highest TOC values are expected in deposits of anoxic environments (Schulz and Zabel, 1999).

The **TOC/S** ratio is commonly used as an index value for coastal runoff and bottom-water oxygenation. Studies suggest that a ratio <2.8 reflects dys- to anoxic conditions, while values >2.8 are related to increased coastal runoff and input of terrestrial organic matter (Berner and Raiswell, 1983; Berner, 1984; Schulz and Zabel, 1999).

$\delta^{18}O$ mainly depends on temperature and salinity (Wefer et al., 1999). Kinetic isotopic fractionation occurs during the evaporation of sea water and the condensation of rain water (Marshall, 1992). Increased $\delta^{18}O$ values in sea water are indicative for phases of cold climate, because relatively more ^{16}O gets trapped in continental ice sheets. Vice-versa, low $\delta^{18}O$ values are indicative for increased freshwater influx and decreased salinity as freshwater is enriched by light ^{16}O (Wefer et al., 1999). In general, meteoric waters show more negative isotopic values than sea water (Marshall, 1992).

$\delta^{13}C$ is commonly used as an indicator for primary productivity (Marshall, 1992). Isotopic fractionation occurs during photosynthesis: ^{12}C gets preferably fixed, thus removing it from surface waters. Therefore, the residual DIC gets enriched with ^{13}C (Marshall, 1992). However, in upwelling areas this pattern might be overwritten by the reintroduction of ^{12}C to the surface waters through upwelled bottom waters, resulting in a more negative isotope signature compared to other eutrophic areas (Wefer et al., 1999).

4.3 Micropaleontological sample preparation

The sample treatment for micropaleontological investigation was carried out by Strahlhofer (2013). At least 100 g of dried sediment material from each of 65 samples of the two sections were treated with gasoline (60/95) for 30 minutes. Afterwards, the gasoline was filtered out and the samples were soaked with about 60°C warm water. After several hours the samples were wet-sieved under running tab water and split into the fractions 60-125 µm, 125-250 µm, 250-500 µm and >500 µm. Four samples (R01, R03-05) did not disintegrate and weren't further treated. After the remaining material of each sieve was dried in an oven at 50°C, the grain-size fractions were weighed to determine the sand content.

4.4 Ostracod treatment and their paleoecological application

The size fractions 250-500 µm and 125-250 µm were investigated in terms of their ostracod content using a Zeiss Discovery V8 light microscope. Because of the rare occurrence of ostracods, the whole material was picked out to get a reasonable sample size. Carapaces were counted as two valves (Aranki, 1987; Gross, 2002). Besides the ostracods, the studied samples contained a small number of echinoid spines and mollusc debris as well as a high quantity of foraminifers.

The identification of the ostracods was carried out at least to the genus level. Ostracods are very sensitive to changes of environmental factors (salinity, temperature, substratum and water-depth; van Morkhoven, 1962, 1963; Hinz-Schallreuter & Schallreuter, 1999; Gross, 2006). These factors are often reflected in the structural details of the ostracod valves (van Morkhoven, 1962). The thickness of the shells, their ornamentation and the branching of the marginal pore canals usually increases with salinity and the size of the ostracods can be indicative for the temperature: reduced growth rates are related to increased temperatures (van Morkhoven, 1963). Marine ostracod faunas can be differentiated into three ecological types of different bathymetric ranges: *littoral*, *shallow marine* (epi- and ?infra-neritic) and *deep marine* (bathyal, ?abyssal; van Morkhoven, 1962). Each of these types is characterised by a number of genera. However, other genera (e.g., *Cytherella*) are not restricted to a bathymetric range and can be encountered in many depths in marine environments (van Morkhoven, 1963).

Due to transport mechanisms, littoral and shallow marine assemblages may overlap towards the shallow marine zone, thus the differentiation between littoral and shallow marine assemblages can be rather difficult in paleoecological studies (van Morkhoven, 1962). In addition, there is no conspicuous structural detail that allows distinguishing littoral forms from shallow marine ones (van Morkhoven, 1962). However, certain genera of both groups exhibit structural features that are uncommon in both deeper marine and fresh to brackish water assemblages. These structural features are: heavy ornamentation, a strong amphidont hinge, conspicuously branching marginal pore canals and a well-developed eye spot (van Morkhoven, 1962). Accordingly, deeper marine assemblages comprise mainly thin-shelled, translucent, mostly unornamented species, rarely with well-developed hinge teeth, like in *Cytherella* and *Krithe* (van Morkhoven, 1962). However, such faunas may also include more ornamented genera like *Henryhowella* (van Morkhoven, 1962). The relationship between the substratum and the carapace was observed by Elofson (1941) and summarised by van Morkhoven (1962), showing the following trend:

- Species that mainly live on plants have mostly thin-shelled, hyaline, elongate, more or less laterally compressed, weak-hinged carapaces.
- The same type of carapace is often found in the few species that live exclusively in very coarse-grained bottom sediments.
- Burrowing species show a twice as high percentage of smooth forms than species living on top of the sediment.
- As a rule, burrowing species have a stronger calcified carapace than non-burrowing benthic forms.
- Species that crawl over the surface often show a pronounced flattening of the ventral surface of the carapace.
- Regarding size, species living on or in sandy sediments are generally shorter than plant-dwelling forms; the largest forms are found living on soft mud.

A detailed description of the ostracod taxa identified in samples from the Old quarry and the Rosenberg quarry is given in chapter 8 “Ostracod systematics".

Due to the low quantity and the poor preservation of the ostracod specimens and in order to create a confident statistical analysis and paleoecological reconstruction, the following taxa were combined into following genera:

Aurila = *Aurila punctata*, *Aurila* cf. *punctata, Aurila* sp., cf*. Aurila, Senesia* cf. *cinctella* (*Senesia cinctella* was previously assigned to the genus *Aurila* and has similar ecological demands; Gross, 2006)

Buntonia = *Buntonia brunensis*, *Buntonia* cf. *brunensis*

Cytherella = *Cytherella* aff. *compressa*, *Cytherella* aff. *russoi, Cytherella* cf. *cercinata*, *Cytherella* sp.

Cytheridea = *Cytheridea acuminata*, *Cytheridea* aff. *acuminata*

Krithe/Parakrithe = *Krithe* aff. *compressa*, *Krithe* sp., *Parakrithe* cf. *soustonsensis*, *Parakrithe* sp. (*Krithe* and *Parakrithe* have similar ecological demands)

Loxocorniculum = *Loxocorniculum hastatum*, *Loxocorniculum* cf. *hastatum*, cf. *Loxocorniculum*

4.5 Statistical analysis

To allow a better comparison between samples with highly variable ostracod content, the total ostracod abundance was transformed into relative abundance data. Statistical analysis of the data was carried out utilising the software PAST v3.14 (2016). For the identification of ostracod assemblages, cluster analysis (CA) applying Ward´s method and non-metrical multidimensional scaling (NMDS; Bray-Curtis similarity) were used. Samples that contained only one taxon were excluded from the statistical dataset (Shi, 1993; samples: R01/06, R01/08, R01/15, R01/17, R01/18 and R02/17). CA merges the samples into groups through hierarchical clustering (Hammer et al., 2001; http://folk.uio.no/ohammer/past/). NMDS plots the results in an n-dimensional space, where the distances between the samples document the faunistic similarity (Clarke & Ainsworth, 1993). In practice, CA and NMDS often give very similar groupings (Murray, 2006). To assess which taxa are primarily responsible for the observed differences between the clusters, a similarity percent analysis (SIMPER) was performed using the Bray-Curtis similarity measure (Clarke, 1993). In addition, the values of the geochemical proxies were correlated with the total abundance of each ostracod taxon in the respective samples using the linear correlation coefficient (Pearson's r; probability value $p < 0.05$). It is important to note that correlation does not imply causation in either direction, but may be due to both variables being dependent on a common, third cause (Hammer & Harper, 2006).

In order to correlate the taxa with the proxies, it is necessary that they occur in a minimum of three samples. Due to this, 5 out of 15 taxa allowed a correlation with the proxies.

5. Ostracod systematics

The subsequent ostracod systematic and the description, ecology and occurrence mostly follow Gross (2006). For terminological explanations see appendix 1, App.1 Fig. 1 – 4.

Subclass Ostracoda LATREILLE 1806
Order Podocopida MÜLLER 1894
Suborder Platycopa SARS 1866
Family Cytherellidae SARS 1866
Genus *Cytherella* JONES 1849

Cytherella* aff. *compressa (MUENSTER 1830)
Plate 1 Fig.: 1, 2, 5

Description: The general shape of the valves in lateral view resembles an elongated oval and the posterior as well as the anterior margin is almost evenly rounded in a wide arc, while the anterior margin appears to be slightly asymmetrically rounded. The dorsal margin of the valve is mostly straight, but can appear slightly convex in few specimens, and the ventral margin is straight. Both margins run approximately parallel to each other. The surface of the valves in general is smooth and does not show significant details except for a few papillae that appear to be randomly scattered.
The inside of the pictured right valve exhibits a distinct contact sulcus that runs parallel to the entire outer margin. The selvage of the other valve interlocks with this contact sulcus.
In dorsal view, the anterior end is rounded while the posterior end is tightly rounded. From the anterior end the outline of the valve runs in an arc, which is very evenly shaped, almost until the posterior end. There, the outline bends and continues almost straight towards the posterior end.
In general, it can be observed that the carapaces are the broadest in the posterior part, and the maximum height is reached slightly after half of the carapace's length, while the greatest length can be seen at the half height of the valve.

Remarks: The form of the outline in dorsal and lateral view as well as the carapace surface are very similar to the specimens described by Gross (2006: 15-17; pl. 1, figs. 1-4, 9-11; pl. 2, figs. 1-4), although they are slightly more rounded, but still less rounded than *Cytherella* aff. *compressa* in Ducasse & Cahuzac (1996: 257, pl. 1, fig. 2).
If no further specification was possible because of the fragmentary character of specimens, missing distinctive characteristics or no comparable description of specimens, the general nomenclature *Cytherella* sp. was chosen. Highly deformed specimens showing structural features that make an affiliation to *Cytherella* probable were named cf. *Cytherella* (see appendix 2; App. 2 Tab. 1-2).

Ecology: In general, *Cytherella* is a eury-bathic filter feeder in marine (seldom brackish) waters (van Morkhoven, 1963; Hartmann, 1975; Gross, 2006). Their appendage morphology is adjusted to a life as filter feeders (Hartmann, 1975; Boomer & Whatley, 1992), allowing enhanced water circulation within the carapace so that specimens of *Cytherella* can survive in areas and during times of low oxygen levels (Boomer & Whatley, 1992; Aiello et al., 1996; Gross, 2006).
Ducasse & Cahuzac (1997) and Gross (2006) describe *Cytherella* aff. *compressa* as a circa-littoral to epi-bathyal form that only seldom inhabits coastal areas or environments influenced by brackish water.

Occurrences in the Paratethys area and/or during the Miocene: According to Gross (2006), *Cytherella* aff. *compressa* occurs in the middle Miocene (Badenian) of eastern and southern Austria (Roemer, 1839; Reuss, 1850; Cernajsek, 1972; Huber-Mahdi, 1984; Gross, 2006). In addition, it occurs in the ?lower Burdigalian to middle Miocene (Langhian) in southwestern France (Moyes, 1965; Ducasse & Cahuzac, 1996).

***Cytherella* sp.1**

Plate 1 Fig.: 3, 4, 6

Description: The shape of the valves is basically that of an elongated oval that appears to be slightly rectangular. Both the anterior and the posterior margins are evenly but slightly asymmetrically rounded. The dorsal and ventral margins run parallel to each other with the dorsal margin being straight to slightly convex and the ventral margin being straight.

The surface of the carapace is covered with papillae that appear to have a concentrical arrangement close to the whole margin, whereas they are more randomly scattered in the central part. Except for this aspect, the surface is smooth.

Because of the filling of the valves, the inner characteristics could not be described with the exception of an only faintly visible contact sulcus at the ventral margin.

The anterior end in dorsal view is slightly rounded and acuminate, while the posterior end is rounded in a wider arc and has a slightly blunt appearance. Between the anterior fifth and the posterior third of the valve, where the outline runs in an even arc towards both the anterior and posterior end, the outline is straight.

In dorsal view, the carapace shows its greatest width at the beginning of the posterior fourth of the valve. In lateral view, the greatest height of the valve is reached approximately at half the length of the carapace and the greatest length occurs at the half height of the carapace.

Remarks: *Cytherella* sp. 1 differs from *Cytherella* aff. *compressa* regarding the shape of the ventral margin and the steeper posteroventral angle. *Cytherella* aff. *compressa* has papillae in the posterior part that are missing in *Cytherella* sp. 1, which in reverse has more prominent simple normal pores.

Specimens that are too poorly preserved for a confident identification as *Cytherella* were named cf. *Cytherella* (see appendix 2; App. 2 Tab. 1-2).

Ecology: Due to the co-occurrence with *Cytherella* aff. *compressa*, it is assumed that *Cytherella* sp. 1 has similar ecological demands.

Cytherella* aff. *russoi SISSINGH 1972

Plate 2 Fig.:1, 2, 4

Description: In lateral view the valves show a pronouncedly ovate shape. The anterior and posterior margins are slightly asymmetrically rounded in a wide arc. The dorsal margin is convex to straight in the central part, the ventral margin is convex. Because of the ovate shape of the valves, both the dorsal and the ventral margin are the straightest in a spatially very restricted central area and then soon start to converge towards both ends.

Aside from a few papillae in the posterior and ventral part of the valves the surface of the carapace is smooth. These papillae are only visible on a few specimens, which is most likely due to bad preservation. The wrinkles that were observed on most of the specimens' surfaces are probably caused by surface corrosion.

The inner characteristics could not be described as no single valves were found.

The anterior end of the valves in dorsal view is acuminate while the posterior end is evenly rounded. The outline broadens from the anterior end towards the beginning of the posterior third of the valve, then progressively decreases towards the posterior end. The planar indentation of the surface on both sides of the hinge is a remarkable feature.

The greatest width of the valve is reached at the beginning of its posterior third. The greatest height in lateral view can be seen in the middle section, the greatest length occurs at the half height of the carapace.

Remarks: The outer morphological characteristics are very similar to *Cytherella* aff. *russoi* described by Gross (2006: 17-18; pl. 1, figs. 5-8, 12-15; pl. 2, figs. 5-10), but the specimens appear to be slightly rounder, but less rounded than *Cytherella russoi* described by Sissingh (1972: 69; pl. 1, figs. 10, 11) and Aiello et al. (1996: 184; pl. 4, figs. 5-8, 11). *Cytherella* aff. *russoi* is smaller and more ovate-shaped than *Cytherella* aff. *compressa* and *Cytherella* sp. 1.

Ecology: In the studied sections *Cytherella* aff. *russoi* occurs together with *Cytherella* aff. *compressa* and is supposed to have comparable environmental demands (see above).

Occurrences in the Paratethys area and/or during the Miocene: According to Gross (2006), *Cytherella* aff. *russoi* occurs during the ?late Miocene of Crete (Sissingh, 1972), the ?early to middle Miocene of Sardinia (Bonaduce & Russo, 1985) and the middle Miocene (Badenian) of eastern and southern Austria (Gross, 2006).

Cytherella* cf. *cercinata AIELLO et al. 1996

Plate 2 Fig.: 3, 5

Description: In lateral view the valves have a more pronounced rectangular shape. The ventral margin and the dorsal margin are almost parallel to each other, but the dorsal margin increases slightly towards anterior. The anterior and the posterior margin are evenly rounded in a wide arc, although the arc of the posterior margin is comparatively narrower. In addition, there is a protrusion of the posteroventral lamella visible at the left valve.

The anterior part of the carapace usually shows a reticulation parallel to the margin, but these features are missing in the depicted specimens, which is probably due to the corrosion of the surface.

The outline of the pictured carapace resembles a rectangle with rounded anterior and posterior ends. The anterior end is slightly acuminate, the posterior end is evenly rounded. Between the anterior fourth and the posterior eighth of the valve the outline runs in an almost straight line.

The greatest width of the valves in dorsal view is reached in the posterior fourth, although the width is almost constant throughout the section where the outline runs in a straight line. In lateral view, the greatest height is reached close to the beginning of the anterior fourth of the valve and the greatest length can be observed at half the height of the valve.

Remarks: Based on the prominent posteroventral lamellar protrusion and the anterior rim of the specimens found in the samples, the differentiation between *Cytherella* cf. *cercinata*, *Cytherella* aff. *compressa*, *Cytherella* aff. *russoi*, and *Cytherella* sp. 1 was considered appropriate. In addition, the found specimens differ from *Cytherella pestiensis postdenticulata* OERTLI 1961 in terms of their more rectangular outline in dorsal view and the different shape of the posterior part, as specimens of *Cytherella pestiensis postdenticulata* have a more lanceolate shape, the anterior part is more pointed and the posterior part is more acutely rounded (Aiello et al., 1996). Therefore, the name *Cytherella* cf. *cercinata* was chosen.

Ecology: In the studied sections *Cytherella* cf. *cercinata* occurs together with *Krithe* and *Henryhowella*. The co-occurrence of these taxa is also described by Gebhardt (2009), who assumes a deeper marine environment.

Occurrences in the Paratethys area and/or during the Miocene: Sissingh (1972) postulated a middle to late Miocene age. *Cytherella* cf. *cercinata* occurs during the (?Serravallian) Tortonian and Pliocene of Crete (Aiello et al., 1996). Gebhardt et al. (2009) and Wessely et al. (2007) described *Cytherella cercinata* as part of Badenian ostracod assemblages in eastern Austria.

Genus *Cytherelloidea* ALEXANDER 1929

***Cytherelloidea* sp.**

Plate 3 Fig.:1, 2, 3

Description: In lateral view the valves have an elongated oval and slightly rectangular shape. The anterior and posterior ends are evenly rounded, but the anterior end is more oblique and the posterior end is more narrowly rounded. The dorsal margin is almost straight while the ventral margin is concave in the central part.

The surface of the valve is highly ornamented, shows a reticulation with oval-elongate meshes. The valves are thick-shelled and no eye tubercle is visible.

There is a contact sulcus parallel to the margins of the valve. Further inner characteristics could not be observed because the valves were filled with sediments.

In dorsal view the outline has a sub-rectangular shape. The anterior end is evenly rounded and slightly acuminate, whereas the posterior end appears to be angular. From the anterior end the outline rapidly runs outward until the anterior eighth of the valve, it then continues slightly concave until the end of the anterior third of the valve. Afterwards, the outline forms a straight and slightly diverging line until the posterior eighth of the valve, from where it rapidly decreases in a slightly convex arc towards the posterior end.

The greatest width in dorsal view is visible in the posterior eighth, the greatest height is reached close to the end of the anterior fourth of the valve and the greatest length can be seen at half height of the valve.

Remarks: Because of the state of preservation of the specimens and resulting uncertainties, a more precise classification than *Cytherelloidea* sp. was not reasonably possible.

Ecology: Preferentially, *Cytherelloidea* inhabit marine environments with warm and shallow waters, but they are sometimes also found in brackish (mesohaline) environments (van Morkhoven, 1963).

Occurrence: They occur from the Jurassic to recent times (van Morkhoven, 1963).

Suborder Podocopa SARS 1866

Superfamily Cytheracea BAIRD 1850

Family Cytherideidae SARS 1925

Subfamily Cytherideinea SARS 1925

Genus *Cythereidea* BOSQUET 1852

Cytheridea acuminata BOSQUET 1852

Plate 4 Fig.: 1, 2, 5

Description: In lateral view, the shape of the carapace resembles a trapeze. The anterior margin is rounded and the posterior margin is straight to a little convex and declines steeply towards the posterior end. The dorsal margin descends from the anterior to the posterior cardinal angle and the ventral margin is straight but shows a retraction in the middle section.

The surface of the valves is ornamented with a network of oval pits. Close to the margins they are arranged in concentrical rows which are separated by ridges, while they appear to be irregularly arranged in the central part. An eye tubercle is not present. At the anteroventral and anterocentral margin better preserved specimens exhibit 6 to 7 spines.

The hinge is amphidont-heterodont and little teeth can be seen in the bar and hinge groove of the right valve. In addition, an inner lamella is visible, which shows a distinct reduction at the concavity of the ventral margin, while it reaches its greatest width in the anterior part.

In dorsal view, the anterior as well as the posterior end shows a distinct truncation. The outline broadens in two steps from the anterior end towards the middle of the valve. From there it runs in an almost straight line towards close to the posterior end, where it steeply bends in an obtuse angle. Additionally, a few of the anterocentral spines can be observed at well-preserved specimens.

The greatest width of the valves in dorsal view occurs close to half of their height. The greatest width is reached in the posterior third at the posterior cardinal angle and the greatest length is achieved half-height of the valve.

Remarks: The shape of the outline in dorsal and lateral view, the carapace surface and inner morphological characteristics are almost identical to *Cytheridea acuminata* described by Gross (2006: 29-30; pl. 11, figs. 1-4, 7-13; pl. 13, figs. 9-10).
Many of the specimens have the characteristic spines on the anterior and posterior margin, though on some specimens these spines are broken off, probably due to transport damage.
On specimens named *Cytheridea* aff. *acuminata* (see appendix 2; App. 2 Tab. 1-2) spines were not observed. Also, the posterodorsal angle and the posteroventral angle differ slightly in comparison to *Cytheridea acuminata*. The dorsal margin is slightly straighter and the posterior margin is more rounded compared to *Cytheridea acuminata*. The posteroventral area is more rounded as well and ascends less steeply towards the posterocentral area.

Ecology: According to van Morkhoven (1963) and Hartmann (1975), *Cytheridea* usually inhabit brackish to epi-neritic environments.
According to Gross (2006), the recent species *Cytheridea neapolitana* KOLLMANN 1960 is comparable to *Cytheridea acuminata.* While preferring sandy pelite (Bonaduce et al., 1976), this species is found in all types of sediments (Montenegro et al., 1998). It inhabits the infra- to upper circa-littoral (5 to 90 metres; Montenegro et al., 1998), and its abundance maxima lie between 20-60 m in the Adriatic Sea (Breman, 1976).

Occurrences in the Paratethys area and/or during the Miocene: According to Gross (2006), *Cytheridea acuminata* occurs during the middle Miocene (Badenian) of eastern Austria (Reuss, 1850; Bosquet, 1852; Goerlich, 1953; Oertli & Key, 1955; Oertli, 1956; Kollmann, 1960; Huber-Mahdi, 1984, Gross, 2006). It is also described from the upper Miocene (Tortonian) of Crete (Sissingh, 1972).

Family Krithidae MANDELSTAM 1960

Genus *Krithe* BRADY, CROSSKEY & ROBERTSON 1874

Krithe* aff. *compressa SEGUENZA 1880

Plate 5 Fig.:1, 2, 5, 6

Description: In lateral view the valves have an elongate-oval form. The anterior margin is evenly rounded, whereas the posterior margin is asymmetrically rounded and truncated at the posterior end. The dorsal margin is straight to slightly convex and the ventral margin is straight but shows a concavity in its middle section.

The surface of the carapace is completely smooth, does not show any ornamentation or spines, and an eye tubercle is missing. The valves are thin-shelled and well preserved shells are translucent.

A selvage is visible which mostly runs near the outer margin, only in the posterior part it is more distant from it.

The outline of the carapace in dorsal view is elongate-oval, it runs in an almost even arc from the anterior to the posterior end. The anterior end is acuminate to pointed and the posterior end is truncated and shows an indentation. The larger left valve overlaps the right valve.

The greatest width is reached at half of the valve. The greatest length in lateral view is reached a little bit below half of the valve's height and greatest height is reached in the middle of the valve.

Remarks: *Krithe* aff. *compressa* has similarities to *Krithe compressa* described by Ruggieri (1991), but due to the poor state of preservation, crystal growth on the valves and the filling of the valves, a more precise identification was not possible. *Krithe* sp. (see appendix 2; App. 2 Tab. 1-2) differs from *Krithe* aff. *compressa* by the missing indented posterior part. Based on the poor preservation of those specimens, a more precise classification than *Krithe* sp. was not reasonably possible. A substantial difference to distinguish *Krithe* sp. from *Parakrithe* cf. *soustonsensis* is the truncated posterior end of *Krithe sp*., which forms a steeper posterior slope, whereas the posterior end of *Parakrithe* cf. *soustonsensis* is more evenly rounded.

Ecology: All species of *Krithe* live infaunal as burrowers in soft substrate and are confined to fully marine waters with salinities above 35 PSU (Coles et al., 1994). *Krithe* is reported to have a wide depth range but primarily inhabits infra-neritic to bathyal environments (van Morkhoven, 1963) with reduced oxygen levels (Zhao & Whatley, 1997). In shallower areas *Krithe* is mainly cryophilic and confined to low-energy soft substrates (Coles et al., 1994). *Krithe* can feed on old organic matter (Didié et al., 2002).

Occurrences in the Paratethys area and/or during the Miocene: According to Aiello & Szczechura (2004), *Krithe compressa* is recorded from the middle Eocene to recent time in the Atlantic (Bold, 1968; Coles et al., 1994; Van Harten, 1995, 1996), in Neogene and Quaternary sediments of the Mediterranean area (Seguenza, 1880; Ruggieri, 1991; Dieci & Russo, 1965, 1967; Russo, 1969; Sissingh, 1972; Aiello et al., 2000; Aiello & Barra, 2001), and also from the lower Badenian of the Czech Republic (Ríha, 1989).

Genus *Parakrithe* BOLD 1958

Parakrithe* cf. *soustonsensis (MOYES 1965)

Plate 5 Fig.: 3, 4, 7

Description: The valves of *Parakrithe* cf. *soustonsensis* in lateral view have an elongate oval shape. The anterior margin is evenly rounded and the posterior margin is asymmetrically rounded, being tightly rounded in the lower half of the valve. The dorsal margin ascends from the end of the anterior fourth of the valve in an almost straight line towards the middle section of the valve, and then it progressively bends in a convex arc towards the posterior end and continues as the posterior margin. The ventral margin is straight.

Except for few normal pore canals that appear to be randomly scattered, the surface is smooth.

The inner lamella is the broadest in the anterior part. Further inner characteristics could not be determined because of the bad preservation of the valves.

The anterior end of the valves is very acuminate. From there the outline runs in a remarkably even arc towards close to the posterior end, where the outline bends more sharply.

The greatest width of the valve is reached slightly below half of its height, and in lateral view the greatest height can be observed close to half of its length and the greatest length slightly below half of its height.

Remarks: The shape of the outline in dorsal and lateral view as well as the carapace surface is very similar to *Parakrithe soustonsensis* figured in Ducasse & Cahuzac (1996: 259, pl. 2, fig. 4) and *Parakrithe* cf. *soustonsensis* of Gross (2006: 31-32; pl. 12, figs. 1-13).

Although several important characteristic features are missing, the identification as *Parakrithe* cf. *soustonsensis* was considered as consistent.

Specimens that were too poorly preserved to be confidently determined were named *Parakrithe* sp. (see appendix 2; App. 2 Tab. 1-2).

Ecology: *Parakrithe soustonsensis* commonly inhabits deep marine environments (infra- and circa-littoral to epi-bathyal; Carbonel, 1985; Aiello et al., 1993; Ducasse & Cahuzac, 1996, 1997). According to Gross (2006), the recent species *Parakrithe dimorpha* BONADUCE, CIAMPO & MASOLI 1976 is morphologically comparable to *Parakrithe soustonsensis*. *Parakrithe dimorpha* lives on pelitic substrate in circa-littoral and bathyal environments (Montenegro et al., 1998). In the studied sections *Parakrithe soustonsensis* frequently occurs together with *Krithe*; thus, similar environmental demands are probable.

Occurrences in the Paratethys area and/or during the Miocene: *Parakrithe soustonsensis* occurs during the middle Miocene (Badenian) of eastern Austria (Reuss, 1850; Cernajsek, 1972; Huber-Mahdi, 1984; Zorn, 2000; Gross, 2006) and the middle Miocene (Badenian) in the Czech and Slovak Republic (Brestenska & Jiricek, 1978; Ríha, 1983, 1984; Ríha & Odehnal, 1988).

Family Trachyleberididae SYLVESTER-BRADLEY 1948

Subfamily Buntoniinae APOSTOLESCU 1961

Tribe Buntiniini APOSTOLESCU 1961

Genus *Buntonia* HOWE 1935

Buntonia brunensis RIHA 1985

Plate 6 Fig.: 1, 2, 5, 6
Plate 12 Fig.: 1

Description: In lateral view the valves show an elongate shape that resembles a drop. The anterior margin is evenly rounded, whereas the posterior margin is slightly asymmetrically rounded and descends steeply. The dorsal margin close to the eye tubercle is a little bit convex, but afterwards it is almost straight until the posterior cardinal angle. The ventral margin is convex.

The surface of the valves is highly ornamented. Besides moderately numerous normal pore canals and an eye tubercle with an adjacent bulge, the surface shows numerous pits that are arranged in concentrical rows close to the margin, while they increase in size towards the central part of the valve. In addition to this, there are several ridges. About 4 ventrolateral ridges can be seen as well as a short minor ridge in the centre of the valve that runs towards posterior.

The internal structure of the valve shows an inner lamella that is the broadest in the anterior part. The central muscle scar field is observable as well. It consists of a v-shaped frontal scar and 4 elongate adductor scars arranged in a vertical line. The hinge of *Buntonia Brunensis* is of the amphidont-heterodont type, as its right valve shows an anterior hinge tooth followed by a roundish hinge groove, a crenulated bar as well as the posterior elongate, semi-oval hinge tooth.

In dorsal view the anterior end is acuminate and flattened. The posterior end is slightly acuminate and flattened as well, but in a lesser degree. The outline runs in an evenly rounded convex arc from the anterior towards the posterior end.

The greatest width can be seen in slightly below half the height of the valve. In lateral view, the greatest height is reached close to the eye tubercle and the greatest length at half-height of the valve.

Remarks: *Buntonia brunensis* found in the studied samples are almost identical to *Buntonia brunensis* described by Gross (2006: 32-33; pl. 13, figs. 1-8). The well preserved specimens show all distinctive inner and outer features and, thus, allow a confident determination. Specimens that show close similarities to *Buntonia brunensis* but are missing distinctive features because of the bad state of preservation were named *Buntonia* cf. *brunensis* (see appendix 2; App. 2 Tab. 1-2).

Ecology: *Buntonia* is a eurybathic genus, it inhabits marine environments at all depths and can even tolerate brackish conditions (van Morkhoven, 1963). *Buntonia brunensis* inhabits greater water depths (?upper bathyal; Ríha, 1985). Montenegro et al. (1998) suggest an infra-littoral to circa-littoral distribution for the similar *Buntonia sublatissima* (Gross, 2006).

Occurrences in the Paratethys area and/or during the Miocene: According to Gross (2006), *Buntonia brunensis* was found in the middle Miocene (lower Badenian) of the Czech Republic (Brestenska & Jiricek, 1978; Ríha, 1985) and the middle Miocene of Eastern Austria (Gross, 2006).

Tribe Costini HARTMANN & PURI 1974

Genus *Costa* NEVIANI 1928

Costa punctatissima RUGGIERI 1962

Plate 6 Fig.: 3, 4, 7

Description: In lateral view the valves have a rectangular shape. The anterior margin is evenly rounded in a wide arc; the posterior margin is straight to slightly concave in the upper section and convex in the lower, posteroventral section. The dorsal margin is straight to slightly concave, it descends from the eye tubercle towards the posterior cardinal angle, and the ventral margin is straight.

The surface of the carapace is highly ornamented with a distinct reticulation, showing a net of triangular to pentagonal meshes in between the ridges. On these ridges and meshes a moderate number of simple normal pore canals can be observed. Most prominent are the three longitudinal ridges (dorsal, median and ventral), but there are additional minor ridges like the short vertical one in the posterior section that runs from the median to the dorsal ridge. Additionally, there is a number of spines at the anterior and posteroventral margin. The eye tubercle below the anterior cardinal angle is clearly visible.

In dorsal view the anterior and the posterior ends appear to be truncated and the outline in between both ends is formed by the median ridge. The rows of spines at the anterior margin are only rudimentarily visible on most of the specimens.

The greatest width of the valves is reached at the posterior end of the median ridge. In lateral view, the greatest height is reached at the anterior cardinal angle, whereas the greatest length can be seen slightly below half the height of the valve.

Remarks: The distinctive outer features are almost identical to *Costa punctatissima* described by Gross (2006: 34-36; pl. 14, figs. 1-11), but the inner features could not be observed because of the bad state of preservation. Nevertheless, the identification as *Costa punctatissima* was considered to be justified.

Ecology: Van Morkhoven (1963) describes *Costa* as a marine neritic faunal element. Ducasse and Cahuzac (1996, 1997) suggest an infra- to circa-littoral environment for *Costa punctatissima*.

Because of their great similarity, Gross (2006) compares *Costa punctatissima* with the recent *Costa edwardsii* ROEMER 1838*,* which, according to Montenegro et al. (1998), lives on sandy pelite to pelite in infra-littoral and upper circa-littoral areas at depths between 5 and 110 m.

Occurrences in the Paratethys area and/or during the Miocene: According to Gross (2006), *Costa punctatissima* occurs during the middle Miocene (Badenian) in eastern Austria (Reuss, 1850; Ruggieri, 1962; van Morkhoven, 1963; Huber-Mahdi, 1984; Gross, 2006), the middle Miocene (Serravallian) to Pliocene in southwest France (Moyes, 1965; Carbonel, 1985; Ducasse & Cahuzac, 1997), the middle Miocene (Badenian) of the Czech Republic (Reuss, 1850; Riha & Odehnal, 1988) and the middle Miocene (middle Badenian) of south Poland (Reuss, 1850).

Subfamily Trachyleberidinae SYLVESTER-BRADLEY 1948

Tribe Trachyleberidini SYLVESTER-BRADLEY 1948

Genus *Henryhowella* PURI 1951

Henryhowella asperrima (REUSS 1850)

Plate 7 Fig.: 1, 2, 5
Plate 12 Fig.: 2, 3
Plate 13 Fig.: 1, 2

Description: The valves in lateral view are mostly elongate and rounded. The anterior margin is evenly rounded, whereas the posterior margin is slightly asymmetrically rounded. The dorsal margin is straight and descends from the anterior to the posterior cardinal angle, the ventral margin is straight.

The surface of the valves does not show an eye tubercle, but it is covered by a net of quadrangular to pentagonal meshes, several ridges and spines. The meshes, which are arranged concentrically in the anterior part of the valve, show spines at their corners with other meshes. The most notable spines are located close to the anterior cardinal angle, and additional rows of spines are located close to the margins of the valves. Furthermore, three major ridges can be observed (dorsal, median and ventral ridge), which are covered with more prominent and bigger spines. Pore canals are located on top of several spines.

The hinge of the specimens is of amphidont-heterodont type. The left valve shows a characteristic structure with an anterior groove followed by a hinge tooth, a crenulated hinge bar and another tooth groove. The inner lamella is the broadest in the anterior and posterior parts of the valve, whereas it shows a reduction where the ventral margin is slightly concave.

In dorsal view most of the outline is overlapped by spines. The anterior end appears to be acuminate and the posterior end is slightly truncated. The outline runs in a convex arc from the anterior to the posterior end.

The greatest width of the valves is reached slightly below their middle. The greatest height in lateral view can be observed at the anterior cardinal angle, the maximum length is reached at the half height of the valve.

Remarks: Specimens found in the prospected samples are almost identical to *Henryhowella asperrima* described by Gross (2006: 37-39; pl. 16, figs. 1-11). Because of the good preservation, all distinctive morphological features are visible and allow a confident determination.

Ecology: *Henryhowella asperrima* prefers circa-littoral to bathyal environments, primarily inhabits areas with water depths greater than 100 m (Kempf & Nink, 1993; Bonaduce et al., 1998, 1999). It is also described as an infaunal species that lives in the uppermost part of fresh, well-ventilated soft substrate with abundant supply of food (Kempf & Nink, 1993; Didié et al., 2002).

Occurrences in the Paratethys area and/or during the Miocene: According to Gross (2006), *Henryhowella asperrima* occurs worldwide since the Eocene until recent time (Bonaduce et al., 1999); in the Central Paratethys of eastern Austria it occurs in the middle Miocene (Badenian; Reuss, 1850; Cernajsek, 1972; Huber-Mahdi, 1984; Kempf & Nink, 1993; Zorn, 2000, Gross, 2006) and in the middle Miocene (Badenian) of the Czech and Slovak Republic (Brestenska & Jiricek, 1978; Riha, 1983; Malz & Jellinek, 1984; Riha & Odehnal, 1988).

Subfamily Phacorhabdotinae GRUNDEL 1969

Genus *Olimfalunia* RUGGIERI 1977

Olimfalunia* cf. *plicatula (REUSS 1850)

Plate 8 Fig.: 1, 2, 5

Description: In lateral view the valves have the shape of a rounded rectangle. The anterior margin is asymmetrically rounded in a wide arc, the posterior margin in the upper section is straight and in the lower section it is convex. The dorsal margin is straight and descends from the anterior to the posterior cardinal angle. The ventral margin is mostly straight but shows a slight concavity in the middle section.

Rounded ridges and pits of variable depth and size dominate the surface of the carapace, simple normal pore canals occur scatteredly. Close to the faintly developed eye tubercle several ridges start (a ventrolateral, median, longitudinal and dorsal ridge, respectively). Further subordinate ridges are visible in between the major ridges. Additionally, there are up to 11 little teeth in a row at the anteroventral margin and 4 bigger conical spines at the posterior end of the valve. Both of the latter features are mostly broken.

The inner lamella of most of the specimens is narrow and only broadens in the anterior part of the valve. If preserved, the central muscle scar field consists of 4 adductor scars and a v-shaped frontal scar.

The anterior as well as the posterior end show a truncation. In general the outline runs in a convex arc from the anterior to the posterior end, but the part between the anterior eighth and the middle of the valve is almost straight.

The greatest width in dorsal view is visible close to the middle of the valve. In lateral view, the greatest height can be observed below the anterior cardinal angle and the greatest length is achieved at half the height of the valve.

Remarks: Specimens found in the studied samples show close similarities to *Olimfalunia plicatula* described by Gross (2006: 39-41; pl. 17, figs. 1-10), but because of the bad state of preservation a more precise classification than *Olimfalunia* cf. *plicatula* was not reasonably possible.

Ecology: The ecological range of *Olimfalunia plicatula* reaches from the littoral-phytal to the epibathyal (Carbonel, 1985; Gross, 2006). Ducasse & Cahuzac (1996, 1997) describe *Olimfalunia plicatula* as part of infra-littoral to circa-littoral areas with brackish water influences.

Occurrences in the Paratethys area and/or during the Miocene: According to Gross (2006), *Olimfalunia plicatula* occurs during the early (?Ottnangian and Karpatian) to middle Miocene (Badenian) of eastern and southern Austria (Reuss, 1850; Kollmann, 1971; Huber-Mahdi, 1984; Zorn, 1998, 2000, Gross, 2006) and the early (Karpatian) to middle Miocene (Badenian) of the Czech and Slovak Republic (Reuss, 1850; Brestenska & Jiricek, 1978).

Subfamily Brachycytherinae PURI 1954

Tribe Brachycytherini PURI 1954

Genus *Pterygocythereis* BLAKE 1933

Pterygocythereis calcarata (BOSQUET 1852)

Plate 8 Fig.: 3, 4, 6

Description: In lateral view, the shape of the valve resembles an elongated oval with a straight dorsal and a bulgy ventral margin. The anterior margin is rounded in a wide arc whose axis of symmetry points towards the posterior cardinal angle. The posterior margin is mostly convex and overlapped by spines. The ventral margin exhibits a bulge-like shape, which is most prominent towards anteroventral. The dorsal margin is perfectly straight between the anterior hinge tooth and the posterior hinge groove.

The surface of the carapace shows a smooth microstructure ornamented with several rows of spatulate spines as well as singular spines. Above the prominent eye tubercle there is a post-ocular spine directed towards posterior, followed by a row of spatulate spines that overlap the central part of the dorsal margin. At the flattened posterior margin a row of 6 rounded spines is visible, most of which are broken. A ridge that is covered with a row of spatulate spines runs parallel to the anterior and ventral margin. In the central area of the valve there are a few singular spines.

The left valve indicates an amphidont-heterodont hinge type, as there is a rounded anteriomedian hinge tooth, a crenulated straight ledge and an elongated oval hinge groove. The inner lamella is the broadest in the anterior section, whereas it is not present in the area of the hinge and becomes narrow at the ventral concavity.

In dorsal view the valve appears to be relatively flat compared to most of the other pictured species. The most prominent features are the eye tubercle and several of the spatulate spines. The anterior and posterior ends are flattened, the anterior end clearly showing the mentioned ridge. In between both ends, the outline is overlapped by spines and shows an evenly rounded convex arc.

The greatest width is reached in the middle section, and in lateral view the greatest height is visible below the post-ocular spine and the greatest length is achieved at half-height of the valve.

Remarks: The shape of the outline in dorsal and lateral view as well as the surface morphology and the inner features are almost identical to *Pterygocythereis calcarata* described by Gross (2006: 41-43; pl. 17, figs. 11-14; pl. 18, figs. 1-10).

Ecology: *Pterygocythereis* is a marine species that avoids wave movements (= kymatophobic; Liebau, 1980). Gross (2006) compares *Pterygocythereis calcarata* with the living species *Pterygocythereis jonesii* BAIRD 1850, which has an ecological range from the infra- to circa-littoral and mainly inhabits sandy substrate (Montenegro et al., 1998). Its maximum abundance in the Adriatic is reported between 80 and 170 m (Bonaduce et al., 1976) or 40 to 100 m (Breman, 1976), but in protected areas it can also occur at water depths of up to 6 m (Liebau, 1980).

Occurrences in the Paratethys area and/or during the Miocene: According to Gross (2006), *Pterygocythereis calcarata* occurs in the middle Miocene (Badenian) of eastern Austria (Huber-Mahdi, 1984, 1986; Zorn, 2000; Gross, 2006) and the middle Miocene (Badenian) of the Czech and Slovak Republic (Brestenska & Jiricek, 1978; Riha, 1983).

uncertain subfamily

Genus *Occultocythereis* HOWE 1951

Occultocythereis* cf. *bituberculata (REUSS 1850)

Plate 7 Fig.: 3, 4, 6

Description: In lateral view the valve exhibits a straight dorsal and ventral margin. The anterior margin is evenly rounded and bordered by a prominent ridge.

The surface of the valves is of a smooth microstructure but shows several ridges and an eye tubercle. The most noticeable ridge at the anterior margin is followed by a wide sulcus. In the ventral section it shows a connection to the ventral ridge. The dorsal ridge starts at the eye tubercle. The posterior margin is also bordered by a ridge, but it could not be described in more detail because of the bad state of preservation.

In dorsal view the thickness of the central section of the carapace is striking, which is probably due to its broadening by the ridges that run parallel to the margins. As a result, both the posterior and anterior end appear to be truncated. From the anterior end the outline diverges in two steps until the beginning of the posterior third of the valve. There, the greatest width is reached. After this point, it sharply decreases in a concave arc towards the flattened area.

The greatest height can be observed at the anterior cardinal angle, the greatest length at the half height of the valve.

Remarks: The outer morphological features of *Occultocythereis* cf. *bituberculata* are very similar to *Occultocythereis bituberculata* described by Gross (2006: 44-45; pl. 19, figs. 4-6, 11). However, because inner features could not be observed due to lack of material and the bad preservation of the specimens, a more detailed identification than *Occultocythereis* cf. *bituberculata* was not reasonably possible.

Ecology: The ecological range of *Occultocythereis* lies mostly in epi-neritic, warm marine environments (van Morkhoven, 1963; Hartmann, 1975; Gross, 2006). The recently living species *Occultocythereis dohrni* PURI 1963 is comparable to *Occultocythereis bituberculata* (Triebel, 1961; Ruggieri, 1992; Gross, 2006). *Occultocythereis dohrni* is a form of the infra-littoral and the upper circa-littoral with maximum water depths of 30-107 m (Montenegro et al., 1998). Its frequency maximum is reported for fine-grained sediments (Uliczny, 1969).

Occurrences in the Paratethys area and/or during the Miocene: According to Gross (2006), *Occultocythereis bituberculata* occurs in the middle Miocene (Badenian) of eastern Austria (Reuss, 1850; Huber-Mahdi, 1984, Gross, 2006), the middle Miocene (Badenian) of the Czech and Slovak Republic (Reuss, 1850; Brestenska & Jiricek, 1978) and the middle Miocene (lower Badenian) of South Poland (Reuss, 1850)

Family Hemicytheridae PURI 1953

Subfamily Hemicytherinae PURI 1953

Tribe Aurilini PURI 1973

Genus *Aurila* POKORNY 1955

Aurila punctata (MUENSTER 1830)

Plate 9 Fig.: 1, 2, 5
Plate 12 Fig.: 4
Plate 13 Fig.: 5

Description: The anterior margin of the valve is asymmetrically rounded, the posterior margin above the caudal process is straight, and below this process it is convex. From anterior to posterior, the dorsal margin first is convex, then straight, whereas the ventral margin posteriorly is convex but shows a concavity in the anterior section.

The surface of the valves is covered with big pits, simple normal pore canals can be observed as well as a faintly developed eye tubercle. In the marginal regions the pits are arranged in a concentrical way, in general showing the tendency of becoming bigger towards posterior and being more roundish and isolated by broad walls (muri) in the centre of the valve.

The characteristic "*Aurila* tooth" can be seen in the posterior hinge groove of the left valve. The hinge itself is of amphidont-heterodont type. The central muscle scar field shows 4 adductor scars (5, as the second from the top actually consists of two separate ones) and 3 roundish frontal scars in a row.

The anterior as well as the posterior end in dorsal view is acuminate. Between both ends the evenly shaped outline mostly is convex (middle part) to straight (between middle part and both ends).

The greatest width is reached in the middle, whereas in lateral view the greatest length is achieved at the height of the caudal process and the greatest height is reached at the half length of the valve.

Remarks: The outer and inner distinctive features of the specimens found in the studied samples are almost identical to *Aurila punctata* described by Gross (2006: 56-57; pl. 29, figs. 10-11; pl. 30, figs. 1-8).
Specimens that show close similarities to *Aurila punctata* but are missing distinctive features due to the bad state of preservation were named *Aurila* cf. *punctata.* Specimens that did not allow any further differentiation than *Aurila* were named *Aurila* sp. Highly deformed specimens that show structural features that make an affiliation to *Aurila* probable were named cf. *Aurila* (see appendix 2; App. 2 Tab. 1-2).

Ecology: As reported by Gross (2006), *Aurila punctata* is similar to *Aurila convexa* BAIRD 1850, which is an infra to inner circa-littoral faunal element and lives on sandy pelite (Montenegro et al., 1998). Its maximum occurrences are documented between 20-40 m (Breman, 1976) or 50-70 m (Bonaduce et al., 1976).

Occurrences in the Paratethys area and/or during the Miocene: According to Gross (2006), *Aurila punctata* occurs in the middle Miocene (Badenian) of eastern Austria (Reuss, 1850; Cernajsek, 1971; Huber-Mahdi, 1984; Gross, 2006), the middle Miocene (Badenian) in Romania (Olteanu, 1971) and the middle Miocene (Badenian) in the Czech and Slovak Republic (Reuss, 1850; Brestenska & Jiricek, 1978; Riha, 1983).

Genus *Senesia* Jiricek 1974

Senesia* cf. *cinctella (REUSS 1850)

Plate 9 Fig.: 3, 4, 6

Description: The valve has an ear-like (auriculate) and elongate shape. The anterior margin of the right valve is asymmetrically rounded, whereas the posterior margin above the pronounced caudal process is concave, and below this process it is convex. From anterior to posterior, the dorsal margin first is straight to slightly concave, then straight to convex. The ventral margin is straight in the posterior section but shows a concavity in the anterior section just below the anterior cardinal angle.

The eye tubercle is faintly developed, and numerous little teeth are located at the posteroventral and anteroventral margin, although most of them were eroded and only stumps are visible. The surface of the carapace is covered by numerous small roundish pits in partly concentrical rows. In the central part of the valve these pits are bigger and appear more isolated.

The hinge appears to be amphidont-heterodont, but because of the bad preservation more details could not be obtained.

In dorsal view, both hinge teeth of the right valve are distinctive features. The anterior as well as the posterior end in dorsal view is acuminate. Between both ends the evenly shaped outline mostly is convex (middle part) to straight (between the middle part and both ends).

The greatest width is reached in the middle, whereas in lateral view the greatest length is achieved at the height of the caudal process and the greatest height is reached below the anterior cardinal angle.

Remarks: Distinctive outer and inner features of the specimens in the studied samples are almost identical to *Senesia cinctella* described by Gross (2006: 57-58; pl. 31, figs. 1-5).

The more elongate-auriculate shape of the *Senesia cinctella* carapace, its surface ornamentation as well as the numerous little teeth at the anteroventral margin are the characteristics that distinguish *Senesia cinctella* from *Aurila* specimens.

Ecology: *Senesia* has very similar ecological demands to *Aurila* (Gross, 2006). Cernajsek (1971) and Zorn (1998) described *Senesia cinctella*, *Senesia trigonella* and *Senesia vadaszi* from littoral and/or epineritic environments (Gross, 2006).

Occurrences in the Paratethys area and/or during the Miocene: According to Gross (2006), *Senesia cinctella* occurs in the middle Miocene (Badenian to lower Sarmatian) of the Czech and Slovak Republic (Reuss, 1850; Brestenska & Jiricek, 1978) and in the middle Miocene (Badenian) of eastern Austria (Cernajsek, 1971; Huber-Mahdi, 1984; Gross, 2006).

Tribe Oertliellini Liebau 1975

Genus *Grinioneis* LIEBAU 1975

Grinioneis* cf. *haidingeri (REUSS 1850)

Plate 10 Fig.: 1, 2, 3

Description: The valves have an elongated rectangular shape, the dorsal and ventral margins are straight and the anterior and posterior margins are rounded. The anterior margin is a little asymmetrically rounded, the posterior margin in the upper section is straight to concave and convex in the lower section.

A reticulation is visible on the surface of the valves, even though the specimens are badly preserved. Additionally, a pronounced eye tubercle is visible in the area of the anterior cardinal angle. A prominent ventral ridge can be seen that gains height towards posterior and terminates abruptly at the beginning of the posterior fourth of the valve.

In dorsal view, the carapace shows a broad rim in its centre at the contact of both valves, possibly caused by ridges bordering the margins. As a result, both ends appear to be flattened and truncated. Until the posterior fourth, the outline is formed by the ventral ridge. In ventral view some better preserved meshes are visible, showing a triangular to pentagonal structure.

The greatest width is reached at the termination of the ventral ridge. In lateral view, the greatest height is reached at the anterior cardinal angle and the greatest width a little below half the height of the valve.

Remarks: The shape of the outline in dorsal and lateral view as well as the carapace surface of *Grinioneis* cf. *haidingeri* found in the studied samples are very similar to *Grinioneis haidingeri* described by Gross (2006: 62-64; pl. 34, figs. 1-13). However, due to the poor preservation of the specimens the inner features were not visible; thus, a more precise classification than *Grinioneis* cf. *haidingeri* was not possible.

Ecology: *Grinioneis haidingeri* is an epi-neritic (infra- and ?circa-littoral) faunal element with a certain tolerance towards brackish waters (Aranki, 1987; Ducasse & Cahuzac, 1996, 1997; Gross, 2006).

Occurrences in the Paratethys area and/or during the Miocene: According to Gross (2006), *Grinioneis haidingeri* occurs in the lower Miocene (?Eggenburgian, Ottnangian) to middle Miocene (Badenian) of eastern Austria (Reuss, 1850; Huber-Mahdi, 1984; Malz & Jellinek, 1984; Zorn, 1995; Gross, 2006), the lower (Karpatian) to middle Miocene (Badenian) of the Czech and Slovak Republic (Brestenska & Jiricek, 1978) and the middle Miocene (Badenian) in Romania (Olteanu, 1971).

Family Loxoconchidae SARS 1925

Subfamily Loxoconchinae SARS 1925

Genus *Loxocorniculum* BENSON & COLEMAN 1963

Loxocorniculum hastatum (REUSS 1850)

Plate 11 Fig.: 1, 2, 3, 4

Description: The shape of the valve resembles an elongated oval, although the dorsal margin is straight. The anterior and posterior margin are asymmetrically rounded and the ventral margin is convex.

Even though the surface's sculpture is partly filled with sediments, a reticulation is visible, consisting of roundish meshes separated by broad ledges. An eye tubercle is visible close to the anterior cardinal angle, a short ridge or tubercle is located below the posterior cardinal angle. Most notably, there is a round, broad and acuminate tubercle in the posteroventral area.

In dorsal view, the prominent posteroventral tubercle dominates the outline, which continuously increases in a slightly convex arc from the acuminate anterior end towards the end of the tubercle. Afterwards, the outline sharply decreases towards the highly pointed posterior end. In addition to this, the short ridge or tubercle close to the posterior cardinal angle is a prominent feature and has an eye-like shape when looking at the whole carapace.

The greatest width is reached at the posteroventral tubercle. In lateral view, the greatest height is reached close to the eye tubercle, whereas the greatest length can be observed a little above half the height of the valve.

Remarks: Specimens found in the studied samples are almost identical to *Loxocorniculum hastatum* described by Gross (2006: 74-76; pl. 42, figs. 1-10; pl. 43, figs. 7, 10-11) in shape of the outlines in dorsal and lateral view as well as the carapace surface. Because of the poorly preserved specimens, the hinge and other inner characteristics could not be observed.

Although the inner characteristics could not be observed because the valves were sediment-filled, the identification of these specimens as *Loxocorniculum hastatum* based on the observable, distinct characteristics is considered to be certain and follows Gross (2006).

Specimens which show close similarities to *Loxocorniculum hastatum*, but are missing distinctive features because of the bad state of preservation, were named *Loxocorniculum* cf. *hastatum.* Poorly preserved specimens which show structural features that make an affiliation to *Loxocorniculum* probable were named cf. *Loxocorniculum* (see appendix 2; App. 2 Tab. 1-2).

Ecology: Ducasse & Cahuzac (1996, 1997) suggest *Loxocorniculum hastatum* as an epi-neritic (infra-littoral) species with a certain tolerance for reductions in salinity (Mitrovic, 1998; Gross, 2006).

Occurrences in the Paratethys area and/or during the Miocene: According to Gross (2006), *Loxocorniculum hastatum* occurs in the lower Miocene (Ottnangian, Karpatian) and middle Miocene (Badenian) of eastern Austria (Reuss, 1850; Kollmann, 1971; Cernajsek, 1974; Brestenska & Jiricek, 1978, Huber-Mahdi, 1984; Zorn, 1998; Gross, 2006) and the lower Miocene (Karpatian) to middle Miocene (Badenian) in the Czech and Slovak Republic (Reuss, 1850; Riha & Odehnal, 1988).

Family Xestoleberididae SARS 1928

Genus *Xestoleberis* SARS 1866

***Xestoleberis* sp.**

Plate 11 Fig.: 5, 6, 7

Description: The valves in lateral view exhibit a shape that resembles an oval, as all of the margins are mostly convexly rounded, with the exception of the almost straight posterior part of the dorsal margin and a little concavity at the posteroventral margin. The anterior margin is asymmetrically rounded in a broad arc and the posterior margin is evenly rounded in a narrower arc. The anterior part of the ventral margin is bulgy.

The surface of the valves is extraordinarily smooth, no eye tubercle or normal pores could be observed. A small ridge runs parallel to the dorsal and posterior margin.

The anterior end of the valves in dorsal view is slightly acuminate, whereas the posterior end is more rounded. The outline runs in a convex arc of variable curvature from the anterior to the posterior end. The whole carapace in dorsal view has a drop-like shape.

The valves show the greatest width at the beginning of the posterior third of the valves. In lateral view, the greatest height is reached shortly after the end of the anterior third of the valve and the greatest length can be seen at half the height of the valve.

Remarks: The shape of the outline in dorsal and lateral view as well as the carapace surface of the specimens of *Xestoleberis* found in the studied samples show similarities to *Xestoleberis tumida* described by Gross (2006: 85-86; pl. 48, figs. 1-10; pl. 49, figs. 1-5; pl. 51, fig. 7). However, because no isolated valves were found, it was not possible to observe the internal characteristics. Thus, the classification is given as *Xestoleberis* sp.

Ecology: *S*pecies of *Xestoleberis* are usually classified as phytal ostracods that mainly inhabit the photic zone (littoral and sub-littoral) and live on sandy substrate or algae. Some species also occur in brackish waters or in marine interstitial or bathyal habitats (Hartmann, 1975; Athersuch, 1976; Bonaduce & Danielopol, 1988).

Occurrences in the Paratethys area and/or during the Miocene: The specimens of *Xestoleberis* found in the samples show similarities to *Xestoleberis tumida* which occurs in eastern Austria during the early Miocene (Karpatian) to middle Miocene (Badenian and ?Sarmatian; Reuss, 1850; Huber-Mahdi, 1984; Zorn, 1998; Gross, 2006) and in the middle Miocene (Badenian) of the Czech and Slovak Republic (Brestenska & Jiricek, 1978).

6. Results

6.1 Ostracod distribution in the Retznei quarries

Out of the two studied sections from the Old quarry and the Rosenberg quarry, 61 samples were investigated in terms of their ostracod content. In comparison to the foraminiferan abundance, ostracods are very rare in the Retznei quarries. Altogether, 1206 valves were determined. 23 different ostracods taxa were identified. 1132 highly deformed valves and fragments remained undetermined.
A detailed distribution of the ostracods is reported in the Appendix.

6.1.1 Old quarry section

In five samples (R01/14 and R02/24-27) no ostracods could be determined or found. While samples R02/26 and R02/27 contained highly deformed valves, samples R01/14 and R02/24-25 did not contain any ostracods. In the remaining 43 samples, the number of taxa per sample varies between 1 and 11 (A = 4.32, σ = 2.46). The number of valves (v) per sample is highly fluctuating throughout the section. The number of determined valves per sample varies between 1 and 93 with an average of 23.97 and a standard deviation of 22.11. Taking the undetermined valves into account, the number of valves per sample varies between 1 and 187 (A = 57.53, σ = 39.71).
Sample **R01/02** from a marl layer within the carbonate complex at the base of the section (bed 02, fig. 2) contains *Parakrithe* sp. (4 v) and *Parakrithe* cf. *soustonsensis* (2 v); 7 valves remained undetermined.
Sample **R01/06** represents the top of the carbonate complex (bed 11, fig. 2) and contains *Cytherelloidea* sp. (4 v); 14 valves remained undetermined.
Sample **R01/07** contains *Henryhowella asperrima* (5 v), *Aurila punctata* (4 v), *Cytherella* sp.1 (4 v), *Grinioneis* cf. *haidingeri* (3 v), *Occultocythereis* cf. *bituberculata* (2 v) and *Senesia* cf. *cinctella* (1 v); 67 valves remained undetermined.
Sample **R01/08** originates from a tuffitic layer on top of the carbonate complex (bed 13, fig. 2) and contains only one valve of *Aurila sp.*

Sample **R01/09** represents the base of the clayey silt layers overlying the carbonate body (bed 14, fig. 2). It contains *Krithe* sp. (4 v) and *Parakrithe* cf. *soustonsensis* (2 v); 24 valves remained undetermined.

The samples **R01/10 – 12** also originate from bed 14 (fig. 2). Sample **R01/10** contains cf. *Cytherella* (2 v), *Cytherella* sp. (1 v) and *Henryhowella asperrima* (2 v); 15 valves remained undetermined. Sample **R01/11** contains *Henryhowella asperrima* (30 v), *Parakrithe* sp. (11 v), *Parakrithe* cf. *soustonsensis* (14 v), *Cytherella* sp. (6 v), *Krithe* aff. *compressa* (2 v), *Pterygocythereis calcarata* (3 v), *Buntonia brunensis* (2 v), *Costa punctatissima* (2 v), *Occultocythereis* sp. (2 v), *Xestoleberis* sp. (2 v) and *Cytherella* cf. *cercinata* (1 v); 36 valves remained undetermined. **R01/12** contains *Henryhowella asperrima* (14 v), *Cytherella* sp. (8 v), *Buntonia brunensis* (6 v), *Loxocorniculum* cf. *hastatum* (3 v), *Cytherella* cf. *cercinata* (2 v) and *Krithe* sp. (2 v); 21 valves remained undetermined.

Sample **R01/13** originates from a marly limestone layer (bed 15, fig. 2) and contains *Parakrithe* sp. (4 v); 48 valves remained undetermined.

Sample **R01/14** and **R01/15** were taken from a tuffitic layer (bed 16, fig. 2). In sample **R01/14** no ostracods were found. Sample **R01/15** has a very low ostracod content. Out of three found valves, one valve of *Henryhowella asperrima* could be determined.

Sample **R01/16** contains *Henryhowella asperrima* (8 v), *Krithe* sp. (3 v), *Costa punctatissima* (2 v), *Cytherella* cf. *cercinata* (2 v) and *Cytherella* sp. (2 v); 36 valves remained undetermined.

Sample **R01/17** was taken from a sandy layer (bed 18, fig. 2) and contains cf. *Aurila* (1 v) and *Aurila* sp. (1 v) and 9 valves remained undetermined.

Sample **R01/18** contains *Henryhowella asperrima* (1 v) and 32 valves remained undetermined.

Samples **R01/19 – 27** originate from a clayey silt layer (bed 22, fig. 2). Sample **R01/19** contains *Henryhowella asperrima* (14 v), *Krithe* aff. *compressa* (6 v), *Buntonia brunensis* (5 v), *Parakrithe* cf. *soustonsensis* (4 v) and *Pterygocythereis calcarata* (1 v); 43 valves remained undetermined. Sample **R01/20** contains *Henryhowella asperrima* (15 v), *Krithe* sp. (7 v), *Parakrithe* sp. (2 v) and *Buntonia brunensis* (1 v); 32 valves remained undetermined. Sample **R01/21** contains *Parakrithe* cf. *soustonsensis* (14 v), *Krithe* sp. (4 v), *Parakrithe* sp. (2 v), *Cytherella* aff. *compressa* (1 v) and

Henryhowella asperrima (1 v); 57 valves remained undetermined. Sample **R01/23** contains *Henryhowella asperrima* (11 v), *Parakrithe* sp. (6 v), *Krithe* sp. (4 v), and *Cytherella* cf. *cercinata* (2 v); 14 valves remained undetermined. Sample **R01/24** contains *Krithe* sp. (15 v), *Henryhowella asperrima* (7 v), *Cytherella* cf. *cercinata* (2 v) and *Pterygocythereis calcarata* (1 v); 35 valves remained undetermined. Sample **R01/25** contains *Parakrithe* cf. *soustonsensis* (8 v), *Henryhowella asperrima* (7 v), *Krithe* sp (6 v), *Occultocythereis* cf. *bituberculata* (4 v), *Cytherella* aff. *compressa* (2 v), *Costa punctatissima* (2 v), *Krithe* aff. *compressa* (1 v), , *Cytherella* sp. (1 v) and *Pterygocythereis calcarata* (1 v); 126 valves remained undetermined. With 187 valves, sample **R01/26** contains the highest ostracods quantity of the Old quarry section. It contains *Parakrithe* sp. (46 v), *Krithe* sp. (19 v), *Krithe* aff. *compressa* (13 v), *Buntonia brunensis* (6 v), *Cytherella* sp. (5 v) and *Cytherella* cf. *cercinata* (4 v); 94 valves remained undetermined. Sample **R01/27** contains *Krithe* sp. (12 v), *Parakrithe* sp. (6 v), *Krithe* aff. *compressa* (5 v), *Xestoleberis* sp. (2 v), *Parakrithe* cf. *soustonsensis* (2 v), *Buntonia brunensis* (2 v), *Cytherella* cf. *cercinata* (2 v) and *Henryhowella asperrima* (2 v); 51 valves remained undetermined.

The samples **R01/28** and **R01/29** originate from a sand layer (bed 23, fig. 2). Sample **R01/28** contains *Aurila punctata* (14 v), *Aurila* sp. (10 v), *Henryhowella asperrima* (3 v), *Loxocorniculum hastatum* (3 v), *Krithe* sp. (3 v), *Cytherella* sp.1 (2 v), cf. *Aurila* (1 v), Cytherelloidea sp. (2 v) and *Cytherelloidea* sp. (1 v); 88 valves remained undetermined. Sample **R01/29** contains *Aurila* sp. (50 v), *Aurila punctata* (25 v), *Cytherella* sp.1 (3 v), *Henryhowella asperrima* (2 v), *Loxocorniculum hastatum* (2 v), and *Cytherelloidea* sp. (1 v); 55 valves remained undetermined.

The samples **R02/05** and **R02/06** originate from a clayey silt layer (bed 25, fig. 2) which marks the base of sub-section R02. Sample **R02/05** contains *Parakrithe* sp. (8 v), *Krithe* sp. (5 v), *Henryhowella asperrima* (2 v), *Krithe* aff. *compressa* (2 v), *Krithe* sp. (2 v) and *Parakrithe* cf. *soustonsensis* (2 v); 9 valves remained undetermined. Sample **R02/06** contains *Krithe* sp. (30 v), *Henryhowella asperrima* (7 v), *Buntonia brunensis* (4 v), *Parakrithe* cf. *soustonsensis* (4 v), *Krithe* aff. *compressa* (2 v), Aurila sp. (1 v) and *Aurila punctata* (1 v); 25 valves remained undetermined.

Samples **R02/07 - 09** originate from bed 27, a clayey silt horizon (fig. 2). Sample **R02/07** contains *Krithe* sp. (20 v), *Krithe* aff. *compressa* (4 v), *Parakrithe* cf. *soustonsensis* (3 v)

and *Henryhowella asperrima* (2 v); 4 valves remained undetermined. Sample **R02/08** contains *Krithe* sp. (35 v), *Parakrithe* sp. (15 v), *Cytherella* aff. *russoi* (3 v), *Buntonia brunensis* (2 v), *Krithe* aff. *compressa* (2 v), *Parakrithe* cf. *soustonsensis* (2 v) and *Henryhowella asperrima* (1 v); 13 valves remained undetermined. Sample **R02/09** contains *Henryhowella asperrima* (11 v), *Krithe* sp. (8 v), *Buntonia brunensis* (4 v) and *Costa punctatissima* (2 v); 18 valves remained undetermined.

Sample **R02/10** originates from a sand horizon (bed 28, fig. 2). It contains *Henryhowella asperrima* (5 v), *Krithe* sp. (2 v), *Parakrithe* cf. *soustonsensis* (2 v) and *Buntonia* cf. *brunensis* (1 v); 36 valves remained undetermined.

Samples **R02/11 - 19** originate from a clayey silt layer (bed 29, fig. 2). Sample **R02/11** contains *Henryhowella asperrima* (11 v), *Krithe* aff. *compressa* (6 v), *Parakrithe* cf. *soustonsensis* (6 v), *Cytherella* sp. (3 v), *Olimfalunia* cf. *plicatula* (2 v) and *Parakrithe* sp. (2 v); 42 valves remained undetermined. Sample **R02/12** contains *Henryhowella asperrima* (21 v), *Parakrithe* sp. (6 v), *Parakrithe* cf. *soustonsensis* (4 v), *Buntonia brunensis* (4 v), *Cytherella* cf. *cercinata* (2 v), *Grinioneis* cf. *haidingeri* (2 v) and *Xestoleberis* sp. (2 v); 62 valves remained undetermined. Sample **R02/13** contains *Henryhowella asperrima* (4 v), *Olimfalunia plicatula* (2 v), *Parakrithe* cf. *soustonsensis* (2 v) and *Parakrithe* sp. (2 v); 25 valves remained undetermined. Sample **R02/14** contains *Krithe* aff. *compressa* (12 v), *Parakrithe* cf. *soustonsensis* (8 v), *Henryhowella asperrima* (7 v), *Krithe* sp. (2 v) and *Cytherella* cf. *cercinata* (1 v); 32 valves remained undetermined. Sample **R02/15** contains *Krithe* sp. (8 v), *Parakrithe* cf. *soustonsensis* (8 v), *Buntonia brunensis* (2 v) and *Henryhowella asperrima* (2 v); 28 valves remained undetermined. Sample **R02/16** contains *Cytherella* sp. (12 v), *Henryhowella asperrima* (11 v), *Parakrithe* sp. (8 v), *Xestoleberis* sp. (4 v), *Buntonia brunensis* (2 v) and *Cytherella* cf. *cercinata* (1 v); 17 valves remained undetermined. Sample **R02/17** contains *Henryhowella asperrima* (4 v); 33 valves remained undetermined. Sample **R02/18** contains *Henryhowella asperrima* (7 v) and *Krithe* aff. *compressa* (3 v); 49 valves remained undetermined. Sample **R02/19** contains *Krithe* sp. (8 v), *Parakrithe* sp. (6 v), *Henryhowella asperrima* (6 v), *Parakrithe* cf. *soustonsensis* (4 v) and *Cytherella* cf. *cercinata*. (3 v); 34 valves remained undetermined.

Samples **R02/20 – 22** originate from a clayey silt layer (bed 31, fig. 2). Sample **R02/20** contains *Cytherella* sp. (7 v), *Krithe* sp. (5 v), *Parakrithe* cf. *soustonsensis* (3 v) and

Henryhowella asperrima (2 v); 44 ostracod fragments remained undetermined. Sample **R02/21** contains *Henryhowella asperrima* (4 v), *Krithe* aff. *compressa* (3 v), *Krithe* sp. (3 v), *Cytherella* sp. (2 v) and *Cytherella* cf. *cercinata* (2 v); 41 valves remained undetermined. Sample **R02/22** contains *Cytherella* sp. (1 v) and *Henryhowella asperrima* (1 v); 38 valves remained undetermined.

Sample **R02/23** originates from a silty sand horizon (bed 33, fig. 2) and contains cf. *Aurila* (2 v) and *Cytherella* cf. *cercinata* (2 v); 47 valves remained undetermined.

Samples **R02/24 – 25** did not contain any ostracods at all, while samples **R02/26 – 27** only contain undetermined valves (24 in sample R02/26 and 16 in sample R02/27).

Sample **R02/28** from a silty sand horizon on the top of the old quarry section contains *Henryhowella asperrima* (2 v) and *Olimfalunia plicatula* (1 v); 12 valves remained undetermined.

6.1.2 Rosenberg quarry section

From 5 out of the 13 samples taken from the Rosenberg quarry section, no ostracods could be determined. While samples RB01/04 and RB01/11 did not contain any ostracods at all, samples RB01/01 – 02 and RB01/08 only contained undeterminable fragments and highly deformed valves.

In the remaining 8 samples, the number of taxa per sample varies between 1 and 12 (A = 4.12, σ = 3.6). The number of valves per sample is highly fluctuating throughout the section. The number of determined valves per sample varies between 2 and 94 (A = 21.87, σ = 29.89). Taking the undetermined valves into account, the total number of valves per sample varies between 2 and 123 (A = 42.18, σ = 38.78).

Sample **RB01/03** originates from a fine to medium sand layer (bed 02, fig. 3) and contains *Aurila* sp. (7 v), *Aurila punctata* (4 v) and *Costa punctatissima* (4 v); 35 valves remained undetermined.

Sample **RB01/05** was taken from a clayey silt layer (bed 03, fig. 3) and contains only two valves of *Loxocorniculum hastatum*.

Sample **RB01/06** represents the top of the carbonate body. It contains cf. *Loxocorniculum* (9 v) and *Aurila* sp. (8 v); 68 valves remained undetermined.

Sample **RB01/07** originates from a fine to medium sand layer (bed 12, fig. 3) and contains *Loxocorniculum hastatum* (8 v), *Aurila* sp. (4 v), *Cytheridea* aff. *acuminata* (4 v), *Aurila* cf. *punctata* (3 v) and cf. *Aurila* (1 v); 53 valves remained undetermined.

Sample **RB01/09** was taken from a silty sand layer (bed 15, fig. 3) and contains a total of 123 valves. This sample shows the highest number of ostracod specimens and taxa in the Rosenberg quarry section. It contains *Cytherella* sp. (40 v), *Cytherella aff. russoi* (14 v), *Buntonia* cf. *brunensis* (12 v), *Cytherella* aff. *compressa* (7 v), *Pterygocythereis calcarata* (6 v), *Cytheridea acuminata* (5 v), cf. *Loxocorniculum* (3 v), *Costa punctatissima* (2 v), *Xestoleberis* sp. (2 v) *Grinioneis* cf. *haidingeri* (1 v), *Olimfalunia* cf. *plicatula* (1 v) and *Krithe* sp. (1 v); 29 valves remained undetermined.

Sample **RB01/10** originates from a medium sand layer (bed 16, fig. 3) and contains 2 valves of *Cytheridea* aff. *acuminata*.

Sample **RB01/12** was derived from a clayey silt layer (bed 18, fig. 3). It contains *Cytherella* sp. (9 v), *Cytherella* aff. *compressa* (3 v), *Cytherella* sp.1 (2 v) and *Cytherella* aff. *russoi* (1 v); 6 valves remained undetermined.

Sample **RB01/13** originates from a fine sand layer (bed 21, fig. 3) and contains *Senesia* cf. *cinctella* (3 v), cf. *Aurila* (2 v), *Olimfalunia* cf. *plicatula* (2 v), *Cytherella* aff. *russoi* (1 v), *Cytheridea* aff. *acuminata* (1 v) and *Pterygocythereis calcarata* (1 v); 11 valves remained undetermined.

6.2 Ostracod assemblages

6.2.1 Old quarry

The most abundant ostracod taxa are *Cytherella*, *Henryhowella*, *Krithe* and *Parakrithe*, which occur throughout the section.

Four assemblages were identified using cluster analysis (CA, fig. 7) and non-metric multi-dimensional scaling (NMDS). The differences between the clusters were determined using SIMPER analysis. Best results were achieved using relative abundances.

The identified assemblages are:

- *Aurila* assemblage
- *Henryhowella* assemblage
- *Henryhowella* – *Cytherella* assemblage
- *Krithe*/*Parakrithe* assemblage

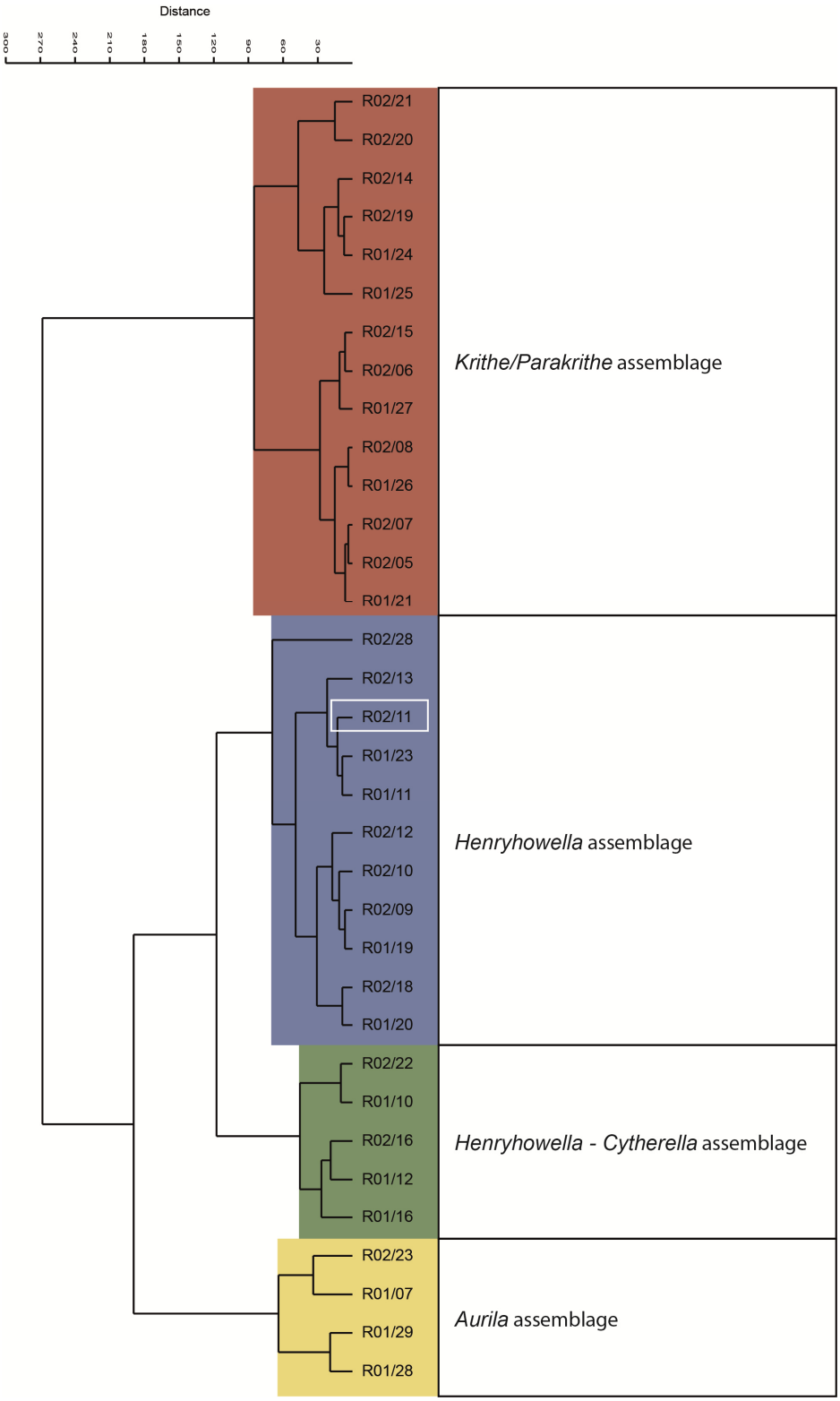

Fig. 7: Q-mode cluster analysis of the Old quarry section (Ward's method, correlation coefficient = 0.53) showing the groupings of four assemblages. Sample R02/11, highlighted with a white box, contains a higher number of *Krithe*/*Parakrithe* than *Henryhowella,* therefore it is assigned to the *Krithe*/*Parakrithe* assemblage.

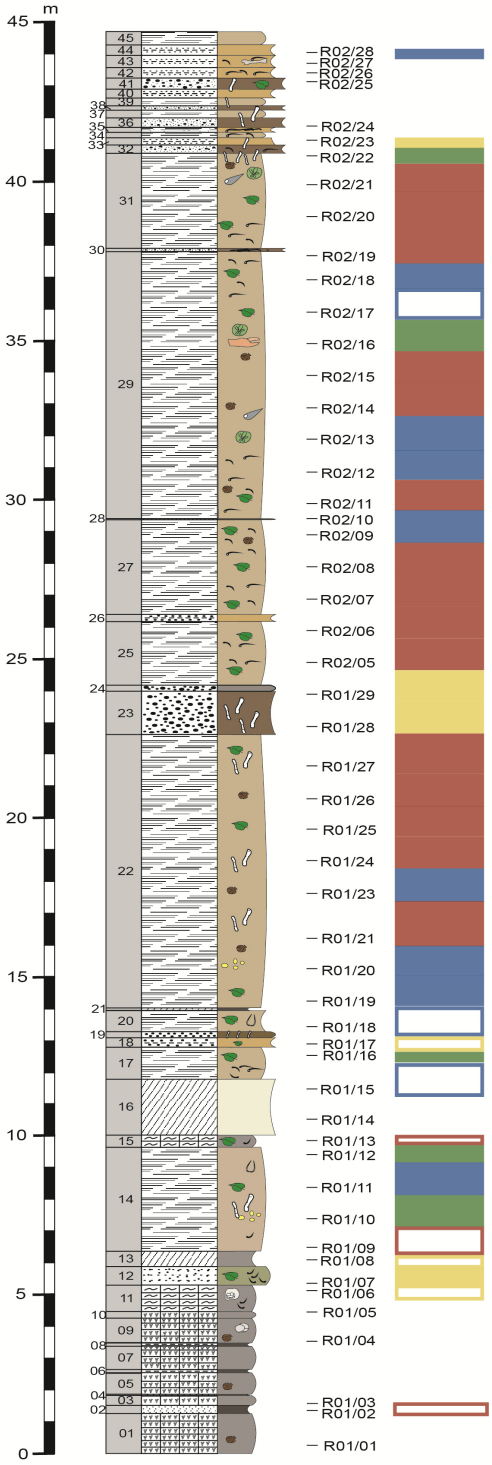

Fig. 8: Ostracod assemblage distribution in the Old quarry section. Boxframes correspond to samples that were excluded from statistical analysis and later assigned to their respective assemblage based on the occurrence of distinctive taxa. White gaps correspond to samples that did not contain any ostracods. For colour codes see fig.7.

Besides sample R01/07 from a sandy silt horizon, the *Aurila* assemblage originates from fine to medium sand layers (fig. 8; Samples R01/28-29, R02/23), which correspond to the yellow cluster. This assemblage is defined by the dominating occurrence of *Aurila* (A = 58.7 %, σ = 26.06 %). It is accompanied by *Cytherella* (A = 19.5 %, σ = 21.5 %), *Henryhowella asperrima* (A = 8.53 %, σ = 10.71 %), *Grinioneis* cf. *haidingeri* (A = 3.57 %, σ = 7.14 %), *Cytherelloidea* (A = 2.81 %, σ = 2.6 %), *Loxocorniculum* (A = 2.58 %, σ = 3.72 %), *Occultocythereis* cf. *bituberculata* (A = 2.38 %, σ = 4.76 %) and *Krithe/Parakrithe* (A = 1.97 %, σ = 3.95 %)
Besides the 4 samples included in the yellow cluster, samples R01/08 and R01/17 (excluded from statistical analysis due to low ostracod content) were assigned to this assemblage based on the occurrence of *Aurila*. Sample R01/06 was assigned to this assemblage based on the occurrence of *Cytherelloidea,* which co-occurs with *Aurila* in the other samples of this section.

The *Henryhowella – Cytherella* assemblage originates from clayey silt layers (fig. 8; Samples R01/10, 12, 16, R02/16 and R02/22) and corresponds to the green cluster. This assemblage is defined by the co-occurrence of *Henryhowella asperrima* (A = 41.2 %, σ = 7.43 %) and *Cytherella* (A = 39.3 %, σ = 15.27 %). They are accompanied by *Krithe/Parakrithe* (A = 8.88 %, σ = 9.91 %), *Buntonia* (A = 4.48 %, σ = 7.43 %), *Costa punctatissima* (A = 2.35 %, σ = 5.26 %), *Xestoleberis* sp. (A = 2.11 %, σ = 4.71 %) and *Loxocorniculum* (A = 1.71 %, σ = 3.83 %).

Besides sample R02/28 from a silty sand layer, the *Henryhowella* assemblage originates from clayey silt layers (fig. 8; Samples R01/11, 19, 20, 23, R02/09, 10, 12, 13, 18 and R02/28), which correspond to the blue cluster. This assemblage is defined by the dominating occurrence of *Henryhowella asperrima* (A = 51.5 %, σ = 10.7 %). It is accompanied by *Krithe*/*Parakrithe* (A = 31.7 %, σ = 12.64 %), *Buntonia* (A = 5.9 %, σ = 6.7 %), *Olimfalunia* cf. *plicatula* (A = 5.33 %, σ = 11.7 %) and *Cytherella* (A = 2.27 %, σ = 3.8 %). Very rare co-occurring taxa are *Costa punctatissima*, *Xestoleberis* sp., *Pterygocythereis calcarata*, *Grinioneis* cf. *haidingeri* and *Occultocythereis* cf. *bituberculata*.

The samples R01/15, 18 and R02/17 were excluded from statistical analysis and later assigned to this assemblage based on the occurrence of *Henryhowella asperrima*.

The *Krithe/Parakrithe* assemblage originates from clayey silt layers (fig. 8: Samples R01/21, 24-27, R02/05-08, 14, 15 and R02/19-21), which correspond to the red cluster. This assemblage is defined by the dominating occurrence of *Krithe/Parakrithe* (A = 70.4 %, σ = 17.77 %). They are accompanied by *Henryhowella asperrima* (A = 15.1 %, σ = 11.02 %), *Cytherella* (A = 9.34 %, σ = 11.36 %) and *Buntonia* (A = 2.26 %, σ = 3.57 %). Very rare co-occurring taxa are *Occultocythereis* cf. *bituberculata*, *Pterygocythereis calcarata*, *Costa punctatissima*, *Xestoleberis* sp. and *Aurila*.
The samples R01/02, 09 and R01/13 were excluded from statistical analysis and later assigned to this assemblage based on the occurrence of *Krithe*/*Parakrithe*.
The cluster analysis assigned sample R02/11 to the *Henryhowella* assemblage, but it contains a higher amount of *Krithe/Parakrithe* than *Henryhowella*. To allow a more precise paleoecological reconstruction it was assigned to the *Krithe/Parakrithe* assemblage.

Taxon	Av. dissim	Contrib. %	Cumulative %	1	2	3	4
Krithe / Parakrithe	21,71	34,21	34,21	1,97	31,7	8,88	70,4
Henryhowella	14,15	22,31	56,52	8,53	51,5	41,2	15,1
Cytherella	9,84	15,51	72,03	19,5	2,27	39,3	9,34
Aurila	8,97	14,14	86,17	58,7	0	0	0,272
Buntonia	2,64	4,161	90,33	0	5,9	4,48	2,26
Olimfalunia	1,747	2,753	93,08	0	5,33	0	0,444
Costa	0,8391	1,323	94,4	0	1,06	2,35	0,417
Xestoleberis	0,7061	1,113	95,52	0	0,748	2,11	0,404
Occultocythereis	0,7039	1,11	96,62	2,38	0,26	0	0,833
Loxocorniculum	0,6799	1,072	97,7	2,58	0	1,71	0
Grinioneis	0,6783	1,069	98,77	3,57	0,488	0	0
Cytherelloidea	0,4265	0,6721	99,44	2,81	0	0	0
Pterygocythereis	0,3569	0,5625	100	0	0,723	0	0,475

Table 1: SIMPER analysis using the Bray-Curtis similarity showing the percentile contribution of the ostracod taxa towards their respective assemblages. Ostracod values are given in relative abundances. 1 = *Aurila* assemblage, 2 = *Henryhowella* assemblage, *3 = Henryhowella – Cytherella* assemblage, *4 = Krithe/Parakrithe* assemblage. Overall average dissimilarity = 63.45.

SIMPER analysis (Tab. 1) shows that the assemblages are generally defined by the occurrences of *Krithe*/*Parakrithe*, *Henryhowella*, *Cytherella* and *Aurila*, which in combination make up 86.33 % of the overall average dissimilarity between the assemblages.

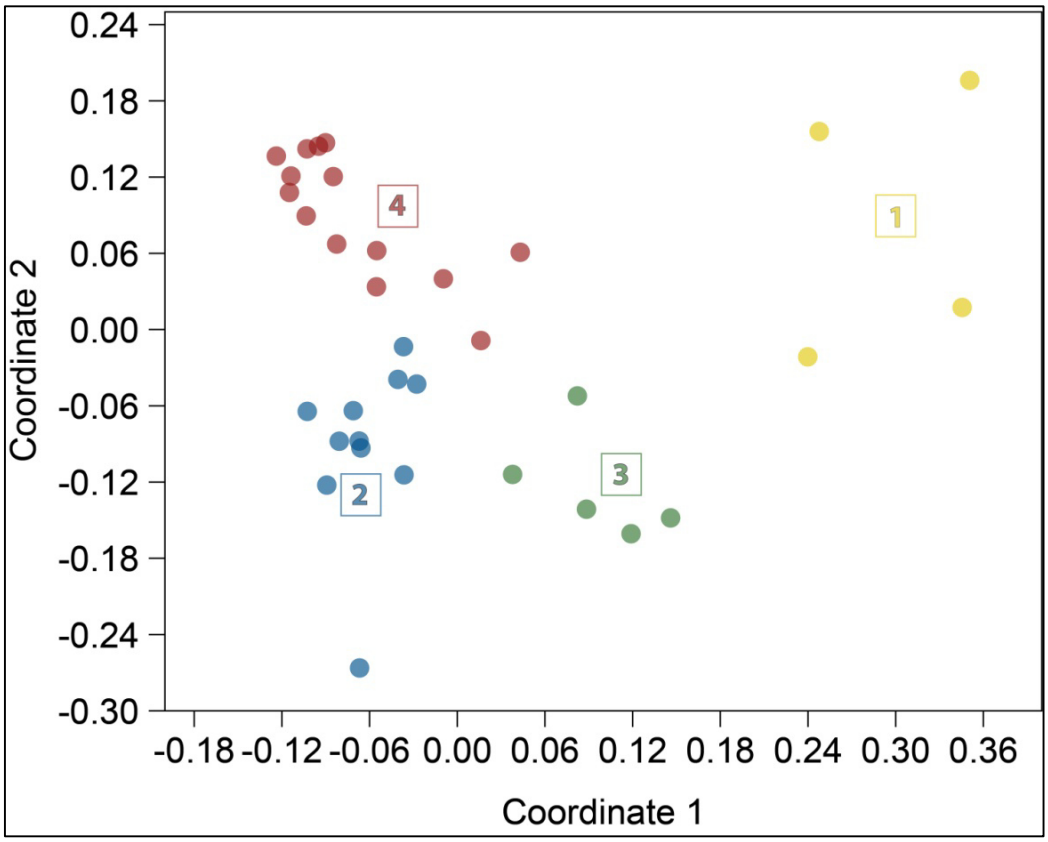

Fig. 9: Non-metric multidimensional scaling (Bray-Curtis; 1 = *Aurila* assemblage, 2 = *Henryhowella* assemblage, 3 = *Henryhowella* – *Cytherella* assemblage, 4 = *Krithe/Parakrithe* assemblage.

To visualise the results of the performed cluster analysis, non-metric multidimensional scaling (NMDS) using Bray-Curtis similarity was performed (fig. 9). The NMDS supports the grouping into four clusters, although some of them plot in close proximity to each other, which may indicate similar ecological demands.

6.2.2 Rosenberg quarry

The ostracod content in the Rosenberg quarry is very low. Only 8 out of 13 samples contained determinable valves. In three samples the ostracods are highly deformed or broken and could not be determined. Two samples contain no ostracods at all. Out of the remaining 8 samples, only 175 valves were determined, with more than half of them in sample RB01/09. Therefore, a statistical analysis of the Rosenberg quarry's ostracod assemblages does not yield any results of statistical significance. However, a co-occurrence of *Aurila* and *Loxocorniculum* cf. *hastatum* is present in samples RB01/06-07 from the top of the carbonate build-up. In addition, samples from the upper part of the section (RB01/09 and RB01/12) show increased numbers of *Cytherella*.

6.3 Ostracod occurrences correlated with geochemical proxies

A correlation of ostracod occurrences with geochemical proxies was only possible for the Old quarry, not for the Rosenberg quarry, due to the sparse ostracod content.

Only five ostracod taxa occur in enough samples to allow a correlation with the geochemical proxies. With the p-value set < 0.05, only 3 correlations show a statistical significance (tab. 2).

The occurrence of *Aurila* shows a positive correlation with the TOC/S value (r = 0.898, p = 0.006), *Buntonia* shows a negative correlation with the $\delta^{18}O$ value (r = -0.587, p = 0,035) and *Krithe/Parakrithe* show a positive correlation to the S (wt. %) content (r = 0.432, p = 0.02).

Proxy / Taxon	CaCO3 (%)		S (%)		TOC (%)		TOC/S		δ13C(‰)		δ18O(‰)	
	r	p	r	p	r	p	r	p	r	p	r	p
Aurila	0.197	0.67	-0.59	0.16	-0.65	0.11	0.898	0.006	-0.65	0.11	-0.45	0.311
Buntonia	-0.18	0.57	0.011	0.97	0.088	0.78	-0.14	0.65	0.256	0.4	-0.587	0.035
Cytherella	-0.18	0.41	0.153	0.49	-0.22	0.32	-0.21	0.34	0.041	0.85	0.037	0.868
Henryhowella	0.326	0.06	0.035	0.84	0.083	0.64	-0.24	0.168	-0.32	0.06	0.054	0.758
Krithe/Parakrithe	-0.06	0.76	0.432	0.02	-0.1	0.61	-0.3	0.105	0.019	0.92	-183	0.313

Table 2: Ostracod taxa correlated with geochemical proxies. r = linear correlation coefficient (Pearson's r); p = p-value. p-values < 0.05 are highlighted in blue.

7. Discussion

In order to describe differences in the depositional regimes within each assemblage, the ostracod assemblages were discussed individually prior to the paleoecological reconstruction.

The ostracod assemblages are interpreted according to Gross (2002, with further references therein), who suggests an in-situ preservation of most life-cycles if adult and juvenile individuals occur together. Information about transport distances and sedimentation rates is given by the degree of disarticulation of the carapaces. High sedimentation rates and/or short transport distances can be assumed if there are high amounts of complete carapaces.

7.1 Ostracod assemblages

7.1.1 Ostracod assemblages of the Old quarry

In the following description, sub-section R01 is referred to as the lower part of the section, whereas sub-section R02 is referred to as the upper part of the section. The two sub-sections are separated by a 1.5 m thick turbiditic layer in the middle of the section (fig. 8).

The ***Aurila* assemblage** occurs in the sandy layers of the section, which are intercalated in a clayey silt succession (fig. 8). This assemblage is characterised by the dominating occurrence of *Aurila,* which makes up to 58.7 % of the ostracods occurrence. This genus is indicative for a coastal, shallow marine environment with sandy substrate (Cernajsek, 1972; Gross, 2006). *Aurila* is also described to show a tolerance towards changes in salinity. Their valves and limbs are robust, which allows them to live in areas with high water energy (Cernajsek, 1972).
Within the *Aurila* assemblage two depositional regimes can be differentiated.

The co-occurring shallow water indicators *Cytherelloidea*, *Grinioneis*, *Occultocythereis* and Senesia (van Morkhoven, 1963; Ducasse & Chahuzac, 1996, 1997; Mitrovic, 1998; Gross, 2006) as well as the position on top of the carbonate body indicate an autochthonous deposition for sample R01/07.
The samples R01/28, 29 and R02/23 are considered to represent turbiditic events based on the high amount of broken *Aurila* specimens and the internal sedimentary structures of the sand layers (fining-upwards trend). The co-occurring genera in these samples are *Cytherelloidea* and *Loxocorniculum*, which also indicate shallow marine environments.

The ***Henryhowella – Cytherella*** **assemblage** includes samples from clayey silt layers that mainly originate from the lower part of the siliciclastics that were deposited above the carbonate body (fig. 8). This assemblage is defined by the dominant co-occurrence of the genera *Henryhowella* (41.2 %) and *Cytherella* (39.3 %). *Henryhowella* usually prefers deeper water (100 m and more; Kempf & Nink; Bonaduce et al., 1998, 1999), living in the uppermost part of fresh, well-ventilated soft substrate with abundant supply of food (Kempf & Nink, 1993; Didié et al., 2002). Members of *Cytherella* are filter feeders in deeper marine waters (Ducasse & Cahuzac, 1997; Gross, 2006; Gebhardt, 2009), which can survive low oxygen levels (Boomer & Whatley, 1992; Aiello et al., 1996; Gross, 2006).
Accessory genera are only represented by a low number of specimens and their occurrence differs between samples. The shallow-water indicators *Xestoleberis* and *Loxocorniculum* (Hartmann, 1975; Athersuch; 1976; Bonaduce & Danielopol, 1988; Ducasse & Cahuzac, 1996, 1997) occur in samples from the lower part of the section. Therefore, in the lower part of the section this assemblage may represent an environmental transition from a shallow marine into a deeper, more open marine environment.
The co-occurrence of *Krithe* and *Parakrithe* is indicative for reduced oxygen levels (van Morkhoven, 1963; Coles et al., 1994; Zhao & Whatley, 1997).

The ***Henryhowella* assemblage** mainly occurs in samples that originate from clayey silt layers (fig. 8). This assemblage is defined by the prominent occurrence of *Henryhowella* (51.53 %), which indicates deeper marine environments with water depths of more than 100 m and muddy substrate (Kempf & Nink, 1993; Bonaduce et al., 1998, 1999; Gross, 2006). *Henryhowella* lives infaunal in the uppermost part of fresh, well-ventilated soft substrate with abundant supply of newly produced food (Kempf & Nink, 1993; Didié et al., 2002; Sciuto & Rosso, 2008).

Except of *Aurila*, *Loxocorniculum* and *Cytherelloidea,* which indicate near-shore settings (van Morkhoven, 1963; Cernajsek, 1972; Ducasse & Cahuzac, 1996, 1997; Gross, 2006), all other identified genera in the Old quarry section occur in this assemblage.

Besides *Krithe* and *Parakrithe*, which occur in higher amounts in all samples, accessory genera are generally low in numbers and vary between the samples.

The eurybathic *Olimfalunia* (Carbonel, 1985; Gross, 2006) occurs only in the upper part of the section. The shallow water genus *Occultocythereis* (van Morkhoven, 1963; Hartmann, 1975; Gross, 2006) and the mainly deeper water indicating kymatophobic *Pterygocythereis* (Liebau, 1980; Montenegro et al., 1998) appear in the lower part of the section. *Grinioneis*, an indicator for shallow water (Aranki, 1987; Ducasse & Cahuzac, 1996, 1997; Gross, 2006), occurs in the upper part of the section, which does not fit to the estimated paleo-depths. In addition, *Grinioneis* specimens are only poorly preserved or broken, which points towards transport. The genera *Cytherella*, *Buntonia* and *Costa* appear all over the section.

It can be assumed that the environmental demands of *Henryhowella*, such as well-ventilated bottom sediments and the abundance of freshly produced food, are also suited for the other occurring taxa and, thus, lead to the relatively high diversity of this assemblage.

All samples of the *Henryhowella* assemblage contain co-occurring *Krithe*, *Parakrithe* and a high amount of planktic foraminifers (as described by Strahlhofer, 2013), and originate from very fine-grained sediments. According to Kempf & Nink (1993), this indicates water depths of at least 200 m.

The ***Krithe*/*Parakrithe* assemblage** occurs in samples which originate from clayey silt layers (fig. 8) and is defined by the dominant occurrence of *Krithe* and *Parakrithe* (70.44 %). They are indicative for fully marine environments and greater water depths (Coles et al., 1994; Zhao & Whatley, 1997). *Krithe* and *Parakrithe* are psychrospheric or cryophilic and inhabit low-energy soft substrates with reduced oxygen levels, like fine sands, muds or oozes of nannofossils and deep-water planktic foraminifers (Coles et al., 1994; Zhao & Whatley, 1997). In addition, *Krithe* is reported to feed on old organic matter (Didié et al., 2002). In this assemblage all identified genera of the Old quarry section appear, except *Cytherelloidea*, *Grinioneis* and *Loxocorniculum*, which usually inhabit shallower, coastal areas (van Morkhoven, 1963; Ducasse & Cahuzac, 1996, 1997; Gross, 2006). The co-occurring genera are only represented by low numbers of specimens, and not all of these genera occur in every sample. Also, their number varies between each sample. *Costa*, *Pterygocythereis* and *Occultocythereis* only occur in samples from the lower part of the section, whereas *Cytherella*, *Buntonia* and *Henryhowella* appear throughout the section. *Olimfalunia*, *Aurila* and *Xestoleberis* are very rare; each specimen of them only appears in one sample (of this assemblage), spread throughout the section.

Based on the dominant occurrence of *Krithe* and *Parakrithe* and the remarkably low quantity of co-occurring genera, it can be assumed that this assemblage represents a muddy, deeper marine environment with reduced oxygen contents and cooler water temperatures.

Compared to the *Henryhowella* assemblage, the *Krithe*/*Parakrithe* assemblage is considered to represent a cooler and less oxygenated depositional environment.

7.2 Paleoenvironmental reconstruction

The combination of the ostracod distribution, the ecological preferences of the recorded taxa, geochemical analysis and lithology can provide valuable information for the reconstruction of the paleoenvironment in which the sediments of the Retznei quarries were deposited. A detailed comparison of the different paleoenvironments of the two sections is not possible due to the sparse ostracod fauna, especially in the Rosenberg quarry.

7.2.1 Old quarry section

Due to the low ostracod content, samples of different ostracod assemblages often show only minor differences in their ostracod composition; therefore, it was regarded as necessary to interpret smaller groups of samples separately in order to make a conscientious reconstruction of the paleoenvironment.

Sample **R01/02** at the bottom of the section originates from a marl layer within the carbonate complex and shows an elevated TOC content and a high TOC/S ratio. The marl layers within the carbonate complex are interpreted to represent short term crises in carbonate production due to volcanic ash-fall (Reuter & Piller, 2011; Reuter et al., 2012). The ostracod fauna is only represented by a few valves of *Parakrithe*, which usually inhabits greater water depths. However, based on the high TOC/S ratios, turbid waters and reduced light levels that cause deeper water taxa to appear in shallower environments (Reuter & Piller, 2011) may be assumed.
Despite the very low ostracod content, the benthic foraminifers are high in numbers and diversity (Strahlhofer, 2013). High productivity, which is indicated by a high TOC value, is not indicated by the ostracods. However, the rich and diverse benthic foraminifer fauna described by Strahlhofer (2013) points towards fertile waters.
Sample **R01/06** shows higher TOC contents and a low S content. This sample only contains 2 valves of *Cytherelloidea*, which indicates warm, shallow marine environments and is also described to tolerate brackish influences. This fits the position of this sample within the shallow-water carbonates.

Sample **R01/07** originates from a sandy layer on top of the carbonates. The ostracods are represented by the *Aurila* assemblage, which indicates coastal, shallow marine environment.

Sample **R01/08** originates from a tuffitic layer directly above the shallow-water carbonates and only contains *Aurila,* which suggests a shallow-water marine environment. The high TOC/S ratio points towards increased external input (ash-fall). When comparing this sample with the other samples from tuffitic layers, which also contain little to no ostracods and very few benthic foraminifers (Strahlhofer, 2013), it becomes obvious that volcanoclastic sedimentation represents clear disturbances in the benthic fauna.

Sample **R01/09** originates from a clayey silt layer and shows an elevated TOC content, which indicates fertile water conditions. The ostracods are represented by a very low number of *Krithe and Parakrithe*, probably because of reduced light levels due to turbid water.

The ostracod content in sample **R01/10** is represented by the *Henryhowella – Cytherella* assemblage. The occurrence of *Henryhowella* in combination with the elevated TOC values indicates ventilated sediments and sufficient food supply.

Sample **R01/11** contains a relatively high amount of ostracods. This diverse ostracod fauna is represented by the *Henryhowella* assemblage. A high TOC content indicates high productivity and increased amounts of organic matter on the sea floor. A higher number of co-occurring *Krithe/Parakrithe* is probably caused by turbid water conditions. The accessory *Pterygocythereis* indicates stagnant bottom water, which can also be seen in the higher sulphur content of this sample.

Sample **R01/12** shows high TOC and S contents and contains the *Henryhowella – Cytherella* assemblage. Compared to sample R01/11, the higher content of *Cytherella* is probably due to its being better suited for lower oxygen levels than *Henryhowella*.

Sample **R01/13** originates from a marl layer and shows a high TOC content. The S content decreases compared to the previous sample. The ostracods are represented by a few individuals of *Parakrithe*, probably due to turbid water conditions.

The samples **R01/14** and **R01/15** originate from a tuffitic layer. The massive positive shift in TOC/S is caused by volcanic ashes. Sample R01/14 contains no ostracods at all and sample R01/15 contains only 1 valve of *Henryhowella*. These samples also contain very low amounts of benthic foraminifers (Strahlhofer, 2013).

Sample **R01/16** shows an elevated TOC content and contains the *Henryhowella* – *Cytherella* assemblage. High TOC content and the occurrence of *Henryhowella* indicate well-ventilated sediments and abundant food supply.

Sample **R01/17** originates from a sandy layer which is interpreted to represent a turbiditic event and contains only one individual of *Aurila*.

Sample **R01/18** shows an elevated TOC content and contains only one adult valve of *Henryhowella.*

The samples **R01/19** to **R01/27** show constant elevated TOC contents, while the S contents show an extreme increase towards the middle of the section (sample R01/27). This indicates that the initially well-ventilated substrate became more and more anoxic due to constant flux of organic matter to the sea-floor. This assumption is strengthened by the occurrence of *Pterygocythereis*, which indicates stagnant water that might have led to stratified water masses. The reduction of the oxygen levels is also indicated in the transition from the *Henryhowella* assemblage towards the *Krithe/Parakrithe* assemblage. Sample R01/23 was assigned to the *Henryhowella* assemblage, because the amount of *Henryhowella* specimens is only slightly higher than the amount of *Krithe/Parakrithe*. However, with the co-occurrence of *Cytherella* the number of taxa that can tolerate low oxygen levels are dominant.

The samples **R01/28** and **R01/29** originate from a sand layer and are characterised by remarkably high TOC/S values. This, in combination with the internal sedimentary structures within the sand layer (fining upwards), clearly points towards turbiditic deposition. The ostracods are represented by the *Aurila* assemblage, which indicates a shallow marine, probably coastal environment. This sand layer is expected to originate from a much shallower environment.

Above this sand layer, constantly low TOC/S ratios indicate lower oxygen levels in the upper part of the section.

The following samples **R02/05** to **R02/08** show lower TOC contents and higher S contents compared to the average of the lower part of the section. The ostracods are represented by the *Krithe/Parakrithe* assemblage. These samples are supposed to represent an environment with lower oxygen levels and lower productivity.

The following part of the section (samples **R02/09-22**) is characterised by the alternating occurrence of the *Henryhowella* assemblage and the *Krithe/Parakrithe* assemblage. In the samples of this part of the section, the differences in the numbers of *Henryhowella* and *Krithe/Parakrithe* are smaller than in the lower part of the section. Their alterations are probably caused by the fluctuating primary production, indicated by relatively high variations in the TOC contents, and the related supply of freshly produced food. In these samples, the number of *Krithe/Parakrithe* is generally higher than the number of *Henryhowella*, which may indicate low oxygen conditions.

Sample **R02/23** originates from a turbiditic sand layer. It contains a very low amount of ostracods that are represented by the *Aurila* assemblage.

Samples **R02/24-27** did not contain any ostracods, in sample **R02/28** ostracods are also very sparse and represented by the *Henryhowella* assemblage.

Comparison with previous studies

The upwards deepening within the siliciclastics above the carbonate body in the Old quarry section from 150 to 300 m as suggested by Hohenegger et al. (2009) and Strahlhofer (2013) could be observed in the ostracod distribution.

Directly above the carbonate platform occurs an autochthonous *Aurila* assemblage, which indicates shallow water conditions. After a nearly ostracod-free tuffitic layer, deep-water indicating ostracod assemblages are dominating the rest of the section. This confirms the aforementioned upwards-deepening trend.

Strahlhofer (2013) also suggests a slight deepening and cooling from sub-section R01 to sub-section R02. This trend could not be confirmed based on the ostracod distribution, because deep-water indicating genera occur throughout the section.

7.2.2 Rosenberg quarry section

Due to the extremely low ostracod content in the Rosenberg quarry it was not possible to carry out a confident statistical analysis or paleoenvironmental reconstruction. Five out of 13 samples did not contain any ostracods (sample RB01/01-02, 04, 08, 11), whereas a lot of foraminifers occur in the Rosenberg quarry section.

Sample **RB01/03** from the basal siliciclastics contains a larger amount of *Aurila,* which is accompanied by *Costa punctatissima*. Both taxa indicate very shallow, sandy areas. *Aurila* also shows tolerance towards reduced salinity (Cernajsek, 1972; Gross, 2006). The high amount of complete carapaces of adults together with the absence of juvenile forms suggests transportation.

Sample **RB01/0**5 contains only few valves of *Loxocorniculum hastatum*.

The top of the carbonate body (**RB01/06** and **RB01/07**) is characterised by the co-occurrence of *Aurila* and *Loxocorniculum* pointing towards a full marine, inner-neritic phytal environment (Gross, 2002).

With 123 valves, sample **RB01/09** contains more than half of the ostracods of the Rosenberg quarry and also shows the highest diversity (*Cytherella*, *Cytheridea*, *Krithe*, *Pterygocythereis calcarata*, *Buntonia* cf. *brunensis*, *Grinioneis* cf. *haidingeri*, *Loxocorniculum hastatum*, *Costa punctatissima, Olimfalunia* cf*. plicatula* and *Xestoleberis* sp.). The high ostracod diversity in combination with the high TOC content in this sample indicates elevated productivity.

The samples **RB01/09** and **RB01/12** contain relatively high amounts of *Cytherella,* which indicates increasing water depths and reduced oxygen levels (van Morkhoven, 1963; Hartmann, 1975; Boomer & Whatley, 1992; Aiello et al., 1996).

Sample **RB01/13** at the top of the Rosenberg quarry section (bed 21, fig. 3) contains *Aurila*, *Olimfalunia* cf. *plicatula*, *Cytherella, Cytheridea* and *Pterygocythereis calcarata*. The co-occurrence of the shallow water taxa *Aurila* and *Cytheridea* with the eurybathic taxa *Cytherella* and *Olimfalunia* cf. *plicatula* as well as the kymatophob taxon *Pterygocythereis calcarata* may indicate a shallow marine environment with reduced water energy.

Comparison with previous studies

According to the study of Strahlhofer (2013) on planktic and benthic foraminifers, the basal siliciclastic succession exposed in the Rosenberg quarry section indicates a partly freshwater-influenced marginal-marine to fluvial-marine environment with well oxygenated water and low productivity. The benthic foraminiferal assemblages in the siliciclastics above the Leitha limestone body suggest the transition from an oligotrophic, photic and well oxygenated inner-neritic setting with sea grass meadows (samples RB01/06-08) towards a middle neritic environment with lower oxygen levels and increased terrigenous input.

The ecological demands of the occurring ostracods match the paleoecological reconstruction of Strahlhofer (2013), but because of the low ostracod content in the Rosenberg quarry section the detailed conclusions of Strahlhofer (2013) could not be reached.

8. Conclusion

A multiproxy approach was used on the siliciclastics of the Old quarry and the Rosenberg quarry in Retznei, which lie below and above the approximately 25 m thick lower Badenian Leitha Limestone bioherm. By utilising ostracod assemblages in combination with geochemical and sedimentological data new information about the paleoenvironmental conditions after the MMCO were obtained.

Based on the count of ostracod valves as well as cluster analysis and non-metric multidimensional scaling, four ostracod assemblages (*Aurila* assemblage, *Henryhowella* assemblage, *Henryhowella* – *Cytherella* assemblage and *Krithe*/*Parakrithe* assemblage) were defined for the Old quarry section.

In the Old quarry, the ostracod fauna in the siliciclastics above the carbonate body indicates a circa-littoral to bathyal environment with decreasing temperatures and reduced oxygen contents. This corresponds to the climate change that is related to the expansion of the East Antarctic Ice Sheet.

This paleoenvironmental change is also reflected in the distribution of the ostracod assemblages throughout the section. At the base of the siliciclastic succession, topping the Leitha Limestone body, an autochthonous *Aurila* assemblage (sample R01/07) indicates a warm, shallow-marine, coastal environment. The siliciclastics above sample R01/07 are dominated by deep-water indicating ostracod assemblages. The lower part of these deep-water taxa domintated siliciclastics (R01/10 – R01/20) mainly represents the *Henryhowella*- and the *Henryhowella* – *Cytherella* assemblage and is indicative for a circa-littoral to bathyal environment with muddy substrate and a relatively productive setting. Towards the middle part of the section (R01/21 – 27), reduced oxygen levels caused by stagnant bottom waters and constant influx of organic matter led to the change from the *Henryhowella* assemblage to the *Krithe*/Parakrithe assemblage. The *Krithe/Parakrithe* assemblage is indicative for a euhaline, infra-neritic to epibathyal environment with reduced oxygenation, soft substrate, cool temperatures and reduced productivity. The samples represented by the *Krithe*/*Parakrithe* assemblage are interrupted by an allochthonuos *Aurila* assemblage. This assemblage occurs in the intercalated sandy layers and corresponds to turbiditic events.

Sub-section R02 is characterised by the alternation of the *Henryhowella*- and the *Krithe/Parakrithe* assemblage. These changes are related to fluctuations in primary production caused by reduced temperatures.

The ostracod distribution in the Old quarry section confirms the increasing water depths, which were proposed in previous studies. The slight deepening and cooling from sub-section R01 to sub-section R02 in the Old quarry section, proposed by Strahlhofer (2013), could not be observed based on the ostracod content.

Because of the extremely low ostracod content, the Rosenberg quarry was excluded from multivariate statistics; a descriptive approach was used to evaluate paleoecological conditions. Although a detailed reconstruction was not possible, the ecological demands of the few identified taxa seem to confirm the paleoenvironmental model suggesting a deepening-upwards trend from an oligotrophic, photic and well oxygenated inner-neritic setting with sea grass meadows towards a middle neritic environment with lower oxygen levels and increased terrigenous input.

9. Ostracod plates

Plate 1

Figures 1, 2, 5: ***Cytherella*** aff. ***compressa*** (MUENSTER 1830)

Fig. 1: *Cytherella* aff. *compressa* right valve

Fig. 2: *Cytherella* aff. *compressa* right valve interior view (same specimen as Fig. 1)

Fig. 5: *Cytherella* aff. *compressa* dorsal view (same specimen as Fig. 1)

Figures 3, 4, 6: ***Cytherella* sp. 1**

Fig. 3: *Cytherella* sp. 1 left valve

Fig. 4: *Cytherella* sp. 1 left valve interior view (same specimen as Fig. 3)

Fig. 6: *Cytherella* sp. 1 dorsal view (same specimen as Fig. 3)

Plate 1

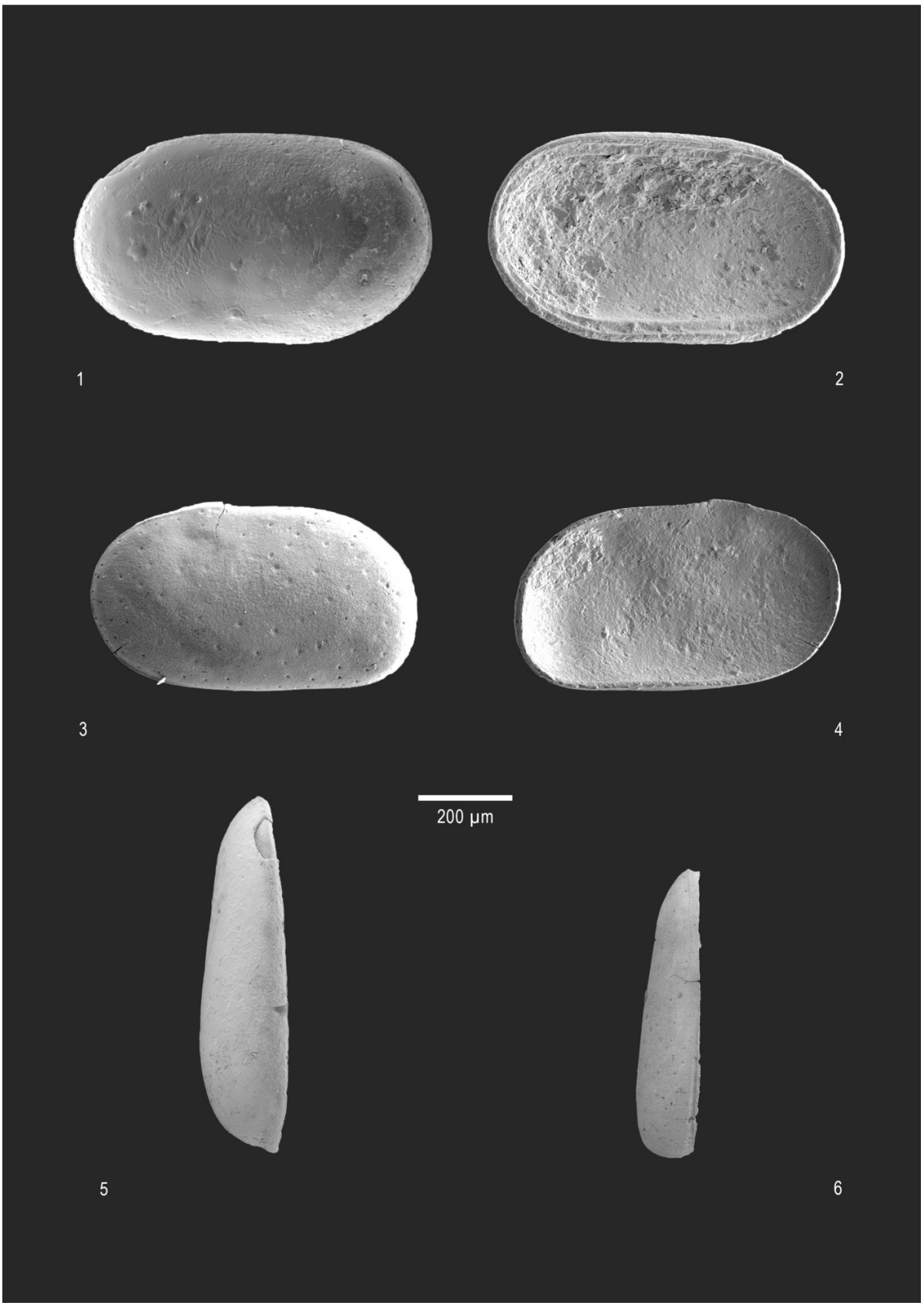

Plate 2

Figures 1, 2, 4: ***Cytherella*** aff. ***russoi*** SISSINGH 1972

Fig. 1: *Cytherella* cf. *russoi* left valve

Fig. 2: *Cytherella* cf. *russoi* left valve interior view

Fig. 4: *Cytherella* cf. *russoi* dorsal view

Figures 3, 5: ***Cytherella*** cf. ***cercinata*** AIELLO et al. 1996

Fig. 3: *Cytherella* cf. *cercinata* left valve

Fig. 5: *Cytherella* cf. *cercinata* dorsal view (same specimen as Fig. 3)

Plate 2

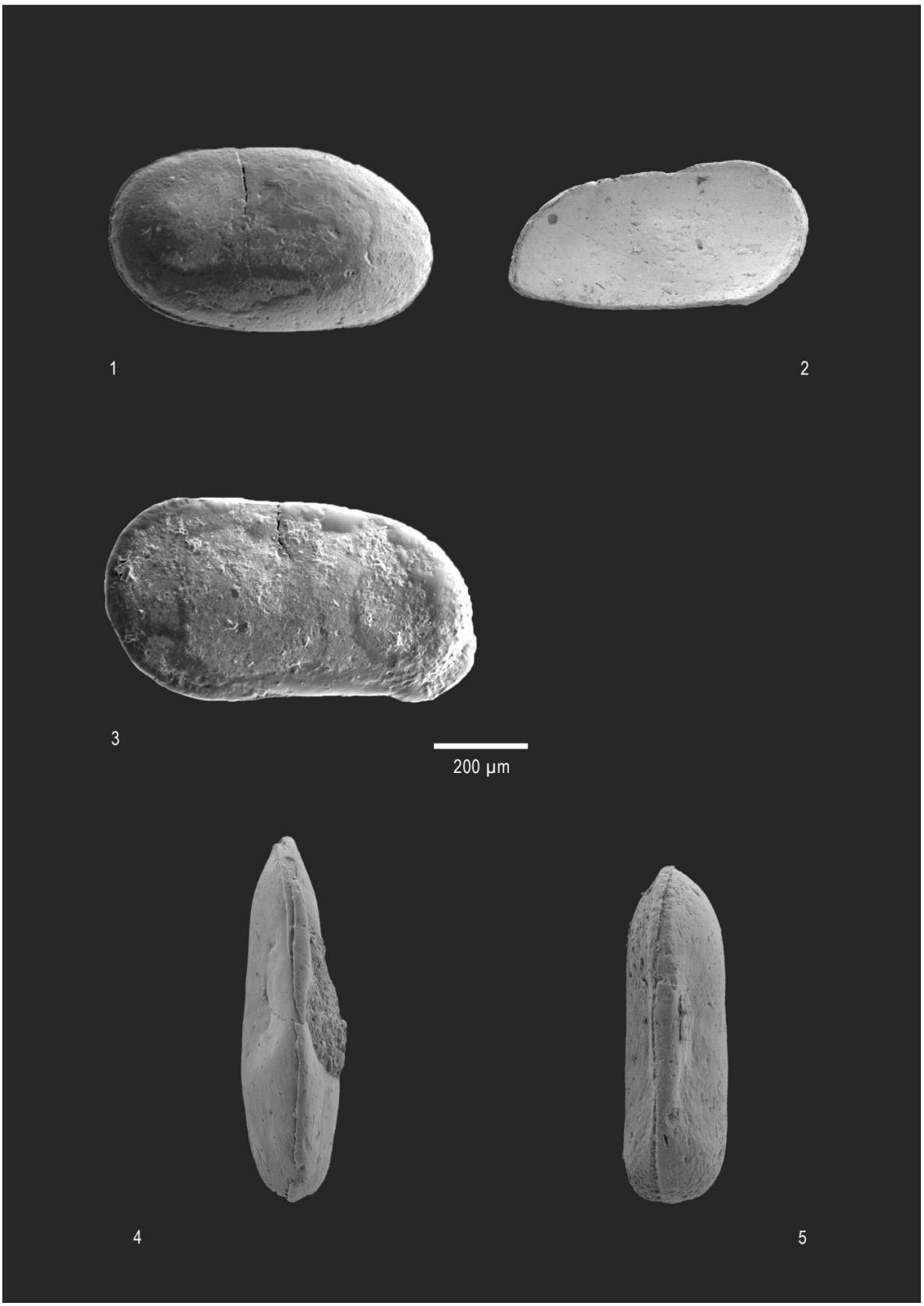

Plate 3

Figures 1, 2, 3: ***Cytherelloidea* sp.** ALEXANDER 1929

Fig. 1: *Cytherelloidea* sp. right valve

Fig. 2: *Cytherelloidea* sp. right valve interior view (same specimen as Fig. 1)

Fig. 3: *Cytherelloidea* sp. dorsal view (same specimen as Fig. 1)

Plate 3

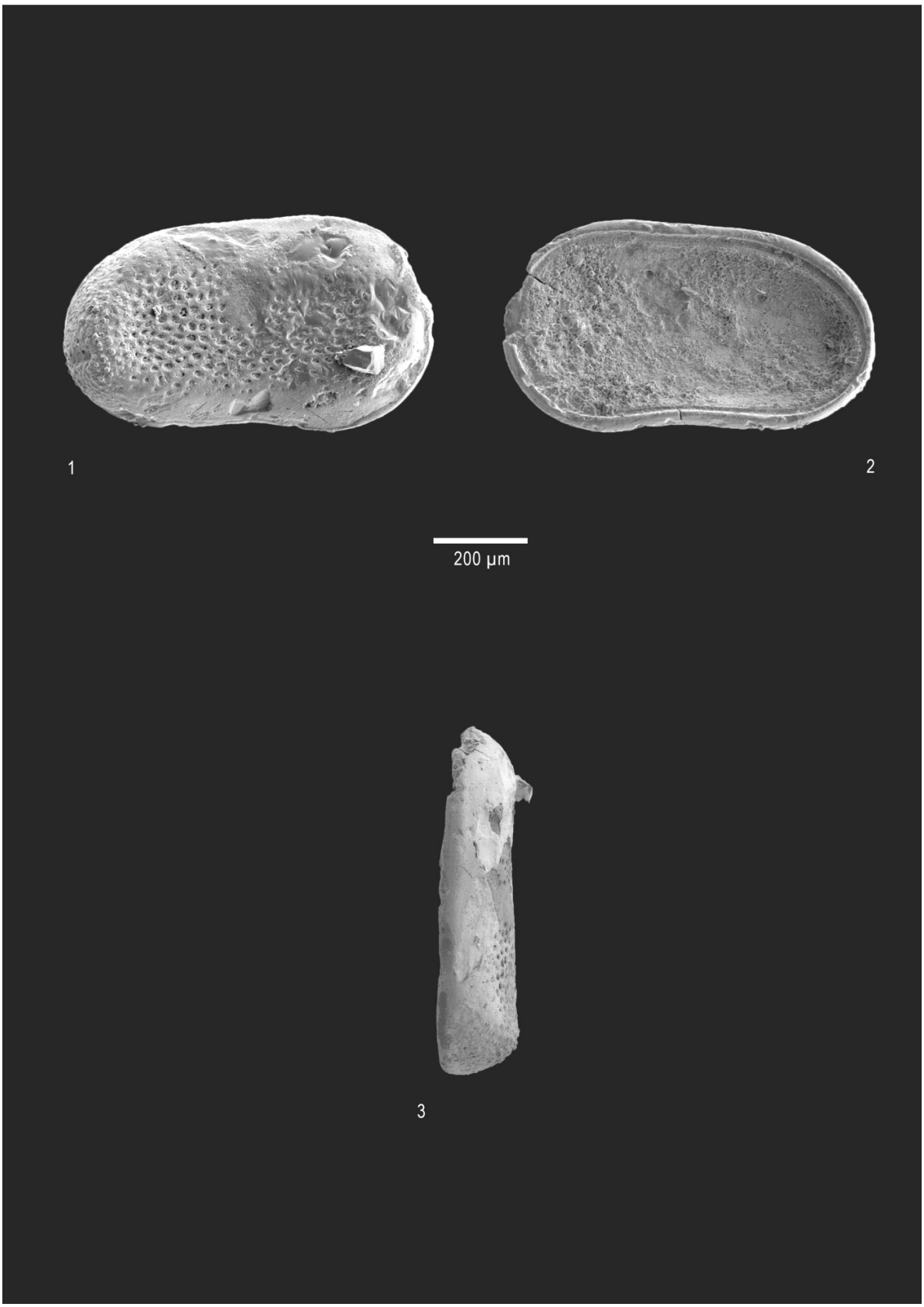

Plate 4

Figures 1, 2, 5: ***Cytheridea acuminata*** BOSQUET 1852

Fig. 1: *Cytheridea acuminata* right valve

Fig. 2: *Cytheridea acuminata* right valve interior view (same specimen as Fig. 1)

Fig. 5: *Cytheridea acuminata* dorsal view

Figures 3, 4, 6***: Cytheridea*** aff. ***acuminata*** BOSQUET 1852

Fig. 3: *Cytheridea* aff*. acuminata* left valve

Fig. 4: *Cytheridea* aff. *acuminata* left valve interior view (same specimen as Fig. 3)

Fig. 6: *Cytheridea* aff. *acuminata* dorsal view (same specimen as Fig. 3)

Plate 4

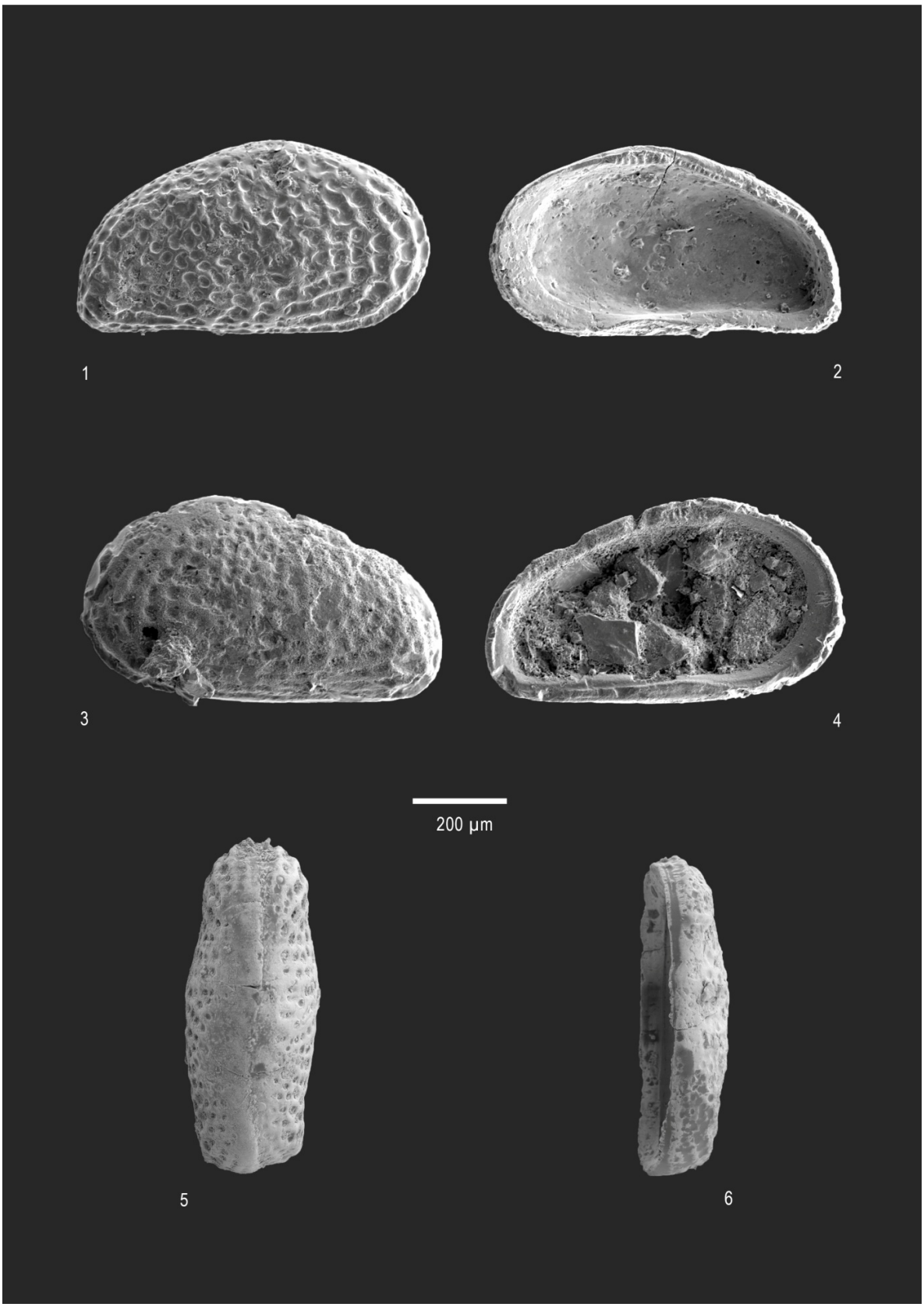

Plate 5

Figures 1, 2, 5, 6: ***Krithe*** aff. ***compressa*** SEGUENZA 1880

Fig. 1: *Krithe* aff. *compressa* right valve

Fig. 2: *Krithe* aff. *compressa* right valve interior view (same specimen as Fig. 1)

Fig. 5: *Krithe* aff. *compressa* dorsal view

Fig. 6: *Krithe* aff. *compressa* ventral view (same specimen as Fig. 6)

Figures 3, 4, 7: ***Parakrithe*** cf. ***soustonsensis*** *(*MOYES 1965)

Fig. 3: *Parakrithe* cf. *soustonsensis* right valve juvenile

Fig. 4: *Parakrithe* cf. *soustonsensis* right valve juvenile interior view
(same specimen as Fig. 3)

Fig. 7: *Parakrithe* cf. *soustonsensis* dorsal view

Plate 5

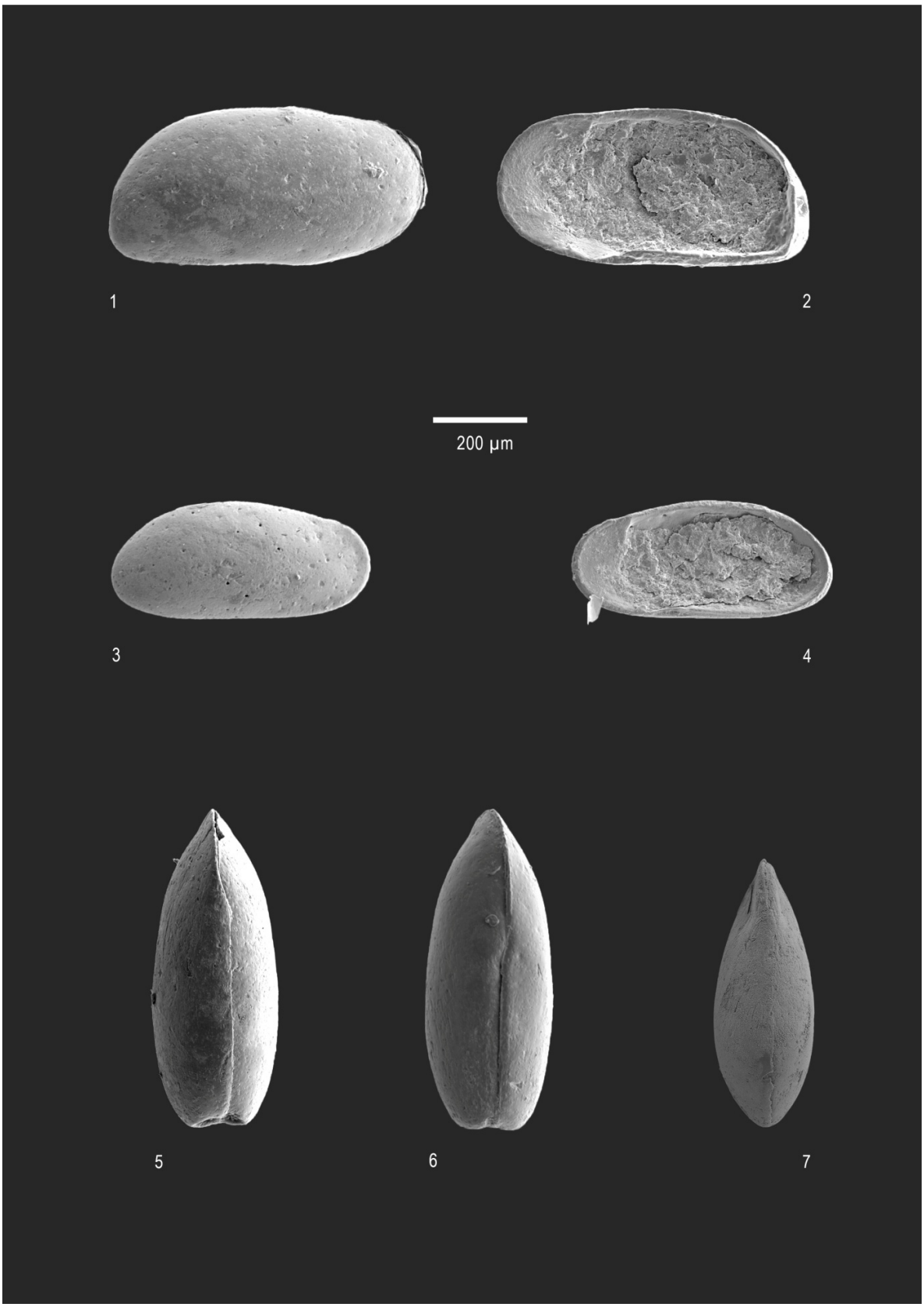

Plate 6

Figures 1, 2, 5, 6: ***Buntonia brunensis*** RIHA 1985

Fig. 1: *Buntonia brunensis* right valve

Fig. 2: *Buntonia brunensis* right valve interior view (same specimen as Fig. 1)

Fig. 5: *Buntonia brunensis* dorsal view

Fig. 6: *Buntonia brunensis* ventral view (same specimen as Fig. 5)

Figures 3, 4, 7: ***Costa punctatissima*** RUGGIERI 1962

Fig. 3: *Costa punctatissima left valve*

Fig. 4: *Costa punctatissima* right valve (same specimen as Fig. 3)

Fig. 7: *Costa punctatissima* dorsal view (same specimen as Fig. 3)

Plate 6

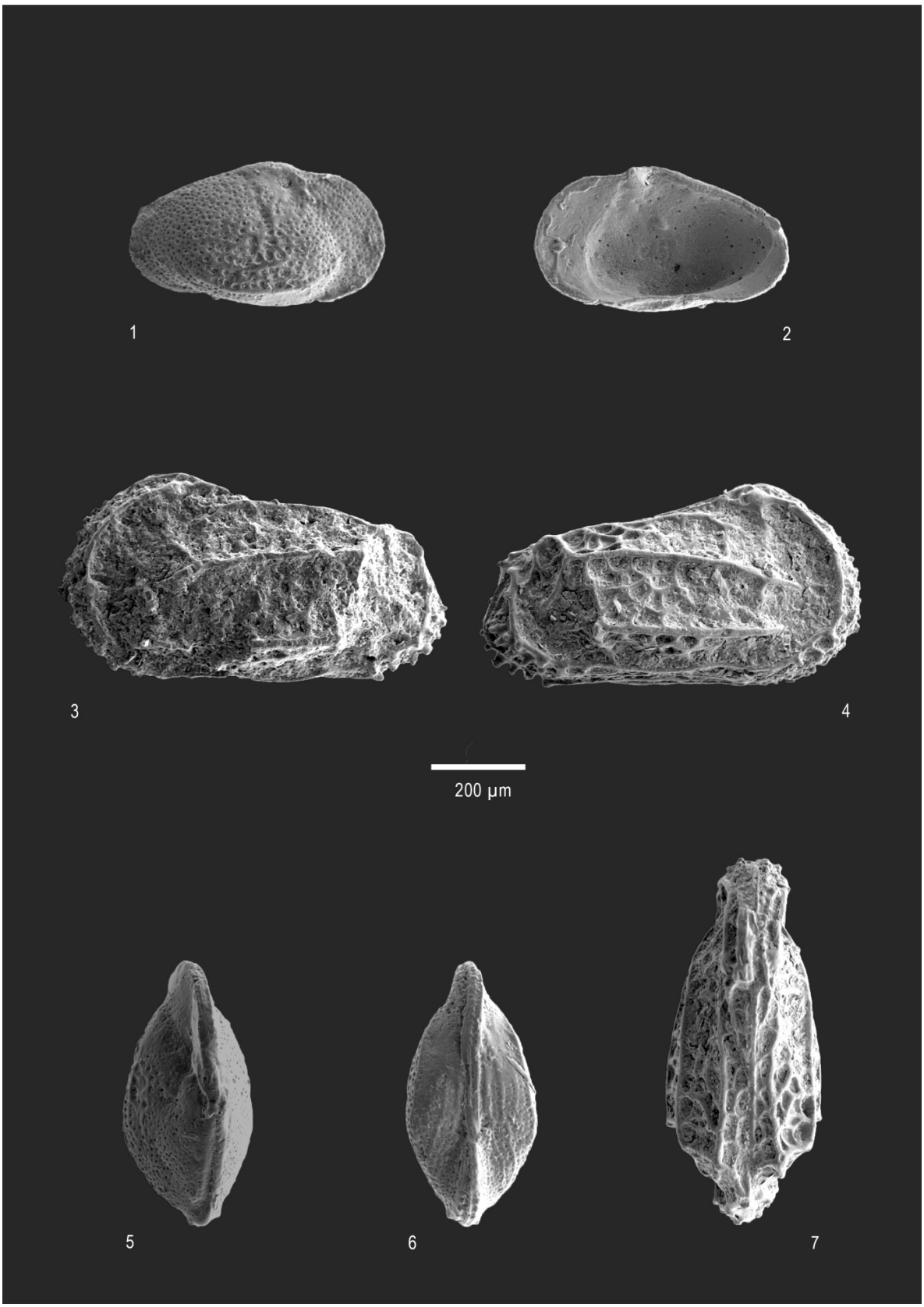

Plate 7

Figures 1, 2, 5: ***Henryhowella asperrima*** (REUSS 1850)

Fig. 1: *Henryhowella asperrima* left valve

Fig. 2: *Henryhowella asperrima* left valve interior view (same specimen as Fig. 1)

Fig. 5: *Henryhowella asperrima* dorsal view

Figures 3, 4, 6: ***Occultocythereis*** cf. ***bituberculata*** (REUSS 1850)

Fig. 3: *Occultocythereis* cf. *bituberculata* view of the left valve

Fig. 4: *Occultocythereis* cf. *bituberculata* view of the right valve (same specimen as Fig. 3)

Fig. 6: *Occultocythereis* cf. *bituberculata* dorsal view (same specimen as Fig. 3)

Plate 7

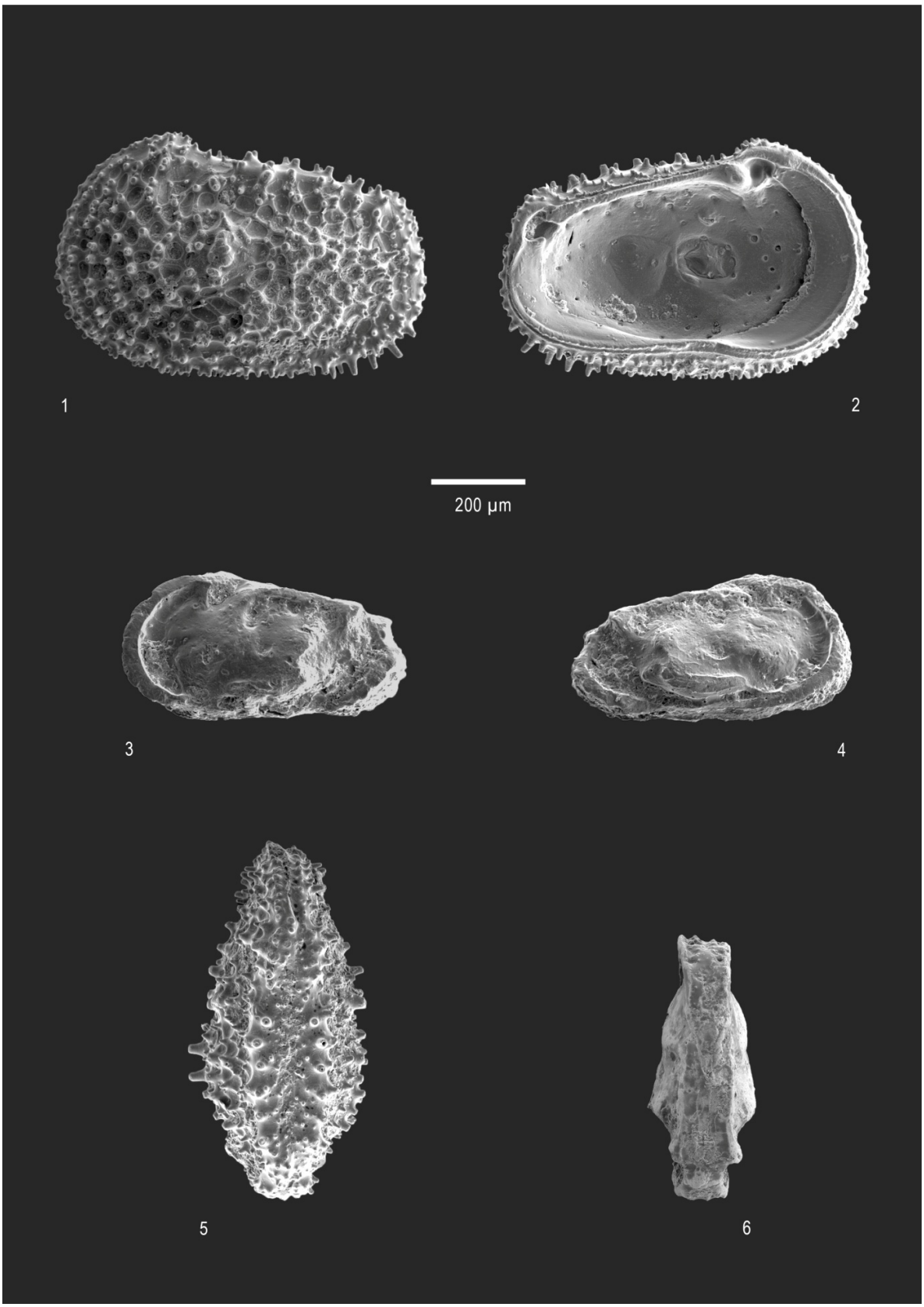

Plate 8

Figures 1, 2, 5: ***Olimfalunia*** cf. ***plicatula*** (REUSS 1850)

Fig. 1: *Olimfalunia cf*. plicatula right valve

Fig. 2: *Olimfalunia cf*. plicatula right valve interior view

Fig. 5: *Olimfalunia cf*. plicatula dorsal view (same specimen as Fig. 1)

Figures 3, 4, 6: ***Pterygocythereis calcarata*** (BOSQUET 1852)

Fig. 3: *Pterygocythereis calcarata* left valve

Fig. 4: *Pterygocythereis calcarata* left valve interior view (same specimen as Fig. 3)

Fig. 6: *Pterygocythereis calcarata* dorsal view (same specimen as Fig. 3)

Plate 8

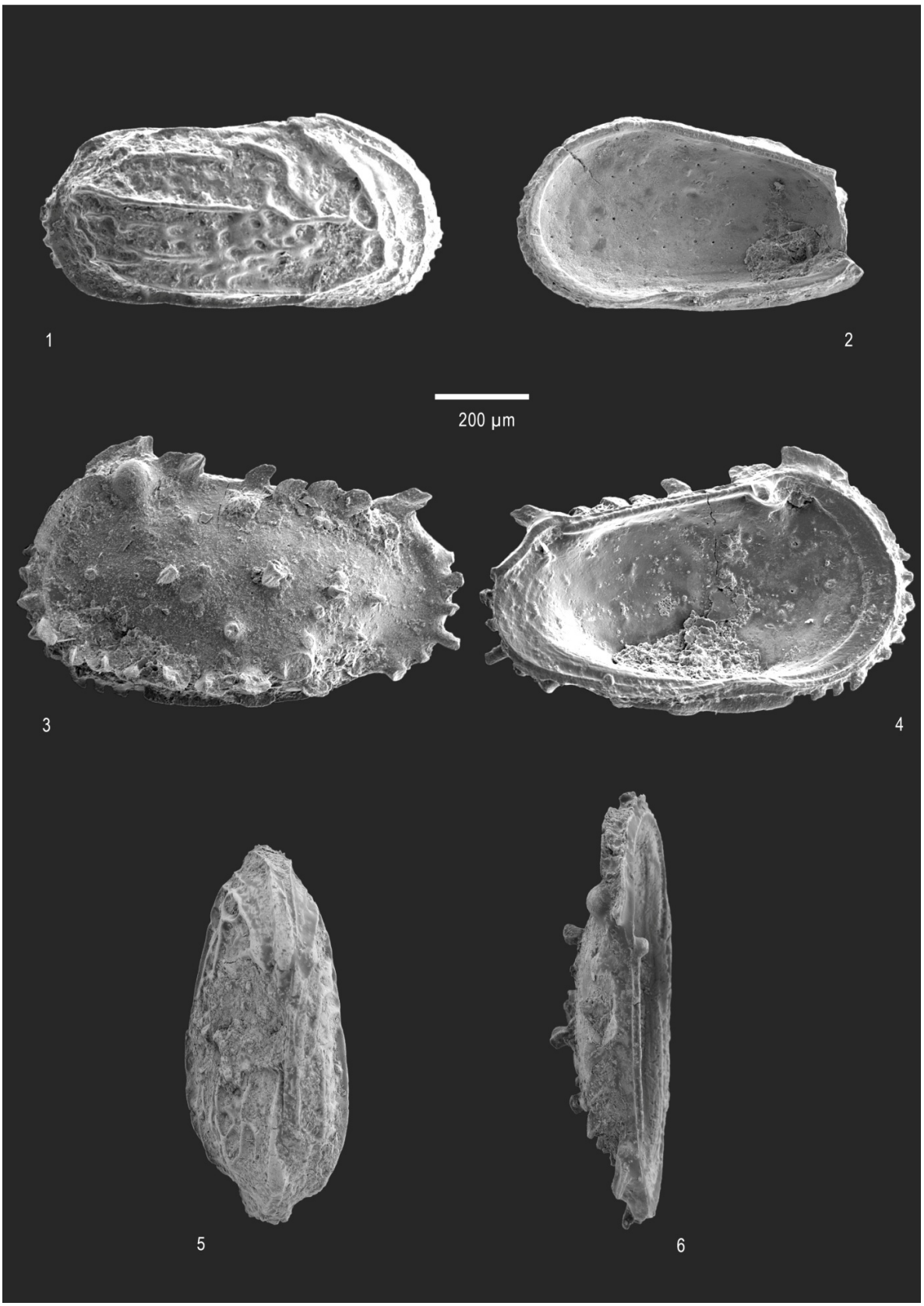

Plate 9

Figures 1, 2, 5: ***Aurila punctata*** (MUENSTER 1830)

Fig. 1: *Aurila punctata* left valve

Fig. 2: *Aurila punctata* left valve inner view (same specimen as Fig. 1)

Fig. 5: *Aurila punctata* dorsal view (same specimen as Fig. 1)

Figures 3, 4, 6: ***Senesia*** cf. ***cinctella*** (REUSS 1850)

Fig. 3: *Senesia* cf. *cinctella* right valve

Fig. 4: *Senesia* cf. *cinctella* right valve inner view (same specimen as Fig. 3)

Fig. 6: *Senesia* cf. *cinctella* dorsal view (same specimen as Fig. 3)

Plate 9

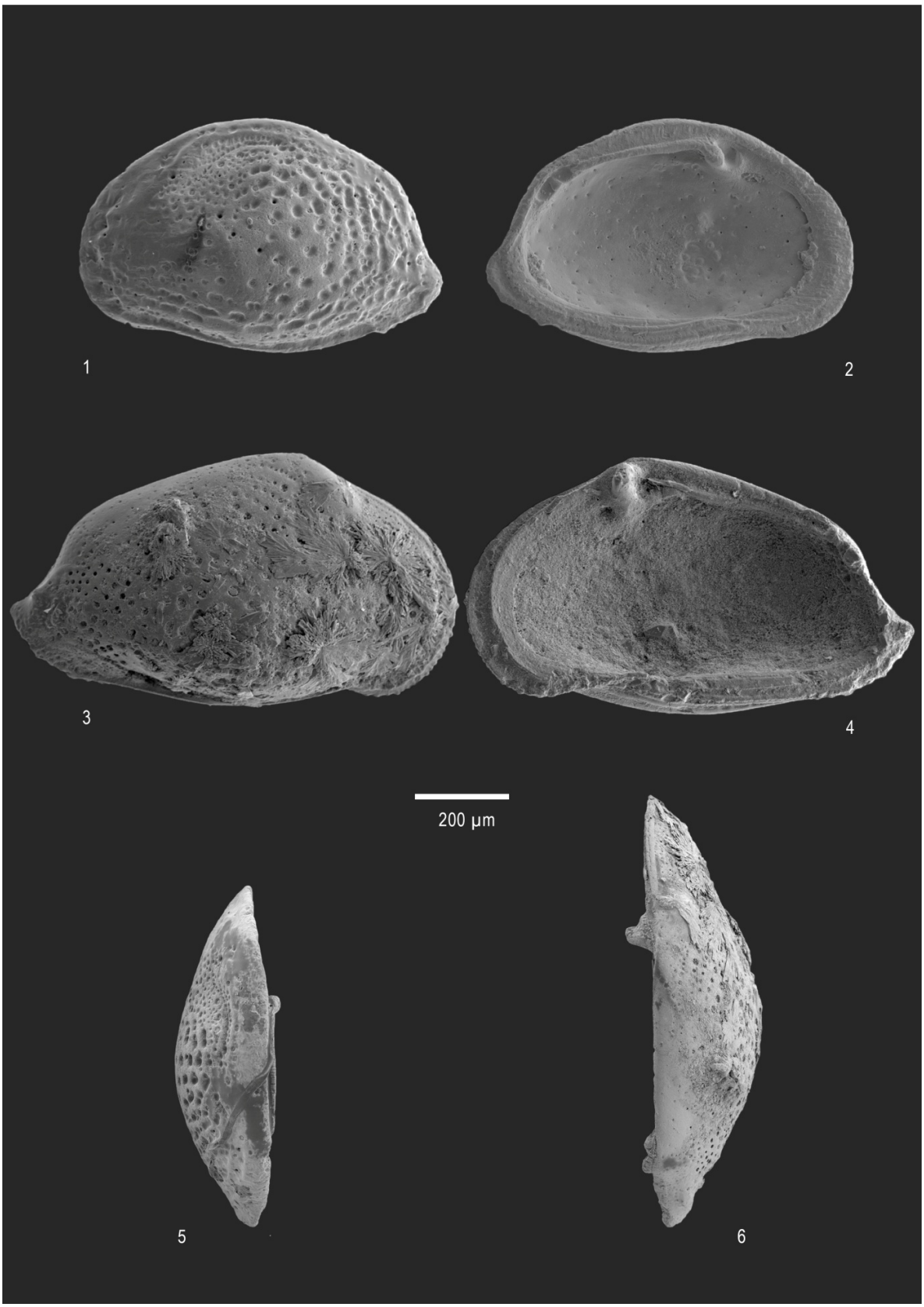

Plate 10

Figures 1, 2, 3: ***Grinioneis*** cf. ***haidingeri*** (REUSS 1850)

Fig. 1 *Grinioneis* cf. *haidingeri* left valve

Fig. 2: *Grinioneis* cf. *haidingeri* dorsal view (same specimen as Fig. 1)

Fig. 3: *Grinioneis* cf. *haidingeri* ventral view (same specimen as Fig. 1)

Plate 10

Plate 11

Figures 1, 2, 3, 4: ***Loxocorniculum hastatum*** (REUSS 1850)

Fig. 1: *Loxocorniculum hastatum* juvenile left valve

Fig. 2: *Loxocorniculum hastatum* juvenile left valve interior view (same specimen as Fig. 1)

Fig. 3: *Loxocorniculum hastatum* juvenile dorsal view

Fig. 4: *Loxocorniculum hastatum* juvenile ventral view (same specimen as Fig. 3)

Figures 5, 6, 7: ***Xestoleberis* sp.** (SARS 1866)

Fig. 5: *Xestoleberis* sp. juvenile left valve

Fig. 6: *Xestoleberis sp.* juvenile dorsal view (same specimen as Fig. 5)

Fig. 7: *Xestoleberis* sp. juvenile ventral view (same specimen as Fig. 5)

Plate 11

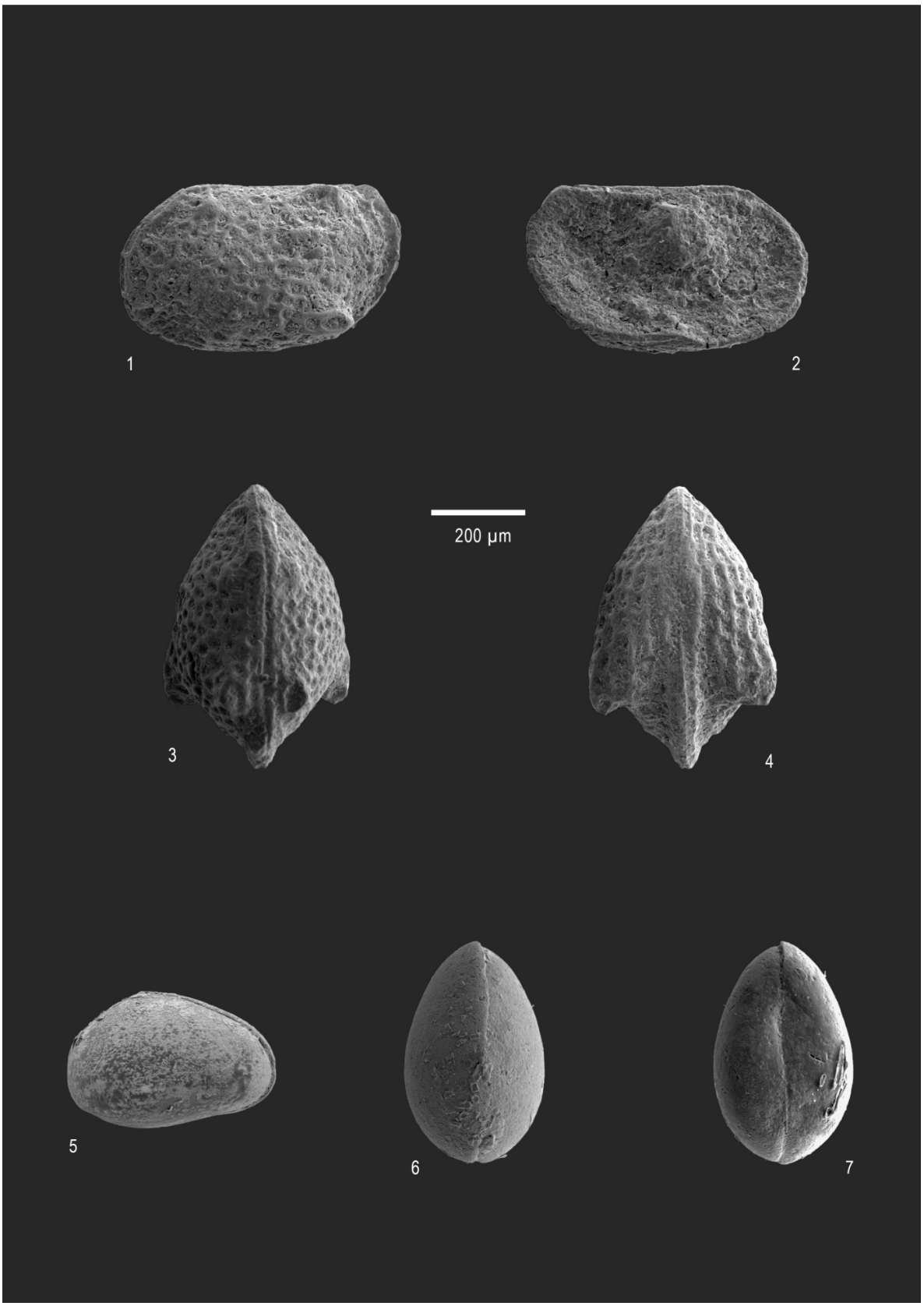

Plate 12

Figures 1, 2, 3, 4: **Muscle scar area**

Fig. 1: *Buntonia brunensis* RIHA 1985

Fig. 2: *Henryhowella asperrima* (REUSS 1850)

Fig. 3: *Henryhowella asperrima* (REUSS 1850)

Fig. 4: *Aurila punctata* (MUENSTER 1830)

Plate 12

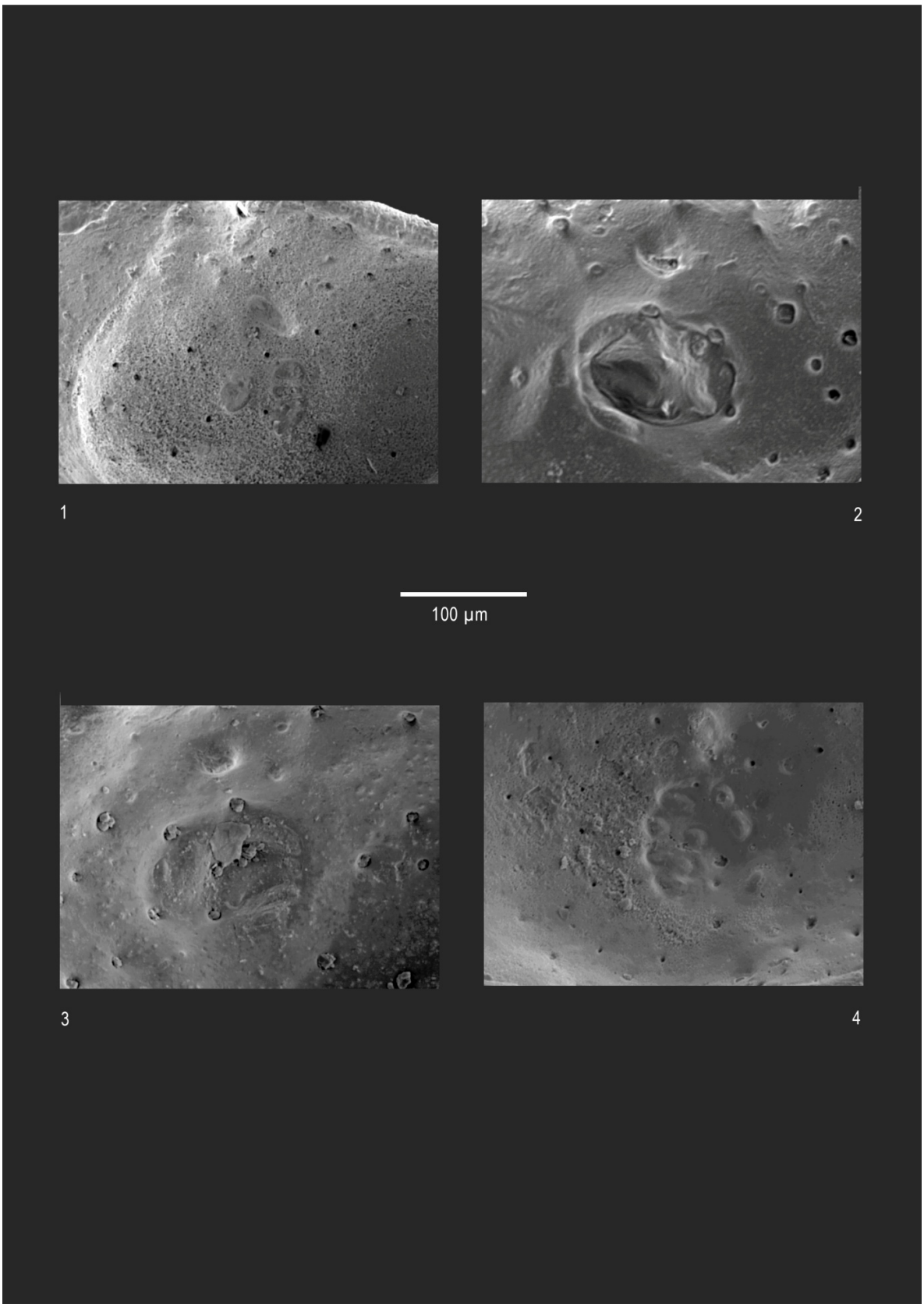

Plate 13

Figures 1, 2, 3, 4, 5 **Hinge details**

Fig. 1: *Henryhowella asperrima* (REUSS 1850)

Fig. 2: *Henryhowella asperrima* (REUSS 1850)

Fig. 3: *Pterygocythereis calcarata* (BOSQUET 1852)

Fig. 4: *Pterygocythereis calcarata* (BOSQUET 1852)

Fig. 5: *Aurila punctata* (MUENSTER 1830)

Plate 13

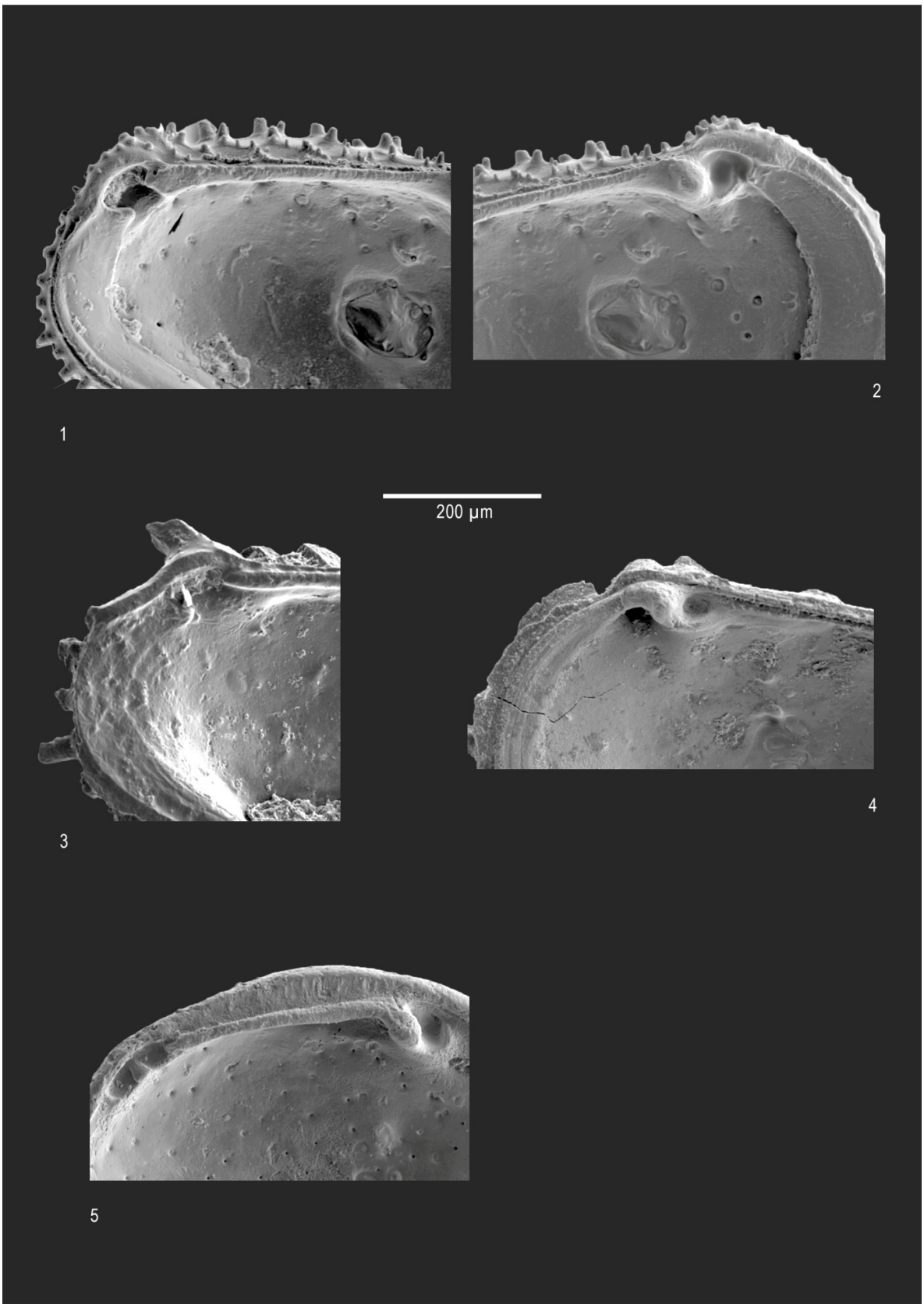

References

Aiello, G., Barra, D., Bonaduce, G., Russo, A., 1996. The Genus Cytherella JONES, 1849 (Ostracoda) in the in the Italian Tortonian – Recent. Revue de Micropaléontologie, 39 (3), 171-190.

Aiello, G. & Szczechura, J. (2004): Middle Miocene ostracods of the For-Carpathian Depression (Central Paratethys, southwestern Poland). Bolletino della Società Paleontologica Italiana, 43 (1-2), 11-70.

Alexander, C.I., 1929. Ostracoda of the Cretaceous of North Texas. University of Texas Bulletin, Austin, vol. 2907, 1-137.

Aranki, J.F., 1987. Marine Lower Pliocene Ostracoda of southern Spain with notes on the Recent fauna. Bulletin of the Geological Institution of the University of Upsala, N.S., 13, 1-94.

Auer, J., 1996. Biostratigraphische und magnetostratigraphische Untersuchungen im Grenzbereich Unter- und Mittelmiozän (Karpatium/Badenium) der Paratethys, Ziegelei Aflenz/Wagna, Steirisches Becken, Steiermark, Österreich. Unpublished PhD Thesis, University of Vienna, 138 pp.

Báldi, T., 1980. A korai Paratethys története. Födtani Köszlöny, 110, 456-472.

Berner, R.A., 1984. Sedimentary pyrite formation: An update. Geochimica et Cosmochimica Acta 48, 605–615.

Berner, R.A., Raiswell, R., 1984. C/S method for distinguishing freshwater from marine sedimentary rocks. Geology 12, 365–368.

Böhme, M., 2003. The Miocene Climatic Optimum: evidence from ectothermic vertebrates of Central Europe. Palaeogeography, Palaeoclimatology, Palaeoecology 195 (3-4), 389-401.

Bojar, A.-V., Hiden, H., Fenninger, A., Neubauer, F., 2004. Middle Miocene seasonal temperature changes in the Styrian basin, Austria, as recorded by the isotopic composition of pectinid and brachiopod shells. Palaeogeography, Palaeoclimatology, Palaeoecology 203, 95-105.

Bold van den, W.A., 1968. Ostracoda of the Yague group (Neogene of the northern Dominican Republic). Bulletin of American Paleontology, 54, 239-266.

Bonaduce, G., Ciampo, G. Masoli, M., 1976. Distribution of Ostracoda in the Adriatic Sea.- Pubblicazioni della Stazione Zoologica di Napoli, 40, 1-304.

Bonaduce, G. & Russo, A., 1985. The Miocene Ostracodes of Sardinia. Bollettino della Società Paleontologica Italiana, 23 (2), 421-437.

Bonaduce, G. & Danielopol, D.L., 1988. To See and Not to Be Seen: The Evolutionary Problems of the Ostracoda Xestoleberididae.- In: Hanai, T., Ikeya, N. & Ishizaki, K. (Eds.): Evolutionary biology of ostracoda.- Developments in Paleontology and Stratigraphy, 11, 375-398.

Bonaduce, G., Barra, D. & Aiello, G., 1998. The areal and bythymetrical distribution of the genus *Henryhowella* Puri (Ostracoda) in the Gulf of Naples. Bulletin du Centre de Recherches Elf Exploration Production, 20, 133-139.

Bonaduce, G, Barra, D., Aiello, G., 1999. The genus *Henryhowella* Puri, 1957 (Crustacea, Ostracoda) in the Atlantic and Mediterranean from Miocene to Recent. Bollettino della Società Paleontologica Italiana, 38 (1), 59-72.

Boomer, I. & Whatley, R., 1992. Ostracoda and dysaerobia in the Lower Jurassic of Wales: the reconstruction of past oxygen levels. Palaeogeography, Palaeclimatology, Palaeoecology, 99, 373-379.

Bosquet, J., 1852. Description des Entomostracés fossiles des terrains Tertiaires de la France et de la Belgique. Mémoires de l'Académie royale des sciences, Belgique, 24, 142 pp.

Breman, E., 1976. The distribution of ostracods in the bottom sediments of the Adriatic Sea. Dissertation University of Amsterdam, 165 pp.

Brestenska, E. & Jiricek, R., 1978. Ostrakoden des Badenien der Zentralen Paratethys.- In: Brestenska, E. (Ed.): Chronostratigraphie und Neostratotypen: Miozän der Zentralen Paratethys, Band VI M4 Badenien (Moravien, Wielicien, Kosovien), 405-439, Verlag Slowakische Akademie der Wissenschaften.

Brestenska, E., 1975. Ostracoden des Egerien.- In: Baldi, T. & Senes, J (Ed.): Chronostratigraphie und Neostratotypen: Miozän der Zentralen Paratethys, Band 5 OM Egerien. Die Egerer, Pouzdraner, Puchkirchener Schichtengruppe und die Bretkaer Formation. 377-435, Verlag Slowakische Akademie der Wissenschaften.

Carbonel, P., 1985. Néogène.- In: Oertli, H.J. (Ed.): Atlas des Ostracodes des France (Paléozoïque-Actuel). Bulletin des centres de recherches exploration-production Elf-Aquitaine, Mem 9, 313-335.

Cernajsek, T., 1971. Die Entwicklung und Abgrenzung der Gattung Aurila Pokorny (1955) im Neogen Österreichs.- Dissertation University of Vienna, 198 pp.

Cernajsek, T., 1972. Zur Palökologie der Ostrakodenfaunen am Westrand des Wiener Beckens.- Verhandlungen der geologischen Bundesanstalt, 1972 (2), 237-246.

Clarke, K.R., 1993. Non-parametric multivariate analysis of changes in community structure. Australian Journal of Ecology 18, 117-143.

Clarke, K.R. & Ainsworth, M, 1993. A method of linking multivariate community structure to environmental variables. Marine Ecology Progress Series 92, 205-219.

Coles, G.P., Whatley, R.C. & Monguilevsky, A., 1994. The ostraced genus Krithe from the Tertiary and Quatemary of the North Atlantic. Palaeontology 37, 71-120.

Ćorić, S., Švábenická, L., Rögl, F., Petrová, P., 2007. Stratigraphical position of Helicosphaera waltrans nannoplankton horizon (NN5, Lower Badenian). Joannea - Geologie und Paläontologie 9, 17-19.

Decker, K. & Peresson, H., 1996. Tertiary kinematics in the Alpine-Carpathian-Pannonian system: links between thrusting, transform faulting and crustal extension. In: Wessely, G. & Liebl, W. (Eds.), Oil and Gas in Alpidic thrustbelts and basins of Central and Eastern Europe. EAGE Special Publications, 5, 69-77.

Demaison, G.J. & Moore, G.T., 1980. Anoxic environments and oil source bed genesis. Organic Geochemistry, 2(1), 9-31.

Didié C., Bauch H.A. & Helmke J.P., 2002. Late Quaternary deepsea ostracods in the polar and subpolar North Atlantic: paleoecological and paleoenvironmental implications. Palaeogeography, Palaeoclimatology, Palaeoecology, 184: 195-212.

Dieci, G. & Russo, A., 1965. Ostracodi tortoniani dell'Appennino settentrionale (Tortona, Montegibbo, Castelvetro). Bollettino della Società Paleontologica Italiana. 3 (1), 38-88.

Ducasse, O. & Cahuzac, B., 1996. Évolution de la faune d'ostracodes dans un cadre paléogéographique et interprétation des paléoenvironnements au Langhien en Aquitaine. Revue de Micropaléontologie, 39 (4), 247-260.

Ducasse, O. & Cahuzac, B., 1997. Les ostracods indicateurs des paléoenvironnements au Miocène moyen (Serravallien) an Aquinaine (Sud-ouest de la France). Revue de Micropaléontologie, 40 (2), 141-166.

Dullo, W.-C., 1983. Diagenesis of fossils of the Miocene Leitha Limestone of the Paratethys, Austria: an example for faunal modifications due to changing diagenetic environments. Facies 8, 1–112.

Ebner, F. & Sachsenhofer, R.F., 1995. Palaeogeography, subsidence and thermal history of the Neogene Styrian basin (Pannonian basin system, Austria). Tectonophysics 242, 133–150.

Elofson, 1941. Zur Kenntnis der marinen Ostracoden Schwedens, mit besonderer Berücksichtigung des Skagerraks. Zoologiska Bidrag fr. Uppsala. 19, 215-534.

Erhart, C., 2004. Fazies und Geometrie von Leithakalken am Beispiel Retznei/Rosenberg. unpublished Master thesis, Karl-Franzens-Universität Graz, 143 pp.

Fenninger, A. & Hubmann, B., 1997. Palichnologie an der Karpatium/Badenium - Grenze des Steirischen Tertiärbeckens (Österreich). Geologische-Paläontologische Mitteilungen Innsbruck, 22, 71-83.

Friebe, J.G., 1988. Paläogeographische Überlegungen zu den Leithakalkarealen (Badenien) der Mittelsteirischen Schwelle (Steiermark). Geologische und Paläontologische Mitteilungen Innsbruck 15, 41-57.

Friebe, J.G., 1989. Stratigraphie und Fazies der Leithakalk-areale der Mittelsteirischen Schwelle (Steirisches Becken, Badenien). unpublished Dissertation, University of Graz, 322 pp.

Friebe, J.G., 1990. Lithostratigraphische Neugliederung und Sedimentologie der Ablagerungen des Badenien (Miozän) um die Mittelsteirische Schwelle (Steirisches Becken, Österreich). Jahrbuch der Geologischen Bundesanstalt, 133(2), 223-257.

Friebe, J.G., 1991. Neotektonik an der Mittelsteirischen Schwelle (Österreich): Die „Steirische Phase“. Zentralblatt für Geologie und Paläontologie I, 41-54.

Friebe, J.G., 1993. Sequence stratigraphy in a mixed carbonate-silicilastic depositional system (Middle Miocene; Styrian Basin, Austria). Geologische Rundschau 82, 281-294.

Frisch, W., Dunkl, I., Kuhlemann, J., 2000. Post-collisional orogen-parallel large-scale extension in the Eastern Alps. Tectonophysics, 327, 239-265

Fritz, I. & Hiden, H., 2001. Fossilgrabung im Steinbruch Retznei (Südsteiermark). Projektmappe für Schulen, 40 pp.

Goerlich, F., 1953. Ostrakoden der Cytherieinae aus der Tertiären Molasse Bayerns. Senckenbergiana, 34 (1/3), 117-148.

Gradstein, F.M., Ogg, J.G., Hilgen, F.J., 2012. On The Geologic Time Scale. Newsletters on Stratigraphy, 45 (2), 171–188.

Gross, M., 2002. Mittelmiozäne Ostracoden aus dem Wiener Becken (Badenium/Sarmatium, Österreich). Unpublished Dissertation, University of Graz, Department of Earth science, 343 pp.

Gross, M., 2006. Mittelmiozäne Ostracoden aus dem Wiener Becken (Badenium/Sarmatium, Österreich). Schriftenreihe der Erdwissenschaftlichen Kommissionen S1 (Ed.: Piller, W.E.), 224pp.

Gross, M., Fritz, I., Piller, W.E., Soliman, A., Harzhauser, M., Hubmann, B., Moser, B., Scholger, R., Suttner, T.J., Bojar, H-P., 2007. The Neogene of the Styrian Basin – Guide to Excursions. Joannea - Geologie und Paläontologie 9, 117-193.

Hammer, Ø. & Harper, D.A.T., 2006. Paleontological Data Analysis. Blackwell Publishing, Oxford.

Hammer, Ø., Harper, D.A.T., Ryan, P.D., 2001. PAST: paleontological statistics software package for education and data analysis. Palaeontologia Electronica 4, 1-9.

Handler, R., Ebner, F., Neubauer, F., Bojar, A.-V., Hermann, S., 2006. 40Ar/39Ar dating of Miocene tuffs from the Styrian part of the Pannonian Basin: an attempt to refine basin stratigraphy. Geologica Carpathica 57, 483–494.

Haq, B.U., Hardenbol, J., Vail, P.R., 1988. Mesozoic and Cenozoic chronostratigraphy and cycles of sea level changes. Wilgus, C.K. (ed.), Sea-level changes - an integrated approach. Society of Economic Paleontologists and Mineralogists, Special Publications 42, 71-108.

Harten van, D., 1995. Differential food-detection: A speculative reinterpretation of vestibule variability in *Krithe* (Crustacea: Ostracoda).- In: Riha, J. (Ed): Ostracoda and Biostratigraphy, Proceedings of the 12th International Symposium on Ostracoda, Prague 1994. 33-36.

Harten van, D., 1996. The case against *Krithe* as a tool to estimate the depth and oxygenation of ancient oceans. - In: Moguilevsky, A. & Whatley, R. (Eds.): Microfossils and oceanic environments. University of Wales, Aberystwyth-Press, Aberystwyth, United Kingdom, 297-304.

Hartmann, G., 1975. Ostracoda.- Dr. H.G. Bronns Klassen und Ordnungen des Tierreichs, 5, 1. Abt., 2. Buch, 4. Teil, 4. Lieferung (1975), 569-786, VEB Gustav Fischer Verlag, Jena.

Harzhauser M., Piller W. E., Müllegger S., Grunert P., Micheels A., 2011. Changing seasonality patterns in Central Europe from Miocene Climate Optimum to Miocene Climate Transition deduced from the Crassostrea isotope archive. Global and Planetary Change 76, 1–2, 77–84.

Harzhauser, M., Piller, W.E., Steininger, F.F., 2002. Circum-Mediterranean Oligo-Miocene biogeographic evolution – the gastropods point of view. Palaeogeography, Palaeoclimatology, Palaeoecology 183, 103-133.

Harzhauser, M., Mandic, O., Zuschin, M., 2003. Changes in Paratethyan marine molluscs at the Early/Middle Miocene transition: diversity, palaeogeography and palaeoclimate. Acta Geologica Polonica 53, 323-339.

Harzhauser, M. & Piller, W.E., 2007. Benchmark data of a changing sea – Palaeogeography, Palaeobiogeographie and Events in the Central Paratethys during the Miocene. Palaeogeography, Palaeoclimatology, Palaeoecology 253, 8-31.

Helmdach, F.-F., 1977. Leitfaden zur Bestimmung fossiler und rezenter Ostracoden.-1. Aufl., 264 pp., de Gruyter, Berlin/New York.

Hinz-Schallreuter, I. & Schallreuter, R., 1999. Ostrakoden.- Haeckel-Bücherei, 4, 169 S., F.Enke Verlag, Stuttgart.

Hohenegger, J., Rögl, F., Ćorić, S., Pervesler, P., Lirer, F., Roetzel, R., Scholger, R., Stingl, K., 2009. The Styrian Basin: A key to the Middle Miocene (Badenian/Langhian) Central Paratethys transgressions. Austrian Journal of Earth Sciences 102, 102-132.

Huber-Mahdi, T., 1984. Beschreibung und Dokumentation von Ostracoden aus dem Badenien von Niederösterreich und Burgenland. Unpublished research paper. Fonds zur Förderung wissenschatflicher Forschung. 178 pp.

Huber-Mahdi, T., 1986. Über neogene Ostracoden im Lavanttal, Kärnten. Unpublished research paper. Fonds zur Förderung wissenschatflicher Forschung. 45 pp.

Hunt, J.M., 1996. Petroleum Geochemistry and Geology. W.H. Freeman and Company, 743 pp.

Kelsing, R. V., 1951. Terminology of Ostracod carapaces. Contributions from the Museum of Paleontology University of Michigan, 9 (4), 93-171.

Kempf, E. K., & Nink, C., 1993. Henryhowella asperrima (Ostracoda) aus der Typusregion (Miozän: Badenian; Wiener Becken). Sonderveröffentlichungen, Geologisches Institut der Universität Köln, 70, 95-114.

Kilenyi, T.I., 1971. Some basic questions in the palaeoecology of ostracods. –In: Oertli, H.J. (Ed.): Paléoécologie des Ostracodes. Bulletin Centre de Recherches, Societé Nationale Pétrole d'Aquitaine, 5, 31-44.

Kollmann, K., 1960. Cytherideinae und Schulerideinae n. subfam. (Ostracoda) aus dem Neogen des östl. Oesterreich.- Mitteilungen der Geologischen Gesellschaft in Wien 51, 89-195.

Kollmann, K., 1965. Jungtertiär im Steirischen Becken. Mitteilungen der Geologischen Gesellschaft in Wien 57 (2), 479-632.

Kovac, M., Barath, I., Harzhauser, M., Hlavaty, I., Hudackova, N., 2004. Miocene depositional systems and sequence stratigraphy of the Vienna Basin. Courier Forschungsinstitut Senckenberg, 246, 187-212.

Kovác, M., Nagymarosy, A., Oszczypko, N., Csontos, L., Slaczka, A., Marunteanu, M., Matenco, L., Márton, E., 1998. Palinspastic reconstruction of the Carpathian – Pannonian region during the Miocene. - In: Rakús, M., (Ed.) Geodynamic development of the Western Carpathians, 189-217.

Kroh, A., 2007. Climate changes in the Early to Middle Miocene of the Central Paratethys and the origin of its echinoderm fauna. Palaeogeography, Palaeoclimatology, Palaeoecology 253, 169–207.

Kröll, A., Flügel, H.W., Seiberl, W., Weber, F., Walach, G., Zych, D., 1988. Erläuterungen zu den Karten über den prätertiären Untergrund des Steirischen Beckens und der Südburgenländischen Schwelle. Geologische Bundesanstalt, 1-49.

Lewis, A.R., Marchant, D.R., Ashworth, A.C., Hemming, S.R., Machlus, M.L., 2007. Major middle Miocene global climate change: Evidence from East Antarctica and the Transantarctic Mountains. Geological Society of America Bulletin 119, 1449-1461.

Liebau, A., 1975. Comment on suprageneric Taxa of Trachyleberididae s.n. (Ostracoda, Cytheracea). Neues Jahrbuch für Geologie und Paläontologie Abhandlungen, 148 (3), 353-379.

Liebau, A., 1980. Paläobathymetrie und Ökofaktoren: Flachmeer-Zonierungen. Neues Jahrbuch für Geologie und Paläontologie Abhandlungen, 160 (2), 173-216.

Malz, H. & Jellinek, T., 1984. Marine Plio-/Pleistozän-Ostracoden von SE-Lakonien (Peloponnes, Griechenland). Senckenbergiana biologica 65 (1/2), 113-167.

Marshall, J.D., 1992. Climatic and oceanographic isotopic signals from the carbonate rock record and their preservation. Geological Magazine 129, 143-160.

Márton, E., 2006. Paleomagnetic constraints for the reconstruction of the geodynamic evolution of the Middle Miocene-Pleistocene. - In: Pinter, N., Grenerczy, G., Weber, J., Stein, S., Medak, D., (Eds.). The Adria Microplate: GPS geodesy, tectonics and hazards, 55-64.

Márton, E., Drobne, K., Cosovic, V., Moro, A., 2003. Palaeomagnetic evidence for Tertiary counterclockwise rotation of Adria. Tectonophysics, 377: 143-156.

Márton, E., Jelen, B., Tomljenovic, B., Pavelic, D., Poljak, M., Márton, P., Avanic, R., Pamic, J., 2006. Late Neogene counterclockwise rotation in the SW part of the Pannonian Basin. Geologica Carpathica, 57, 41-46.

Meisch, C., 2000. Freshwater Ostracoda of Western and Central Europe.- In: Schwoerbel, J. & Zwick, P. (Eds.): Süßwasserfauna von Mitteleuropa.- Bd. 8 (3), 522 pp., Spektrum Akademischer Verlag, Heidelberg/Berlin.

Mitrovic, S., 1998. Sarmatian microfauna from boreholes B-3 and B-4, Belgrade area.- Annales Géologiques de la Péninsule Balkanique, 62, 179-191.

Montenegro, M.E. & Pugliese, N., 1996. Autecological remarks on the ostracods distribution in the Marano and Grado Lagoons (Northern Adriatic Sea, Italy). – Bollettino della Società Paleontologica Italiana, 3, 123-132.

Montenegro, M.E., Pugliese, N., Bonaduce, G., 1998. Shelf Ostracods distribution in the Italian seas. – What about Ostracoda! Actes du 3e Congrès Européen des

Ostracodologistes, 1996 - Bulletin du Centre de Rrecherches Elf Exploration Production 20, 91-101.

Morkhoven van, F.P.C.M., 1962. Post-Palaeozoic Ostracoda, their Morphology, Taxonomy, and Economic use. Volume 1, General.- 204 S., Elsevier, Amsterdam/London/New York.

Morkhoven van, F.P.C.M., 1963. Post-Palaeozoic Ostracoda, their Morphology, Taxonomy, and Economic use. Volume 3, General descriptions.- 478 pp., Elsevier, Amsterdam/London/New York.

Moyes, J., 1965. Les Ostracodes du Miocène aquitan. Essai de paléoécologie stratigraphique et de paléogéographie. 339 pp.

Muenster von, G., 1830. Ueber einige fossile Arten *Cypris* (Mueller, Lamk.) und *Cythere* (Mueller, Latreille, Desmarest). Jahrbuch für Minerologie, Geognosie, Geologie und Petrefaktenkunde, 1, 60-67.

Murray, J.W., 2006. Ecology and Applications of Benthic Foraminifera. Cambridge University Press, 426 pp.

Nevesskaja, L.A., Goncharova, I.A., Paramonova, N.P., Popov, S.B., Babak, E.B., Bagdasarjan, K.G., Voronina, A.A., 1993. Opredelitelj miocenovj ih dvustvorchatjih molljuskov Jugo-Zapadnoi Evrazii. Moskow: Nauka, 412 pp.

Oertli, H. & Key, A.J., 1955. Drei neue Ostrakoden-Arten aus dem Oligozän Westeuropas. Bulletin der Vereinigung Schweizer Petroleum-Geologen und -Ingenieure, 22 (62), 19-28.

Oertli, H.J., 1956. Ostrakoden aus der oligozänen und miozänen Molasse der Schweiz. Abhandlungen der Schweizerischen Paläontologischen Gesellschaft 74, 1-119.

Oertli, H.J., 1971. The aspect of ostracode faunas – a possible new tool in petroleum sedimentology.- In: Oertli, H.J. (Ed.): Paléoécologie des Ostracodes. – Bulletin du Centre de Recherche de Pau, 5, 137-151.

Olteanu, R., 1971. Faune des Ostracodes des dépôts Tortoniens de Lăpugiu de Sus. Memoires Institut Geologique, 14, 125-142.

Olteanu, R., 2000. The *Loxoconcha* genus (Ostracoda, Crustacea) within Paratethys areas. Memoiriile Institutu Iui Geologic al Romaniei, 37, 47-90.

Peters, K.E., Walters, C.C., Moldowan, J.M., 2005. The Biomarker Guide, Volume 2: Biomarkers and Isotopes in the Petroleum Exploration and Earth History, 2nd ed. Cambridge University Press.

Pietrzeniuk, E., 1969. Taxonomische und biostratigraphische Untersuchungen an Ostracoden des Eozäns 5 im Norden der Deutschen Demokratischen Republik. Paläontologische Abhandlungen, A,4 (1), 1-162.

Piller, W.E., Egger, H., Erhart, C., Gross, M., Harzhauser, M., Hubmann, B., van Husen, D., Krenmayr, H.-G., Krystyn, L., Lein, R., Lukeneder, A., Mandl, G., Rögl, F., Roetzel, R., Rupp, C., Schnabel, W., Schönlaub, H.P., Summesberger, H., Wagreich, M., 2004. Die Stratigraphische Tabelle von Österreich 2004 (Sedimentäre Schichtfolge). Commission for the Palaeontological and Stratigraphical Research of Austria, Austrian Academy of Sciences, Vienna.

Piller, W.E., Harzhauser, M., Mandic, O., 2007. Miocene Central Paratethys stratigraphy – current status and future directions. Stratigraphy 4, 151-168.

Piller, W.E., Kleemann, K., 1991. Miocene reefs and related facies in Eastern Austria. 1) Vienna Basin. VI. International Symposium on Fossil Cnidaria including Archaeocyatha and Porifera, Excursion-Guidebook, Excursion B4, 1–28.

Popov, S.V., Rögl, F., Rozanov, A.Y., Steininger, F.F., Shcherba, I.G., Kovác, M. Eds., 2004. Lithological - Paleogeographic maps of Paratethys. 10 Maps Late Eocene to Pliocene. Courier Forschungsinstitut Senckenberg, 250, 1-46.

Pugliese, N. & Stanley D.J., 1991. Ostracoda, depositional environments and late quaternary evolution of the eastern Nile delta, Egypt. – Il Quaternario, 4 (2), 275-302.

Reuss, A.E., 1850. Die fossilen Entomostraceen des österreichischen Tertiärbeckens. Haidingers Naturwissenschaftliche Abhandlungen, 3 (1), 41-92.

Reuter, M. & Piller, W.E., 2011. Volcaniclastic events in coral reef and seagrass environments: evidence for disturbance and recovery (Middle Miocene, Styrian Basin, Austria). Coral Reefs 30, 889-899.

Reuter, M., Piller, W.E., Erhart, C., 2012. A Middle Miocene carbonate platform under silicivolcaniclastic sedimentation stress (Leitha Limestone, Styrian Basin, Austria) - Depositional environments, sedimentary evolution and palaeoecology. Palaeogeography, Palaeoclimatology, Palaeoecology 350-352, 198-211.

Riegl, B. & Piller, W.E., 2000. Reefs and coral carpets in the Miocene Paratethys (Badenian, Leitha Limestone, Austria). Proceedings 9th International Coral Reef Symposium, Bali, Indonesia I, 211-216.

Ríha, J., 1983. Ostrakoden aus der kalkigen Tone (Tegels) des unteren Badenien (Tertiär-Miozän) in Umgebung der Stadt Brünn. Acta Musei Moraviae, Scientiae Naturales 68, 57-83.

Ríha, J., 1984. Ein Beitrag zur Erkenntnis der Ostracodengemeinschaften in den Bunten Tonen der Karpatischen Vortiefe südöstlich von Brno.- Acta Musei Moraviae, Scientiae Naturales 69, 51-74.

Ríha, J., 1985. *Buntonia brunensis* n. sp. (Ostracoda) from the Lower Badenian (Miocene) of Moravia.- Acta Acta Musei Moraviae, Scientiae Naturales 70, 61-65.

Ríha, J. & Odehnal, F., 1988. Badenian ostracode assemblages of the OS-1 Kravare borehole (Northern Moravia, Czechoslovakia). Acta Musei Moraviae, Scientiae Naturales 73, 51-57.

Roemer, F.A., 1839. Mittheilungen an Professor Bronn gerichtet. Neues Jahrbuch für Mineralogie, Geognosie, Geologie und Petrefaktenkunde, 1839, 430-431, Stuttgart.

Rögl, F., 1998. Palaeogeographic Considerations for Mediterranean and Paratethys Seaways (Oligocene to Miocene). Annalen des Naturhistorischen Museums Wien, A, 99, 279-310.

Rögl, F., 1999. Mediterranean and Paratethys, facts and hypotheses of an Oligocene to Miocene paleogeography (short overview). Geologica Carpathica, 50, 339-349.

Ruggeri, G., 1962. Alcuni Ostracodi quaternari e recenti pertinent al genere *Costa* Neviani. Bolletino della Societa Paleontologica Italiana, 1 (2), 3-9.

Ruggieri, G., 1992. Considerazioni tassonomiche su Ostracodi neogenici e pleistocenici resultate dalla revision di vecchi lavori dell scrivente. Bolletino della Societa Paleontologica Italiana, 31 (2), 175-188.

Sachsenhofer, R. F, Lankreijer, A., Cloetingh, S., Ebner, F. 1997. Subsidence analysis and quantitative basin modelling in the Styrian Basin (Pannonian Basin System, Austria). Tectonophysics 272, 175-196.

Schell, F., 1994. Die Geologie der südlichen Windischen Büheln (Raum Arnfels-Leutschach-Langegg). Unpublished Dissertatiion, Karl-Franzens-Universität Graz, 207 pp.

Schreilechner, M.G. & Sachsenhofer, R.F., 2007. High resolution sequence stratigraphy in the Eastern Styrian Basin (Miocene, Austria). Austrian Journal of Earth Sciences, 100, 164-184.

Schulz, H.D, & Zabel, M., 1999. Marine Geochemistry. 574 pp. Springer, Berlin-Heidelberg-New York.

Sciuto, F. & Rosso, A., 2008. Distribution pattern of deep-water ostracod assemblages from Lower Pleistocene sediments from Furnari, Sicily. Bollettino della Società Paleontologica Italiana, 47 (1), 33-43.

Seghedi, I., Downes, H., Szakács, A., Mason, P.R.D., Thirlwall, M.F., Rosu, E., Pécskay, Z., Márton, E., Panaiotu, C., 2004. Neogene-Quaternary magmatism and geodynamics in the Carpathian-Pannonian region: a synthesis. Lithos, 72: 117-146.

Shevenell, A.E., Kennett, J.P., Lea, D.W., 2004. Middle Miocene Southern Ocean Cooling and Antarctic Crysosphere Expansion. Science 305, 1766-1770.

Shi, G.R., 1993. Multivariate data analysis in palaeoecology and palaeobiogeography – a review. Palaeogeography Palaeoclimatology. Palaeoecology, 105. 199-234.

Sissingh, W., 1972. Late Cenocoic Ostracoda of the south Aegean Island Arc. Utrecht Micropaleontological Bulletins, 6, 1-187.

Spezzaferri, S., Ćorić, S., Hohehegger, H., Rögl, F., 2002. Basin-scale paleobiogeography and paleoecology: an example from Karpatian (Latest Burdigalian) benthic and planktonic foraminifera and calcareous nannofossils from the Central Paratethys. Geobios 35 (M.S. 24), 241–256.

Stille, H., 1924. Grundfragen der vergleichenden Tektonik. Bornträger, 443 pp.

Strahlhofer, D., 2013. Paleoenvironmental Reconstruction of Middle Miocene (Badenian/Langhian) Siliciclastic Sections in the Central Paratethys (Styrian Basin, Austria). 132 pp. Unpublished Master thesis, University of Graz, Department of Earth science.

Strauss, P., Harzhauser, M., Hinsch, R., Wagreich, M., 2006. Sequence stratigraphy in a classic pull-apart basin (Neogene, Vienna Basin). A 3D seismic based integrated approach. Geologica Carpathica 57, 185–197.

Szczechura, J., 2006. Middle Miocene (Badenian) ostracods and green algae (Chlorophyta) from Kamienica Nawojowska, Nowy Sącz Basin (Western Carpathians, Poland). Geologica Carpathica 57 (2), 103-122.

Triebel, E., 1961. Geschlechts-Dimorphismus und Asymmetrie der Klappen bei der Ostracodengattung *Occultocythereis*. Senckenbergiana Lethaea, 42 (3/4), 205-225.

Uliczny, F., 1969. Hemicytheridae und Trachyleberididae (Ostracoda) aus dem Pliozän der Insel Kephallinia (Westgriechenland). 152 pp. Unpublished Dissertation, Ludwig-Maximilians-Universität Munich.

Wefer, G., Berger, W.H., Bijima, J., Fischer, G., 1999. Clues to Ocean History: a Brief Overview of Proxies. In: Fischer, G., Wefer, G. (Eds.), Use of Proxies in Paleoceanography - Examples from the South Atlantic. 1-68.

Wessely, G., Ćorić, S., Rögl, F., Draxler, I., Zorn, I., 2007. Geologie und Paläontologie von Bad Vöslau (Niederösterreich). Jahrbuch der Geologischen Bundesanstalt, 147, p 419-448, Wien.

Zachos, J., Pagani, M., Sloan, L., Thomas, E., Billups, K., 2001. Trends, rhythms, and aberrations in global climate 65 Ma to present. Science 292, 686–693.

Zhao, Q. & Whatley R., 1997. Distribution of the ostracod genera Krithe and Parakrithe in bottom sediments of the East China and Yellow seas. Marine Micropaleontology 32, 195-207.

Zlinská, A., Zorn, I., Zágoršek, K., 2013. Foraminifery, ostrakódy a machovky z okolia Devínskej Novej Vsi a Záhorskej Bystrice (slovenská časť Viedenskej panvy). Mineralia Slovaka, 45 (2013), 185-200.

Zorn, I., 1995. Preliminary report on the ostracods from the Ottnangian (Early Miocene) of Upper Austria.- In Riha, J. (Ed.): Ostracoda and Biostratigraphy, Proceedings of the 12th International Symposium on Ostracoda, Prague, Prague 1994. 237-243, A.A.

Zorn, I., 1998. Ostracoda aus dem Karpat (Unter-Miozän) des Korneuburger Beckens (Niederösterreich). Beiträge zur Paläontologie, 23, 175-27.

Zorn, I., 2000. Das Paläogen und Neogen.- In: Schönlaub H.P. (Ed.): Geologie der Österreichischen Bundesländer – Burgenland.- 15-30, Geologische. Bundesanstalt, Wien.

Appendix 1: Terminological explanations

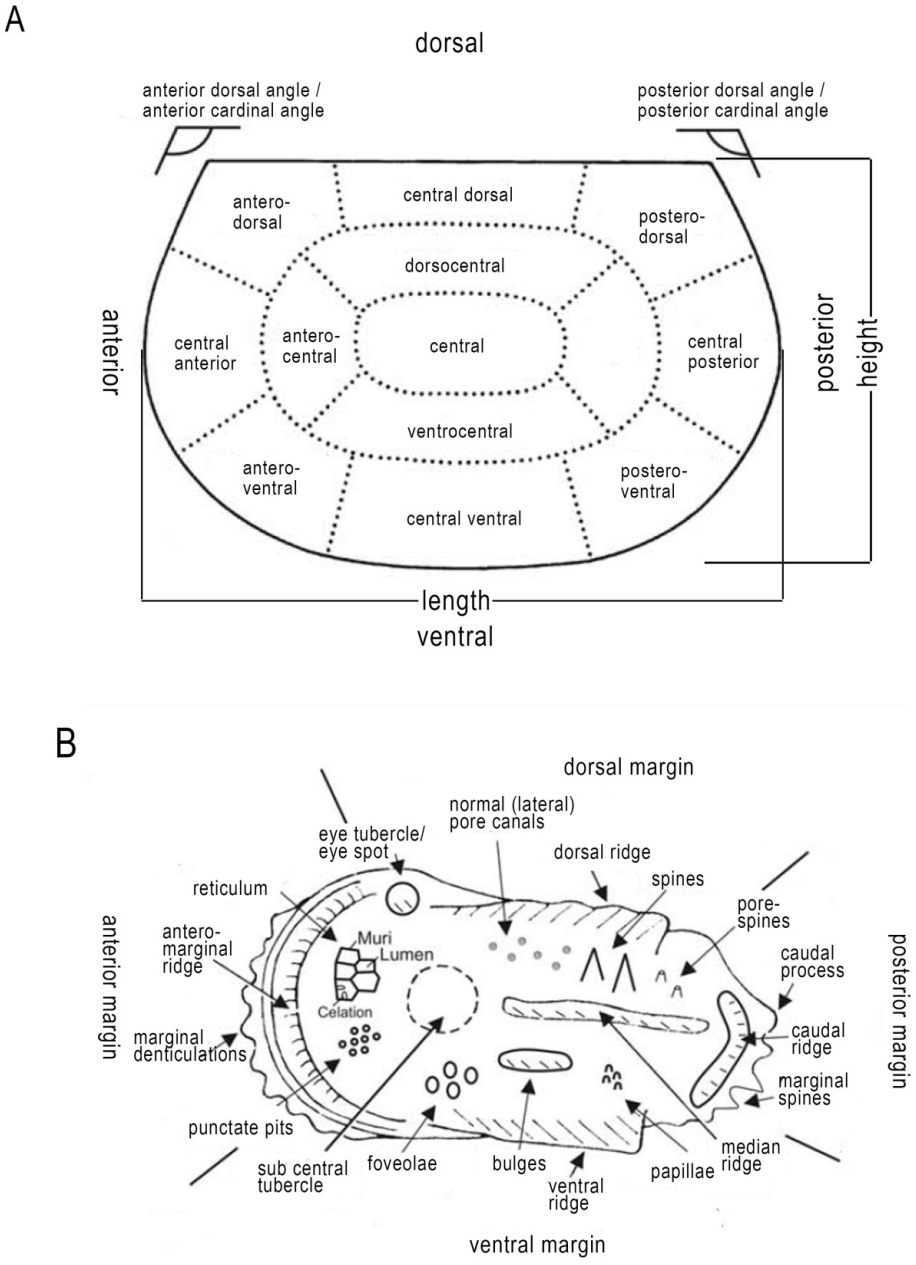

App. 1 Fig. 1: Important morphological features of ostracods valves: A = terminology of the lateral surface of an ostracod valve (after Kelsing, 1951; modified after van Morkhoven, 1962 and Gross, 2006). B = terminology of important sculpture elements (after van Morkhoven, 1962; modified after Gross, 2006).

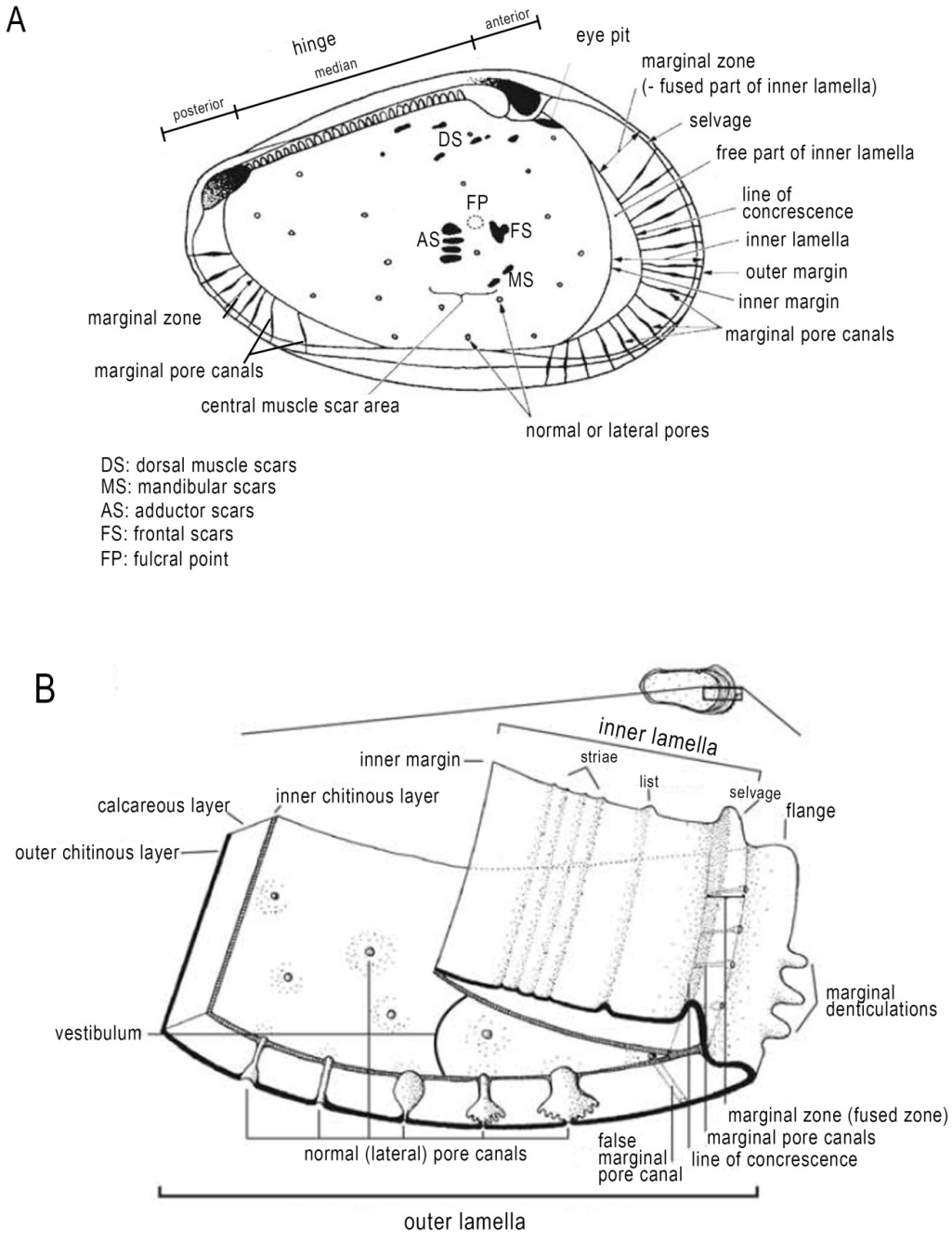

App. 1 Fig. 2: Morphological features of ostracods valves. A = left valve of an ostracod, seen from the inside, showing main structural elements of the calcareous part (after van Morkhoven, 1962; modified after Gross, 2006); B = detailed sketch of the marginal area of a valve (after Helmdach, 1977; modified after Gross, 2006).

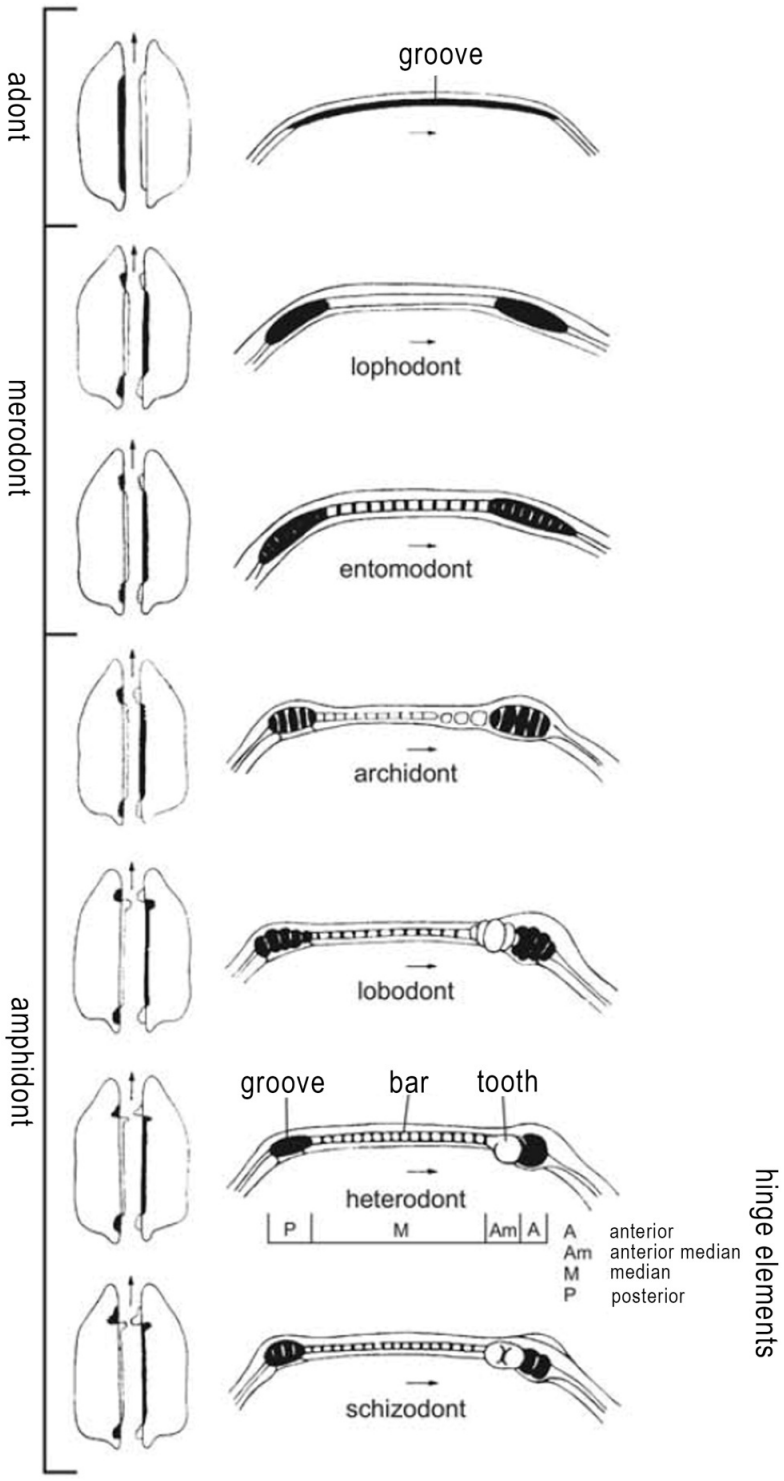

App. 1 Fig. 3: Schematic representation of the main ostracod hinge types after van Morkhoven, 1962; modified after Gross, 2006.

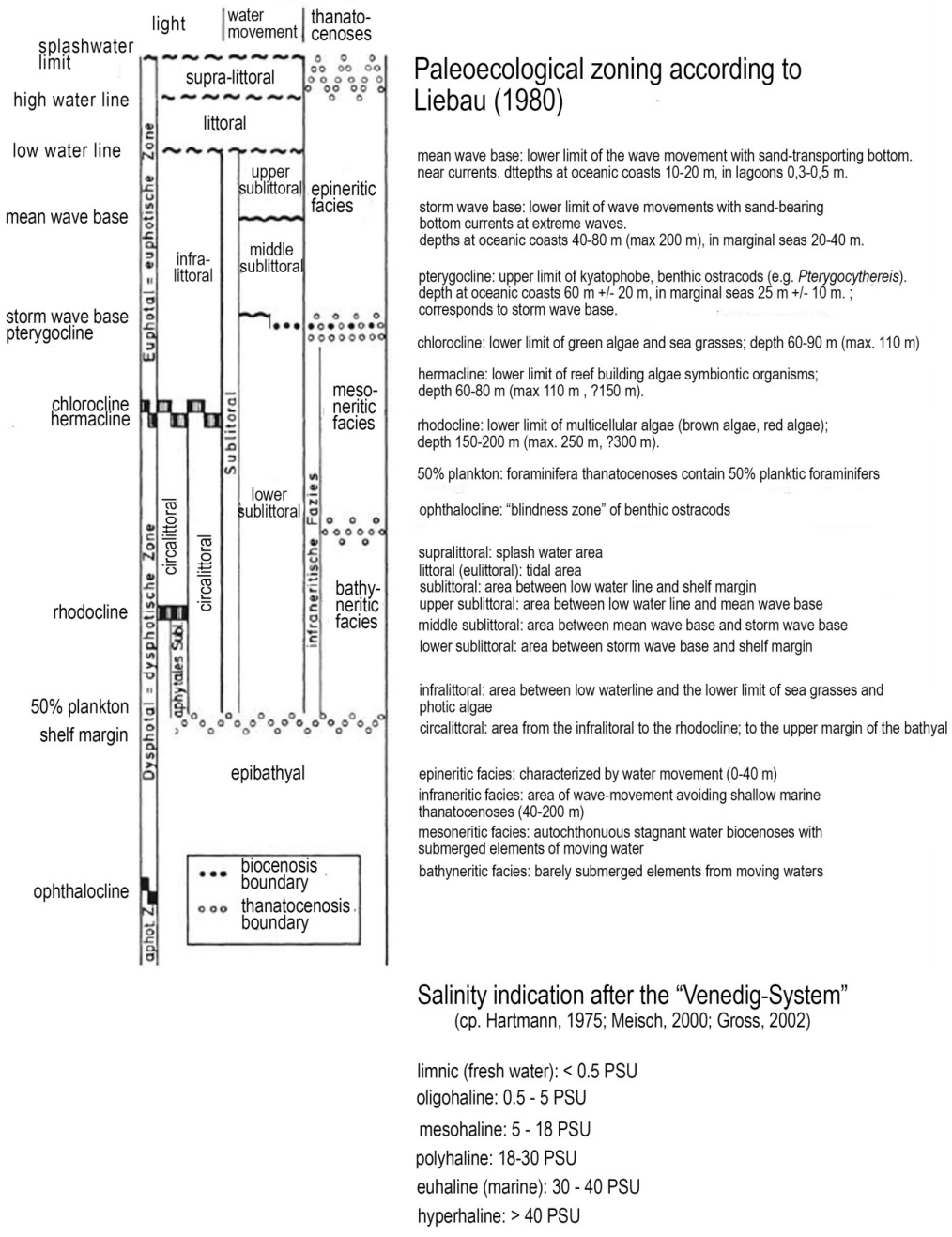

App. 1 Fig. 4: Paleoecological zoning of shallow-marine environments after Liebau (1980) and salinity indication after the "Venedig-System" (both modified after Gross, 2006).

Appendix 2: Ostracod distribution

Ostracod distribution in the Old quarry section

	cf. Aurila				*Aurila* sp.				*Aurila punctata*				*Aurila* cf. *punctata*				*Buntonia brunensis*				*Buntonia* cf. *brunensis*			
	juvenile		adult		juvenile		adult		juvenile		adult		juvenile		adult		juvenile		adult		juvenile		adult	
	c	v	c	v	c	v	c	v	c	v	c	v	c	v	c	v	c	v	c	v	c	v	c	v
R02/28																								
R02/27																								
R02/26																								
R02/25																								
R02/24																								
R02/23			1																					
R02/22																								
R02/21																								
R02/20																								
R02/19																								
R02/18																								
R02/17																								
R02/16																			1					
R02/15																			1					
R02/14																								
R02/13																								
R02/12																			2					
R02/11																								
R02/10																								1
R02/09																			2					
R02/08																			1					
R02/07																								
R02/06						1						1							2					
R02/05																								
R01/29					2	17	4	21			7	11												
R01/28				1			1	8			7													
R01/27																			1					
R01/26																			3					
R01/25																								
R01/24																								
R01/23																								
R01/21																								
R01/20																				1				
R01/19																			1	3				
R01/18																								
R01/17				1				1																
R01/16																								
R01/15																								
R01/14																								
R01/13																								
R01/12																			2	2				
R01/11																				2				
R01/10																								
R01/09																								
R01/08								1																
R01/07												4												
R01/06																								
R01/02																								

App. 2 Tab. 1: Ostracod distribution in the Old quarry section

	Costa punctatissima				cf. *Cytherella*				*Cytherella* sp.1				*Cytherella* aff. *russoi*				*Cytherella* aff. *compressa*				*Cytherella* sp.			
	juvenile		adult		juvenile		adult		juvenile		adult		juvenile		adult		juvenile		adult		juvenile		adult	
	c	v	c	v	c	v	c	v	c	v	c	v	c	v	c	v	c	v	c	v	c	v	c	v
R02/28																								
R02/27																								
R02/26																								
R02/25																								
R02/24																								
R02/23																								
R02/22																								1
R02/21																							1	
R02/20																							2	3
R02/19																								
R02/18																								
R02/17																								
R02/16																							6	
R02/15																								
R02/14																								
R02/13																								
R02/12																								
R02/11																						1	1	
R02/10																								
R02/09			1																					
R02/08															1	1								2
R02/07																								
R02/06																								
R02/05																								
R01/29											1	1												
R01/28											1													
R01/27																								
R01/26																						2		3
R01/25			1															2				1		
R01/24																								
R01/23																								
R01/21																		1						
R01/20																								
R01/19																								
R01/18																								
R01/17																								
R01/16			1																				1	
R01/15																								
R01/14																								
R01/13																								
R01/12																					4			
R01/11				2																				6
R01/10							1																	1
R01/09																								
R01/08																								
R01/07												4												
R01/06																								
R01/02																								

App. 2 Tab. 1: Ostracod distribution in the Old quarry section (continued).

	Cytherella cf. *cercinata*				*Cytherelloidea* sp.				*Cytheridea acuminata*				*Cytheridea* aff. *acuminata*				*Grinioneis* cf. *haidingeri*				*Henryhowella asperrima*			
	juvenile		adult		juvenile		adult		juvenile		adult		juvenile		adult		juvenile		adult		juvenile		adult	
	c	v	c	v	c	v	c	v	c	v	c	v	c	v	c	v	c	v	c	v	c	v	c	v
R02/28																								2
R02/27																								
R02/26																								
R02/25																								
R02/24																								
R02/23			1																					
R02/22																								1
R02/21			1																				1	2
R02/20																							1	
R02/19			1	1																		1	2	1
R02/18																					1		1	3
R02/17																						1	1	1
R02/16				1																		3	3	2
R02/15																						1		1
R02/14				1																		5		2
R02/13																						1	1	1
R02/12			1																1		1	9	1	8
R02/11																							3	5
R02/10																							2	1
R02/09																						6	2	1
R02/08																								1
R02/07																							1	
R02/06																					1	2	1	1
R02/05																							1	
R01/29								1															1	
R01/28								2															1	1
R01/27			1																			1		1
R01/26			2																					
R01/25																						6		1
R01/24			1																					7
R01/23			1																		2	2	2	1
R01/21																								1
R01/20																					1	6	2	3
R01/19																						10	1	2
R01/18																								1
R01/17																								
R01/16			1																			3	1	3
R01/15																								1
R01/14																								
R01/13																								
R01/12			1																			4	3	4
R01/11				1																	2	10	3	10
R01/10																								2
R01/09																								
R01/08																								
R01/07								1											1	1			1	3
R01/06							2																	
R01/02																								

App. 2 Tab. 1: Ostracod distribution in the Old quarry section (continued).

	Krithe aff *compressa*				*Krithe* sp.				cf. *Loxocorniculum*				*Loxocorniculum hastatum*				*Loxocorniculum* cf. *hastatum*				*Occultocythereis* cf. *bituberculata*			
	juvenile		adult		juvenile		adult		juvenile		adult		juvenile		adult		juvenile		adult		juvenile		adult	
	c	v	c	v	c	v	c	v	c	v	c	v	c	v	c	v	c	v	c	v	c	v	c	v
R02/28																								
R02/27																								
R02/26																								
R02/25																								
R02/24																								
R02/23																								
R02/22																								
R02/21			1	1		1	1																	
R02/20							1	3																
R02/19					3	2																		
R02/18			1	1																				
R02/17																								
R02/16																								
R02/15					4																			
R02/14	4		2		1																			
R02/13																								
R02/12																								
R02/11			3																					
R02/10					1																			
R02/09					4																			
R02/08			1		15	3	1																	
R02/07			2		10																			
R02/06	1				14	2																		
R02/05			1		2	1																		
R01/29														2										
R01/28							1	1							1	1								
R01/27		5			6																			
R01/26		1	6			5	7																	
R01/25		1			3																		2	
R01/24					4	1	3																	
R01/23								4																
R01/21						3																		
R01/20					2	3																		
R01/19	3																							
R01/18																								
R01/17																								
R01/16					1	1																		
R01/15																								
R01/14																								
R01/13																								
R01/12					1												1	1						
R01/11	2																						1	
R01/10																								
R01/09					4																			
R01/08																								
R01/07																							1	
R01/06																								
R01/02																								

App. 2 Tab. 1: Ostracod distribution in the Old quarry section (continued).

	Olimfalunia cf. *plicatula*				*Parakrithe* cf. *soustonsensis*				*Parakrithe* sp.				*Pterygocythereis calcarata*				*Senesia* cf. *cinctella*				*Xestoleberis* sp.				indet.		
	juvenile		adult		juvenile		adult		juvenile		adult		juvenile		adult		juvenile		adult		venile		adult				
	c	v	c	v	c	v	c	v	c	v	c	v	c	v	c	v	c	v	c	v	c	v	c	v	c	v	br
R02/28				1																					6		
R02/27																									8		
R02/26																									12		
R02/25																											
R02/24																											
R02/23																									20		7
R02/22																									19		
R02/21																									9		23
R02/20						1	1																				44
R02/19						4			2		1														9		16
R02/18																									13	3	20
R02/17																									11		11
R02/16											4												2		7	3	
R02/15					4																				6	4	12
R02/14					3	2																			16		
R02/13			1				1		1																5	2	13
R02/12						1	1	1	1		2												1		21	20	
R02/11			1		2		1				1														9	5	19
R02/10							1																		18		
R02/09																											18
R02/08					1				6	3															3	4	3
R02/07						3																			1		2
R02/06					2																				5		15
R02/05					1				3		1														2		5
R01/29																									7	37	4
R01/28																									7	7	67
R01/27						2			3												1				12		27
R01/26									15	8	4														3		88
R01/25					3			2								1									36		54
R01/24																1									10		15
R01/23									3																6		2
R01/21					5	2	1				1														3	3	48
R01/20										2															14	4	
R01/19					2											1									11	5	16
R01/18																									12		8
R01/17																									2	5	
R01/16																									13		10
R01/15																										2	
R01/14																											
R01/13									1	2															22		4
R01/12																									6	9	
R01/11					5	1			7						1	1					1				17		5
R01/10																									5		5
R01/09					1																				3	2	16
R01/08																											
R01/07																				2					11	15	30
R01/06																									5		4
R01/02						2			2																2		3

App. 2 Tab. 1: Ostracod distribution in the Old quarry section (continued).

Ostracod distribution in the Rosenberg quarry section

	cf. Aurila				*Aurila* sp.				*Aurila punctata*				*Aurila* cf. *punctata*				*Buntonia* cf. *brunensis*				*Costa punctatissima*			
	juvenile		adult		juvenile		adult		juvenile		adult		juvenile		adult		juvenile		adult		juvenile		adult	
	c	v	c	v	c	v	c	v	c	v	c	v	c	v	c	v	c	v	c	v	c	v	c	v
RB01/13								2																
RB01/12																								
RB01/11																								
RB01/10																								
RB01/09																		7	2	1				2
RB01/08																								
RB01/07				1			1	2								3								
RB01/06								8																
RB01/05																								
RB01/04																								
RB01/03							2	3			2												2	
RB01/02																								
RB01/01																								

App. 2 Tab. 2: Ostracod distribution in the Rosenberg quarry section.

	Cytherella sp.1				*Cytherella* aff. *russoi*				*Cytherella* aff. *compressa*				*Cytherella* sp.				*Cytheridea acuminata*				*Cytheridea* aff. *acuminata*			
	juvenile		adult		juvenile		adult		juvenile		adult		juvenile		adult		juvenile		adult		juvenile		adult	
	c	v	c	v	c	v	c	v	c	v	c	v	c	v	c	v	c	v	c	v	c	v	c	v
RB01/13								1																1
RB01/12				2				1				3	2	5										
RB01/11																								
RB01/10																			1					
RB01/09					3	8					2	3	8	24					1	3				
RB01/08																								
RB01/07																								4
RB01/06																								
RB01/05																								
RB01/04																								
RB01/03																								
RB01/02																								
RB01/01																								

App. 2 Tab. 2: Ostracod distribution in the Rosenberg quarry section (continued).

	Grinioneis cf. *haidingeri*				*Krithe* sp.				cf. *Loxocorniculum*				*Loxocorniculum hastatum*				*Olimfalunia* cf. *plicatula*				*Pterygocythereis calcarata*			
	juvenile		adult		juvenile		adult		juvenile		adult		juvenile		adult		juvenile		adult		juvenile		adult	
	c	v	c	v	c	v	c	v	c	v	c	v	c	v	c	v	c	v	c	v	c	v	c	v
RB01/13																			1					1
RB01/12																								
RB01/11																								
RB01/10																								
RB01/09				1		1				3										1			1	4
RB01/08																								
RB01/07															4									
RB01/06											4	1												
RB01/05													1											
RB01/04																								
RB01/03																								
RB01/02																								
RB01/01																								

App. 2 Tab. 2: Ostracod distribution in the Rosenberg quarry section (continued).

	Senesia cf. *cinctella*				*Xestoleberis* sp.				indet.		
	juvenile		adult		juvenile		adult				
	c	v	c	v	c	v	c	v	c	v	br
RB01/13				3						3	8
RB01/12											6
RB01/11											
RB01/10											
RB01/09							1		1	19	8
RB01/08									2	5	5
RB01/07									11	10	21
RB01/06									15		38
RB01/05											
RB01/04											
RB01/03									5	17	8
RB01/02									24		7
RB01/01									9		

App. 2 Tab. 2: Ostracod distribution in the Rosenberg quarry section (continued).

Appendix 3: Geochemical data

Geochemical data of the Old quarry section.

	CaCO3 (%)	S (%)	TOC (%)	TOC/S	δ13C(‰)	δ18O(‰)
R02/28	19.2	1.5	1.3	0.9	0.5	-0.8
R02/27	57.2	0.7	0.7	1	1.8	0.2
R02/26	21.6	1.3	1.1	0.9	-0.1	-0.1
R02/25	4.8	0.6	0.3	0.6	0.7	-4
R02/24	5.8	0.7	0.7	1	0.5	-3.1
R02/23	28.6	1.2	1.1	0.9	0.5	-1.5
R02/22	39.4	1.1	1.2	1.1	0.6	-1.3
R02/21	34.7	0.9	0.7	0.8	0.7	0.1
R02/20	31.7	0.8	0.9	1.2	1.1	-2.1
R02/19	30.1	0.7	0.8	1.1	-0.3	-2.2
R02/18	31.1	0.7	0.8	1.1	0.5	-2.2
R02/17	35	1.1	1.2	1.1	0.9	-1.5
R02/16	25	1.5	0.8	0.5	0.8	-1.9
R02/15	29.8	0.5	0.7	1.4	0.7	-2.8
R02/14	35.4	0.9	1.2	1.4	0.7	-1.5
R02/13	37.4	0.8	1.1	1.3	0.5	-2.5
R02/12	34.8	1	0.8	0.8	0.4	-2.7
R02/11	30.7	1.3	1.4	1.1	0.8	-1.7
R02/10	24.3	1.3	1.1	0.8	0.8	-2.5
R02/09	33.6	1	1.2	1.2	0.6	-2.9
R02/08	27.6	1.1	0.7	0.7	0.1	-3.4
R02/07	30.5	0.7	0.7	1.1	0.4	-2.8
R02/06	25.4	0.8	0.5	0.7	0.6	-3.6
R02/05	34.9	0.8	0.7	0.9	0.5	-2.9
R01/29	27.1	0	0.4	15	0.1	-4.1
R01/28	31.1	0.1	0.5	9.6	0.5	-4.1
R01/27	30.8	3.4	1.2	0.4	0.1	-2.4
R01/26	30.4	2.3	1.1	0.5	0.9	-2.8
R01/25	30.2	2.1	1.2	0.6	0.9	-3.2
R01/24	29.5	1.5	1.1	0.8	1	-3
R01/23	25.2	0.7	1.1	1.6	0.8	-3
R01/21	28.7	0.4	1.2	3.3	0.7	-3.2
R01/20	49.1	0.4	1	2.9	-0.6	-1.8
R01/19	30.1	0.5	1.2	2.3	0.6	-3.7
R01/18	18.9	0.4	1.3	3.3	0.8	-3
R01/17	20.7	0.9	1.3	1.6	0.4	-3.3
R01/16	23.5	0.4	1.2	2.9	0.5	-2.9
R01/15	0	0.1	1	16.7	0.5	-3.4
R01/14	0	0.1	1	14.6	0.7	-3
R01/13	20.4	0.5	1.1	2	0.3	-1.8
R01/12	30.4	0.9	0.9	0.9	-0.1	-3.1
R01/11	38	0.9	1	1.1	-0.1	-2.2

App. 3 Tab. 1: Geochemical data from the Old quarry section.

	CaCO3 (%)	S (%)	TOC (%)	TOC/S	δ13C(‰)	δ18O(‰)
R01/10	30.4	0.4	1.1	2.6	0.7	-3.3
R01/09	41.7	0.6	1.1	1.8	0.2	-1.5
R01/08	2.2	0.1	1	6.6	0.4	-4
R01/07	39.8	0.4	0.9	2.6	0.2	-2.9
R01/06	72.7	0.2	0.6	2.7	-0.7	-1.6
R01/05	79.3	0.2	0.4	1.9	-0.5	-1.1
R01/04	85.7	0.1	0.3	2.4	0.1	-1.7
R01/03	91.1	0	0.3	6.3	0.2	-2.6
R01/02	34.4	0.2	1.1	5.6	0.4	-2.9
R01/01	92.6	0	0.2	8.6	-0.1	-1

App. 3 Tab. 1: Geochemical data from the Old quarry section (continued).

Geochemical data of the Rosenberg quarry section.

	CaCO3 (%)	S (%)	TOC (%)	TOC/S	δ13C(‰)	δ18O(‰)
RB01/13	18.7	0	0.2	9.6	-0.3	-4.1
RB01/12	18.7	0.9	0.5	0.5	-1.1	-4.2
RB01/11	30.3	0.8	0.7	0.9	-0.9	-5.5
RB01/10	18.6	0.3	0.4	1.1	-0.9	-5
RB01/09	25.1	0.5	0.5	1	0	-3.7
RB01/08	25.6	0.9	0.3	0.3	0.1	-2.9
RB01/07	34.8	0.9	0.4	0.4	-0.2	-2.2
RB01/06	60.2	0.7	0.5	0.7	-0.6	-0.5
RB01/05	21.4	1	0.7	0.7	0	-3.7
RB01/04	33.4	0.8	0.9	1.1	0.2	-2.4
RB01/03	25.1	0.5	0.3	0.5	0.2	-8.2
RB01/02	27.8	1.1	1	0.9	0.2	-2.6
RB01/01	23.9	0.6	0.9	1.5	0	-3.5

App. 3 Tab. 2: Geochemical data of the Rosenberg quarry section.